Designs for Muon Tomography Station Prototypes Using GEM Detectors

by

Leonard Victor Grasso III

Bachelors Degree in Physics
University of Florida, 1998

A thesis
submitted to
Florida Institute of Technology
in partial fulfillment of the requirements
for the degree of

Master of Science
In Physics

Melbourne, Florida
May, 2012

We the undersigned committee hereby recommend
that the attached document be accepted as fulfilling in
part the requirements for the degree of
Master of Science in Physics.

"Designs for Muon Tomography Station Prototypes Using GEM Detectors," a thesis by Leonard Victor Grasso III

Marcus Hohlmann, Ph.D. Associate Professor Physics and Space Sciences	Debasis Mitra, Ph.D. Professor Computer Sciences
Ming Zhang, Ph.D. Professor Physics and Space Sciences	Terry D. Oswalt, Ph.D. Professor and Head Physics and Space Sciences

Abstract

Title: Designs for Muon Tomography Station Prototypes Using GEM Detectors.
Author: Leonard Victor Grasso III
Advisor: Dr. Marcus Hohlmann

The discovery of the muon can be traced back to the era spanning 1930 to 1950, and in the 1960's, Luis Alvarez found one of the first ways to apply muons in experimental physics by using them to develop an imaging technique called shadow radiography and to search for hidden chambers in the ancient Egyptian pyramid of Chephren. Muon tomography is a very different imaging technique, but also exploits the free supply of cosmic ray muons passing through us all the time. Muon tomography was developed by Christopher Morris at Los Alamos National Lab in 2001 and uses detectors to track the incoming and outgoing trajectories of muons as they pass through a volume in order to image material in it.

Our research group is the first to use gas electron multiplier (GEM) detectors, developed in 1997 by Fabio Sauli, for muon tomography. I designed our group's muon tomography station (MTS) prototypes I and II to mount GEM detectors around a cubic foot imaging volume. The prototype I station was designed to mount detector stacks on two sides (top and bottom) of the imaging volume, and the prototype II station is able to mount detector stacks on four sides of the cubic foot volume. Our group receives funding from the Department of Homeland Security, and the goal of our research is to improve the detection of shielded nuclear material (SNM) at our nation's ports and borders. Muon tomography offers advantages over current detection systems because it is based on the scattering of muons, not on the detection of high energy photons emitted from nuclear material as is currently done.

I designed and ran simulations to test what uranium encased in lead boxes 5 mm thick would look like imaged in our MTS prototype II. The shielding was sufficient to absorb 99.9% of the most probable gamma rays emitted from the uranium. Not only was shielded uranium detectable everywhere in the imaging volume, shielded uranium was shown to stand out more than unshielded uranium. In order to fully replace current detection systems, our system may need to make better images in shorter periods of time. The conclusion is that our detection system could at least be used in parallel with current ones as a secondary check for cargo flagged as needing a more thorough scan, thereby improving national security. Finally, I suggest possible improvements that could be implemented in future prototypes that could increase the structural integrity of the station as well as its coverage and efficiency.

Table of Contents

List of Figures

Acknowledgments

I would like to dedicate this thesis to my wife, Magdalena, and two children Gregory and Claire. Without my wife's undying support, I could not have completed my masters program or this thesis. I want to thank her first and foremost for making all this possible.

I would like to thank Dr. Marcus Hohlmann for the position and opportunities he gave me in his research group and for the work he supported me in which lead to this thesis. Along with Dr. Hohlmann, I would also like to thank the following group members for the invaluable help they provided during various phases of my research: Dr. Kondo Gnanvo, Nick Leioatts, Amilkar Quintero, Bryant Benson, Ben Locke, and Mike Staib.

Finally, I would like to thank Jim Tryzbiak and Bill Bailey for the support and training they gave me in Florida Tech's machine shop. Without their guidance, I would not have been able to realize our group's muon tomography station prototypes I and II.

Chapter 1 Introduction

1.1 The Discovery of the Muon

The origins of the history of the muon can be traced back to the era from 1930 to 1950. It was around this time period that physicists began to seriously contemplate a troubling problem. The classical model did not address the question of what holds the atomic nucleus together. Positively charged protons packed together tightly in the nucleus should repel each other violently. It seemed that there must be some other force present, more powerful than the electromagnetic force, that binds the nucleus together, and physicists at the time were already calling it the strong force. Of course one may ask if such a potent force exists in nature, why aren't we overwhelmed by it in our everyday lives? One possibility is that if such a force exists, it could have a very short range, unlike the more familiar electromagnetic and gravitational forces with their theoretically infinite ranges. It was Hideki Yukawa who proposed the first significant theory of the strong force in 1934. He assumed that protons and neutrons in the nucleus are attracted to each other by a new field in the same way that electrons are attracted to the nucleus by the electromagnetic field. Yukawa also postulated that the strong field should be quantized like the electromagnetic field is. Although many were still uncomfortable with quantum theory, not the least of whom was Einstein, it was ironically Einstein himself who showed that the electromagnetic field is unequivocally quantized through the photoelectric effect in 1905, for which he won the Nobel Prize. The quantum of the electromagnetic field turned out to be the photon (light), and Yukawa wondered what the properties of the quantum of the strong force must be to account for its known properties. For example, since the strong force must be a short range force, Yukawa reasoned that its mediator should be heavy, and he calculated that its mass should be nearly three hundred times that

of an electron, or about one sixth that of a proton. Because the mass of his particle was believed to fall between that of the electron and proton, it came to be known as the meson, which means middle weight (by the way, lepton means light weight, and baryon means heavy weight). One troubling fact, however, was that as of 1934, no such particle that fit the description had been observed in the laboratory, and Yukawa began to doubt his idea. By 1937, a number of systematic studies of cosmic radiation were underway, and it was J. Robert Oppenheimer who realized that two separate groups, Anderson and Neddermeyer, and Street and Stevenson, had identified particles matching Yukawa's description [1]. For many, it was Street and Stevenson's group that provided the most convincing evidence for a new particle at the time through a striking photograph they took (fig. 1.1) [2].

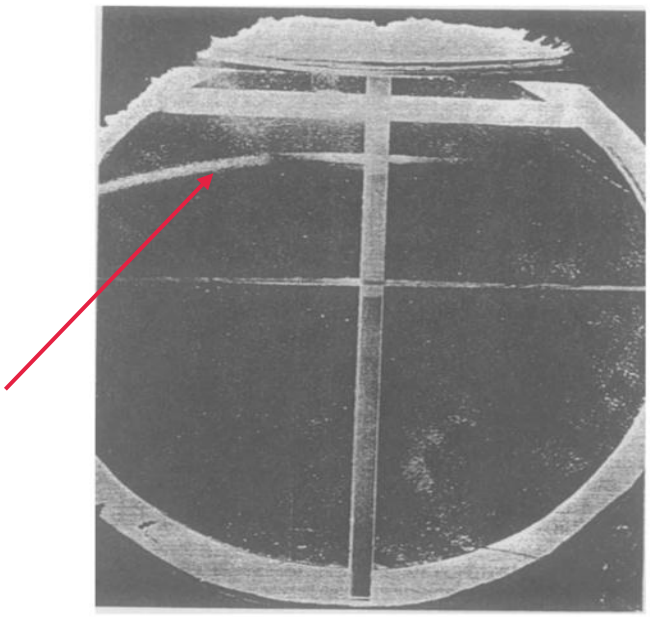

Figure 1.1: Convincing evidence for a new particle provided by Street and Stevenson's group. The arrow points to the curved track swept out by the charged particle moving through the detector's cloud chamber [2].

Measurement of the particle's ionization and momentum showed that its mass must clearly be greater than that of an electron's. (We now know that the particle

observed here was a muon.) This was not only good news for Yukawa, but also good news for quantum electrodynamics in its early stages. Until then, the deep penetrating properties of this new particle were trying to be theoretically accounted for as though it were an electron! A quantum theory of electrodynamics was thought to be breaking down because it could not produce predictions commensurate with experimental observation. Once it was realized that a new particle, more massive than an electron, was being observed, quantum electrodynamics was vindicated and only awaited Richard Feynman, Julian Schwinger, and Sin-Itiro Tomanaga to complete the first quantum field theory, for which they were awarded a Nobel Prize [2]. So, it appeared that the cosmic rays with which we are being bombarded consisted of middle weight particles. Initially, it seemed that Yukawa's particle had been observed, but as more details from the studies came in, disturbing discrepancies arose between Yukawa's predictions and the observed experimental results. For example, the observed particles had the wrong lifetime and were lighter than predicted. To make matters worse, the mass measurements were also inconsistent. To add to the mystery, decisive experiments were carried out in Rome in 1946 demonstrating that the particles resulting from cosmic radiation interacted very weakly with atomic nuclei. This of course posed serious problems if the particles were supposed to mediate the strong force. If that were the case, then they should have interacted quite dramatically with the nuclei. This mystery was finally resolved a year later in 1947 when Powell and his group at Bristol showed that there were actually *two* middle weight particles being detected that were derived from cosmic rays, which they called π (or pion) and μ (or muon). It turns out that the true Yukawa meson is the pion, and that it is produced in large quantities in the upper atmosphere. Powell's group exposed photographic emulsions on mountain tops and observed that one of the decay products of the pi meson is the muon, still referred to by some as the mu meson, even though it is now properly classified as a lepton (fig. 1.2) [3]. They also

determined the mass of the pion and muon to be 286 and 216 electron masses, respectively [4]. Powell and his group provided one of the first measurements of these masses and came close to today's accepted values of 273 and 207 electron masses for the π^- and μ^-, respectively (in MeV/c^2, the masses of e^-, μ^-, and π^- are 0.510999, 105.659, and 139.570 respectively). Now, pi mesons decay before reaching sea level, but the lighter and longer-living muon can be observed at sea level. In fact, of all the products of high energy collisions in our atmosphere (typically incoming protons striking protons in the atmosphere), it is primarily muons that can be observed at the surface of the Earth. It turns out that pions have a lifetime of about 2.6×10^{-8} s, while that of the muon is about 2.2×10^{-6} s (note that the muon's lifetime on average is about one hundred times longer than that of the pion), which means that the fact that muons can be observed at the Earth's surface is a relativistic effect. In fact, the observation of muons at sea level provided strong experimental evidence in support of Einstein's special theory of relativity. According to classical kinematics, we should not be able to observe muons at the surface of the Earth. Assuming that muons are produced at about 8,000 m and travel at about 0.998c, we see that according to the equation:

$$\Delta x = vt \quad \Rightarrow \quad \Delta x = (0.998c)(2.2\times10^{-6}\,s) = 658\,m$$

muons should only be able to penetrate 658 m into the atmosphere, about 7,342 m short of reaching the surface. However, according to relativistic kinematics, we observe time in the muon's reference frame to be slowed down due to time dilation, and the increased lifetime allows the muon to reach the Earth's surface, from our perspective. As measured from our reference frame, the muon's lifetime becomes:

$$\Delta t = \frac{\Delta t_0}{\sqrt{1-\frac{v^2}{c^2}}} \quad \Rightarrow \quad \Delta t = \frac{(2.2\times10^{-6}\,s)}{\sqrt{1-\frac{(0.998c)^2}{c^2}}} = 3.48\times10^{-5}\,s$$

and the muon can now penetrate a distance of:

$$\Delta x = (0.998c)(3.48\times10^{-5}\,s) = 10{,}413\,m$$

enough to reach the Earth's surface and then some. It's interesting to note that what transpires from the muon's point of view is different, although the same net result is achieved. According to special relativity, inside the muon's reference frame its lifetime remains 2.2×10^{-6} s, but the distance to the surface of the Earth becomes shorter due to length contraction. Inside the muon's reference frame, the distance to the surface of the Earth would be measured to be:

$$L = L_o\sqrt{1-\frac{v^2}{c^2}} \quad \Rightarrow \quad L = 8{,}000\,\text{m}\sqrt{1-\frac{(0.998c)^2}{c^2}} = 506\,\text{m}$$

requiring a time of:

$$t = \frac{\Delta x}{v} = \frac{506\,\text{m}}{0.998c} = 1.69\times10^{-6}\,\text{s}$$

to cover, which is well within the muon's mean lifetime. As before, the muon can make it to the Earth's surface and then some. Having a lifetime about one hundred times shorter than that of the muon, not even relativity can help the pion to make it to the surface of the Earth. Relative to an observer on Earth, the pion's lifetime dilates to:

$$\Delta t = \frac{2.6\times10^{-8}\,\text{s}}{\sqrt{1-\frac{(0.998c)^2}{c^2}}} = 4.11\times10^{-7}\,\text{s}$$

and it is only able to penetrate a distance of:

$$\Delta x = (0.998c)(4.11\times10^{-7}\,\text{s}) = 123\,\text{m}$$

Interestingly enough then, it was in the search for Yukawa's meson that the muon appeared as an uninvited guest, having nothing whatsoever to do with strong interactions. Isidore Rabi was once quoted as inquiring, "Who ordered that?" in reference to the discovery of the muon. Sometimes thought of as a heavy version of an electron, Rabi thought it seemed unnecessary for nature to provide more than one kind of the same type of particle [5]. He would have been quite surprised at what lay ahead. As mentioned before, muons are properly classified with leptons.

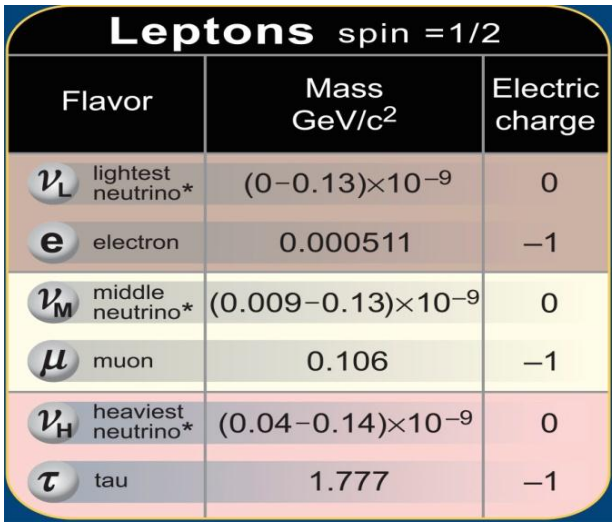

Leptons spin =1/2		
Flavor	Mass GeV/c^2	Electric charge
ν_L lightest neutrino*	$(0-0.13)\times10^{-9}$	0
e electron	0.000511	−1
ν_M middle neutrino*	$(0.009-0.13)\times10^{-9}$	0
μ muon	0.106	−1
ν_H heaviest neutrino*	$(0.04-0.14)\times10^{-9}$	0
τ tau	1.777	−1

Figure 1.2: A table containing information about the six flavors of leptons [3].

Since the search for Yukawa's meson and the pion played such an important role in the discovery of the muon, a table (fig. 1.3) in which the π^+ appears follows.

Mesons $q\bar{q}$ Mesons are bosonic hadrons These are a few of the many types of mesons.					
Symbol	Name	Quark content	Electric charge	Mass GeV/c^2	Spin
π^+	pion	$u\bar{d}$	+1	0.140	0
K^-	kaon	$s\bar{u}$	−1	0.494	0
ρ^+	rho	$u\bar{d}$	+1	0.776	1
B^0	B-zero	$d\bar{b}$	0	5.279	0
η_c	eta-c	$c\bar{c}$	0	2.980	0

Figure 1.3: A table containing information on select mesons [3].

Of course, there are other key particles necessary to fully describe the strong force, but that's another story.

1.2 Imaging Techniques Using Muons

In this section I will discuss two imaging techniques that have been employed using muons. The first is called shadow radiography and was one of the first applications of muons in experimental physics and is therefore historically significant. This technique uses detectors to compare the number of incident muons in certain areas against others. Discrepancies in average muon counts can yield important information about the material they have passed through. Shadow radiography using muons was pioneered by Luis Alvarez in the 1960's to search for hidden chambers in an ancient Egyptian pyramid [6]. The second is called muon tomography and is the technique that my research centers on. Muon tomography (MT) was developed by Christopher Morris at Los Alamos National Lab in 2001 [7]-[11]. This technique uses detectors to track the path of a muon through a volume to image material within it. Detectors developed at CERN to improve the detection and tracking of particles in high energy physics experiments can be used for this purpose. The first such detector used to image material using muons was the drift tube invented by Georges Charpak in 1968 [12]. In 1997, Fabio Sauli invented gas electron multiplier (GEM) detectors, and our research group is the first to use them for muon tomography [13], [14].

Recall from the previous section that high energy cosmic rays are continually bombarding Earth's atmosphere. These rays are approximately comprised of 90% protons, 9% α-particles, and the remainder of heavier nuclei. When the cosmic rays encounter molecules in the Earth's atmosphere, they undergo deep inelastic collisions which produce cascades of lighter particles. We already know that pions are produced, which decay into muons. It turns out that neutrinos are also produced, and the reactions appear as follows, conserving both charge and lepton number:

$$\pi^+ \rightarrow \mu^+ + \upsilon_\mu$$

$$\pi^- \rightarrow \mu^- + \bar{\upsilon}_\mu$$

We also know that muons not only make it to the surface of the Earth, but are able to penetrate well below it due to their relativistic speeds and ability to penetrate through all kinds of matter. The muon flux rate at sea level turns out to be about 10,000 $min^{-1}m^{-2}$, which is approximately one through the surface of your hand every second. The flux rate does, however, depend on a number of factors such as time in the solar cycle, latitude, longitude, and the angle of incidence (usually measured from the vertical). The energy with which muons reach sea level also varies over several orders of magnitude, ranging from about 10 MeV to 10 GeV. However, the average energy, or energy with the highest probability of being measured, is 4 GeV [15]. Now, one might wonder if there is a way to exploit this free source of radiation, or particle influx, with all of its properties for a technological gain in experimental physics, and one of the earliest to do so was Luis Alvarez in the 1960's. Now it so happened that the ancient pyramids of Egypt caught Alvarez's eye, the two largest ever built in particular. They are found near Cairo, are 4,500 years old, and are the pyramids of Cheops and Chephren. At the time there were several known chambers in Cheops' pyramid spread throughout its volume, including a King's Chamber, a Queen's Chamber, a Grand Gallery, and passageways to connect them all, but the only known chamber in Chephren's pyramid was a room at the bottom. Naturally, Alvarez wondered if there were any undiscovered chambers in Chephren's pyramid similar to those known to exist in Cheops' and began to think of possible ways to image the mysterious pyramid. Initially, he thought he might be able to place a strong x-ray source in the chamber beneath the pyramid and to cover the faces of the pyramid with large photographic plates. However, after further consideration Alvarez realized that although the idea was simple in concept, it was also completely impractical. The x-rays would not penetrate the vast amount of rock, and the plates required to cover the faces would have to be too large. He also realized that radar and sonar would not work because

they either would not penetrate the rock or would be too scattered by small gaps between the blocks of rock. The scheme that Alvarez finally conceived involved the new-found muon, and was like his x-ray idea, except run backward. A strong source of muons was already in place via incoming cosmic rays as previously described, and a high energy muon can plow through many meters of rock before stopping [6]. The higher the energy, the more rock can be penetrated. If a detector could be set up in the chamber at the bottom of the pyramid that could discriminate the direction of incoming muons, it should be possible to image the interior volume of the pyramid. If there were hidden chambers, more muons would be incident from those directions because there would be less rock to travel through. Therefore, an image made from the incoming muons should reveal any hollow volumes travelled through, and thus betray any hidden, undiscovered chambers. This method of analysis is referred to as shadow radiography and compares the amounts of muons expected to arrive at a detector to those that actually arrive [15]. So instead of having x-rays emanating outward and detected on the exterior of the pyramid, a constant, free supply of muons would travel inward and be detected at the bottom of the pyramid. It was exactly this scheme that Alvarez was able to make work, and his detector consisted of a series of spark chambers, trigger counters, and 36 tons of iron to insure that only the most energetic muons were being counted. There were many troubles along the way, both technical and political, but Alvarez, and all those who worked with him, were able to complete one of the first and most dramatic muon photography experiments. Unfortunately, the search yielded a negative result, and there were no hidden chambers or treasures to be found. Figures 1.4 and 1.5 show what the expected number of muons might be for no hidden chambers (solid rock all the way through) in the pyramid, and what one might expect to observe if a hidden chamber were present.

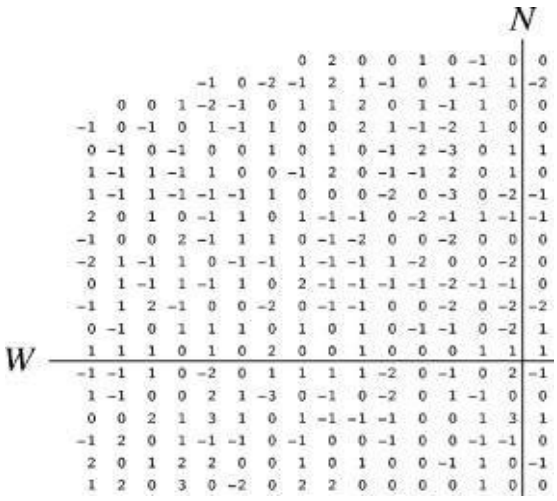

Figure 1.4: No secret chambers to be found would imply solid rock all the way through the pyramid and relatively uniform muon counts throughout the scanned area [6].

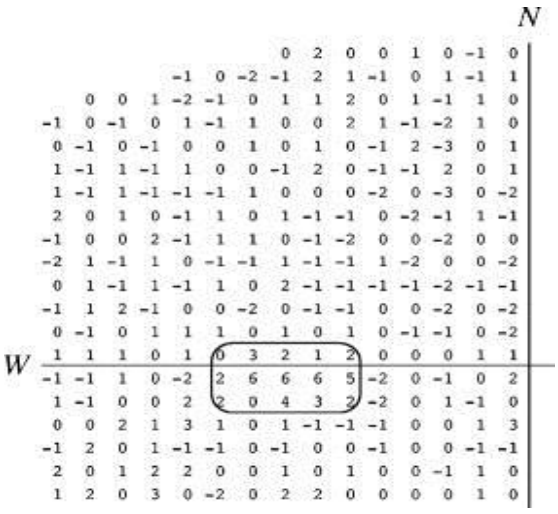

Figure 1.5: A secret chamber in the pyramid would be revealed by a higher than usual muon count within the scanned area. The circled area in the figure reveals how the presence of a hollow volume would be detected by allowing more muons to pass through in that direction [6].

After reading this account, I couldn't help but be reminded of the Michelson-Morley experiment. Michelson and Morley came up with a revised, elaborate, and clever method to measure the speed of the Earth through the ether, which was hypothesized to be the medium through which light propagates. If the ether existed and could be used as an absolute reference frame, then differences in the speed of light should have been able to be detected in their experiment. They were, of course, able to detect no difference in the speed of light, and one would imagine that they were probably somewhat disappointed with their anticlimactic result. Anticlimactic or not, Michelson and Morley's null result is one of the most important experimental results in physics and played a role in shaping and supporting Einstein's theory of special relativity. While the underpinnings of theoretical physics did not hinge on Alvarez's results, there are certainly analogies to be made. His muon photography experiment was absolutely beautiful, and it would have been a picture perfect end to the story had a pot of gold been found at the end of the rainbow, but the fact is that there exists no hidden chambers in the pyramid investigated. When people would say to Alvarez, "So you didn't find any chambers", his response was, "No, *we found* that there are no chambers." Around the same time, in 1968, Luis Alvarez won the Nobel Prize in Physics "For his decisive contributions to elementary particle physics, in particular the discovery of a large number of resonant states, made possible through his development of the technique of using hydrogen bubble chambers and data analysis [6]."

An interesting application of muon tomography using cosmic ray muons involves the pursuit of detecting nuclear (high-Z) material. After being developed by Christopher Morris in 2001, Los Alamos National Lab started to explore the use of MT to detect nuclear contraband at our nation's ports and borders in 2003 [7]-[11]. The threat of nuclear contraband being smuggled across international borders is ever present, and new ways of detecting such contraband are important to national security interests. Muon tomography offers advantages over current

detection systems through its ability to discriminate high-Z material from a lower-Z background, thereby making it more difficult to shield special nuclear material (SNM) [16]. In fact, results of simulations that I will present later suggest that attempting to shield uranium with lead that would make it very difficult to detect using current systems could cause it to show up slightly stronger (than with no shielding) in an image created using muon tomography. Furthermore, if an efficient muon tomography detection based system could be brought to market, it would not only offer certain detection advantages, but may also be more affordable than current systems which are not able to take advantage of a free imaging source. As mentioned previously, to date muon tomography makes use of advanced detectors that have been developed at CERN. Drift tubes have been used by Decision Sciences Corporation in the development of a muon tomography system designed to detect nuclear contraband. In 1992, Georges Charpak won the Nobel Prize in physics for the invention of this kind of detector [12]. Our research group has been funded by the Department of Homeland Security to develop a muon tomography system using GEM detectors, developed by Fabio Sauli. An advantage of using GEM detectors is that they are capable of better spatial resolution than drift tubes are. A disadvantage is that because they are a relatively new technology, very large (>1 m) GEM detectors have yet to be manufactured, making it very difficult to currently image large volumes using them. Although muons have high penetrating properties, they do interact with matter to some degree via Coulomb scattering. Muons are scattered more by atoms with large atomic numbers (high-Z material) than they are by atoms with small atomic numbers. By using detectors that can track incoming and outgoing velocity vectors of muons and using an algorithm that can calculate the position that a deflection occurred along with a scattering angle, material can be imaged using four dimensional data. Three of the dimensions locate a point in space where material exists, and the fourth dimension (scattering angle) indicates the density of the material present. A Point Of Closest

Approach (POCA) reconstruction method is one such algorithm that finds the intersection of incident and exiting muon trajectories and assigns a color coded image to the voxel (a small volume containing the point of interaction) commensurate with the scattering angle [7], [16]. This is the type of reconstruction method our research group uses. Another algorithm involves a Maximum Likelihood / Expectation Maximization (ML/EM) reconstruction method that borrows much from techniques used in medical imaging, but incorporates the statistics of muon scattering [10]. One challenge to overcome in developing a muon tomography system aimed at detecting nuclear contraband is that viable systems should be able to detect SNM within a few minutes, and there is no way to increase the flux of cosmic ray muons. A great reconstruction algorithm could play a key role in overcoming this challenge. Figure 1.6 depicts how a muon tomography system could be used to check a cargo container for nuclear contraband [17].

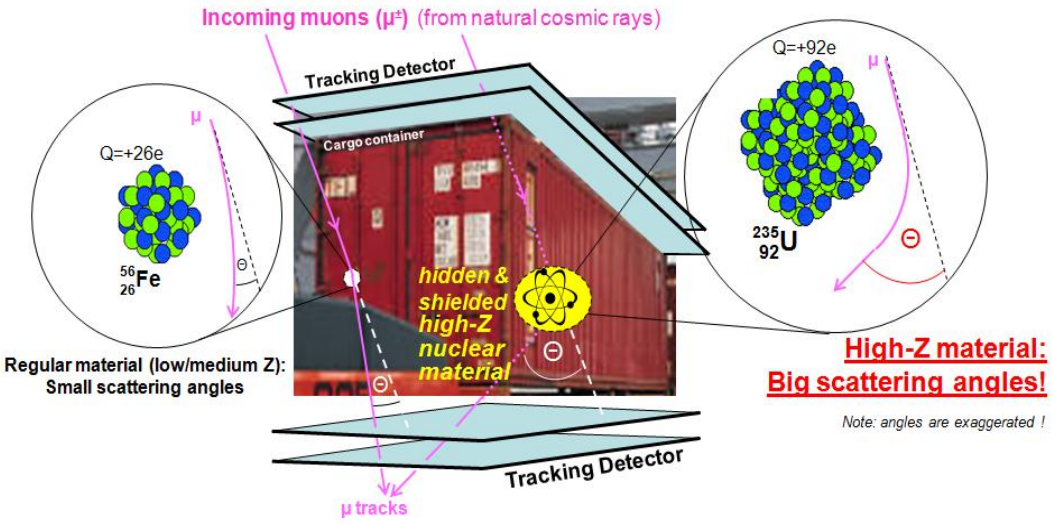

Figure 1.6: The pairs of planes above and below the container represent pairs of GEM detectors used to calculate incoming and outgoing trajectories of muons in a MT based detection system. Muons are scattered more by high-Z material [17].

Because our muon tomography system employs GEM detectors, and accounting for their use primarily drove the designs of the two prototype stations I designed and built, the following section explains the basics of how they work.

1.3 Gas Electron Multiplier (GEM) Detectors

Gas Electron Multiplier (GEM) detectors are micro-pattern gas detectors used for the detection of charged particles [13]. Each GEM detector has five basic components: a honeycomb frame, a drift cathode, foils (referred to as GEM foils), a readout, and a gas mixture which fills the volume of each sealed detector [18]. Fast moving charged particles passing through a detector first ionize the gas filling it in the drift region.

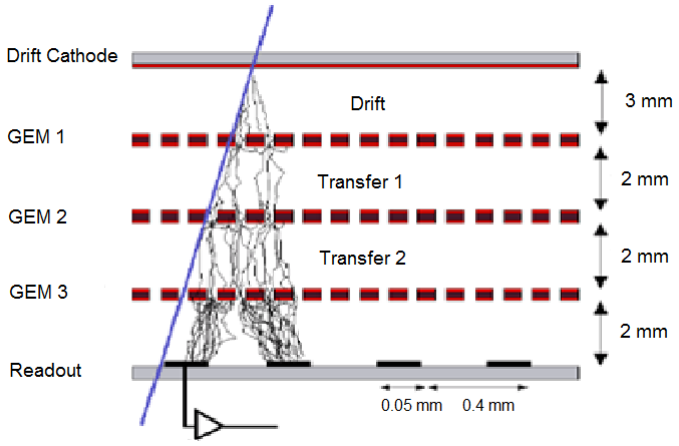

Figure 1.7: Cross section of a triple-GEM detector illustrating the electron multiplication that occurs within the gas-filled detector [19].

The freed electrons are then accelerated through a series of GEM foils (usually two or three) that have a potential difference across them, further ionizing the gas and producing an avalanche of electrons (fig. 1.7) [19]. This is the electron

multiplication that occurs in the gas-filled detectors that their name (Gas Electron Multiplier) implies, and it is the means by which the original signal (in this case a charged particle ionizing gas) is amplified into a measurable current. The avalanche of electrons induces a charge in the readout and thereby produces a current which reveals the position that the fast moving charged particle crossed the detector. Detectors that use two GEM foils for signal amplification are called double-GEM detectors, and those that use three are called triple-GEM detectors.

Each detector has a honeycomb frame which serves to provide strong structural integrity while minimizing the amount of material required to do so (hence the honeycomb geometry). Minimizing the amount of material used for the structural support of each detector is important because it can potentially interfere with the particles sought to be detected [18].

The drift cathode found in each detector is made of kapton and is coated on one side with copper. Kapton is a polymer foil with very strong insulating properties manufactured by the Du Pont Company [20]. It's only about 50 μm thick, and the copper coating is only about 5 μm thick. The side of the drift cathode that is not coated is attached to the honeycomb frame. A negative electric potential is applied to the drift cathode which serves to attract the positive ions created in the ionization process described above. This is important because it helps to prevent positive ions from recombining with freed electrons before they can be propagated downward to the readout [18].

Each GEM foil used in a detector is also made of kapton and is coated with copper on both sides. Again, the kapton is about 50 μm thick and the copper coating on each side is about 5 μm thick. Each foil is pierced by a regular array of chemically etched holes that are about 140 μm apart (this is why GEM detectors are referred to as micro-pattern gas detectors). The holes have a conical shape to them, and the technique used to etch the holes and to give them their desired shape was

developed at CERN (fig. 1.8-9). The outer diameter of the conically shaped holes is 70 μm, and the inner diameter is 50 μm [14], [21].

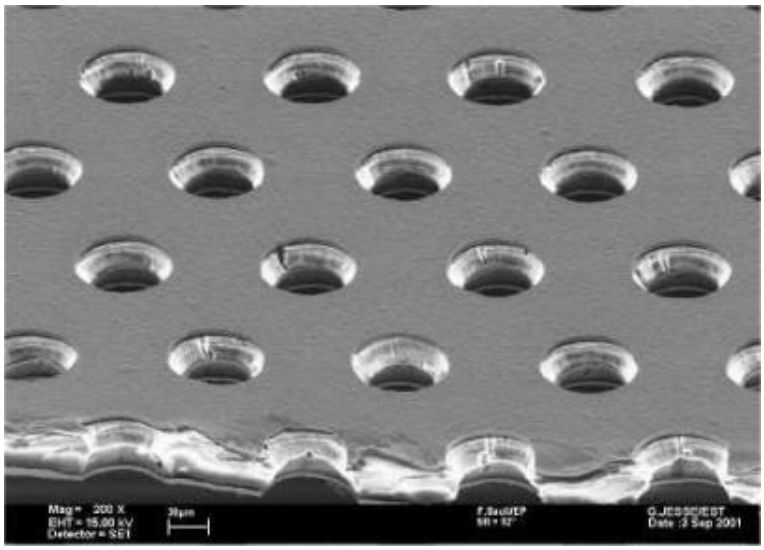

Figure 1.8: Magnified view of the micro-pattern holes etched into each GEM foil [14], [21].

In a triple-GEM detector, the voltage applied across each GEM foil is typically between 400 and 500 volts. The holes piercing each foil have their conical shape for two reasons: to help prevent unwanted and potentially very damaging sparking from one side of the foil to the other, and to help concentrate the electric field lines that fill each hole which serves to amplify the original signal [13]. Free electrons caught in the field filling these holes are accelerated to high enough speeds to further ionize the gas filling each detector, and the number of free electrons able to make it to the readout and produce a measurable current is multiplied. Before being deployed, GEM foils must be stretched and framed. Within a detector it is critical that GEM foils maintain a uniformly flat surface area to function properly [13].

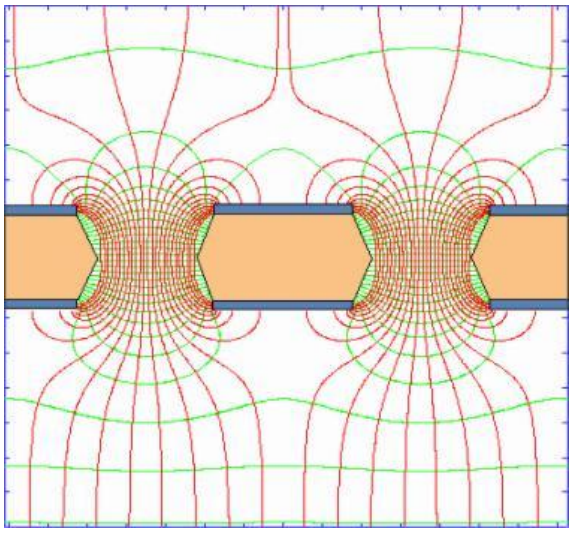

Figure 1.9: The conical shape of the holes etched into each GEM foil helps to concentrate the electric field lines filling them. Here, electric field lines (red) and equipotential lines (green) are shown [14], [21].

A readout must be placed at the bottom of each detector to measure the amplified signal of an interaction (gas being ionized by a cosmic ray muon in our case) and to determine the position at which the interaction occurred. The readouts used for the detectors in the muon tomography station prototypes I designed have two dimensional readout strips with a 400 μm pitch and analog readout and can reach a position resolution of 50 – 80 μm for muons with perpendicular incidence [21]. The two dimensional readout strips can be thought of as x-y, x-z, or y-z strips depending on the choice of coordinate system and the readout's placement within it.

The choice of gas used to fill each detector is a critical one. The gas should be relatively easy to ionize, and electron avalanching should be obtainable in a relatively low electric field because they pose less danger to the detector. The gas should recover quickly from electron avalanching and should be non-corrosive to the GEM foils used in each detector. It turns out that the noble gasses are ideal

candidates to meet all of these criteria, with those having higher atomic numbers being preferred. Because xenon and krypton are so expensive, argon is the most cost effective choice. However, there is a problem with the use of pure argon. The only way for argon to return to ground state is by emitting a photon which can cause secondary ionization on the GEM foils themselves, thereby producing a false signal. To overcome this problem, a polyatomic molecule can be introduced to the gas because they can be very useful in preventing these kinds of secondary ionizations. Carbon dioxide is an excellent choice, and a mixture that optimizes all of the desired characteristics is seventy percent argon and thirty percent carbon dioxide (Ar/CO_2 70:30). Gas composed of this mixture of argon and carbon dioxide is cost-efficient, relatively easy to ionize, facilitates electron avalanching in a relatively low electric field, recovers quickly from electron avalanching, and is non-corrosive to metal inside each detector [18].

The detectors used in the prototype stations I designed are triple-GEM detectors using 30 cm × 30 cm GEM foils, yielding an active area of 900 cm^2 for each detector. The thickness of each detector is about 1.3 cm, from the top of the readout to the top of the honeycomb frame placed over the drift cathode. In our application (muon tomography) of the triple-GEM detectors, cosmic ray muons are the fast moving charged particles ionizing the Ar/CO_2 (70:30) gas mixture in the detectors, and the position that they cross a detector can be read out to a resolution of 50 – 80 μm for muons with perpendicular incidence.

Chapter 2 Muon Tomography Station Prototypes

2.1 Muon Tomography Station Prototype I

One of the long term goals of our research group is to design and commission large scale muon tomography stations that can be used to image cargo containers at our nation's ports and prevent the smuggling of nuclear contraband into our country more efficiently and less expensively than is currently done. When I first joined our group in 2008, we were in the earliest phases of this endeavor. At that time, we had run exhaustive simulations which suggested that our long term goal of developing a muon tomography station using GEM detectors was quite feasible. By early 2009 we were getting ready to collect real data from physical detectors to verify predictions made by our simulations and to refine our imaging techniques. Ultimately, our group would need to design an imaging station that could accommodate detector stacks on at least four sides of an imaging volume. A minimum of two detectors are required in a detector stack because each detector reads out a point in space where a muon crossed it, and it takes at least two points to define a line (the muon's incoming or outgoing trajectory). If more than two detectors are used in a stack, then lines of best fit can be calculated to determine trajectories. The reality in 2009 was that we were going to have fewer than eight detectors at our disposal, which meant that even if we had a station that could accommodate detector stacks on four sides, we would only be able to actually employ detector stacks on the top and bottom of our imaging volume. A decision was therefore made that our first muon tomography station (MTS) prototype would be both simple and elegant and able to accommodate detector stacks on the top and bottom of an imaging volume only. This kind of design could be produced quickly and allow for the collection of real data by the fall of 2009. I was tasked to design and build our group's prototype I station accounting for the

use of GEM detectors with 30 cm × 30 cm active areas that are 1.3 cm thick during the summer of 2009. In 2010 I would design and build our group's MTS prototype II, capable of mounting detector stacks on four sides of an imaging volume and the subject of the following section.

I decided that the simplest way to implement a design accommodating top and bottom detector stacks only would be to take advantage of fixation holes that readouts we use have drilled into them during manufacturing. Each readout has three fixation holes that are a quarter inch in diameter in close proximity to three of the four corners where each detector is attached to it. I pursued a design that employed quarter inch stainless steel threaded rods emanating upward from a base support plate made of aluminum. Detectors would be supported by the rods directly, which would pass through the fixation holes in each readout. Support for the detectors (and readouts) on three sides would be sufficient due to their low mass and to the fact that there would be no excess mass, or mass concentration, close to the corner with no support. Using three support rods would work fine for the detectors, but would not be a practical solution to support the target plate which would be placed between the top and bottom detector stacks. The target plate is the element in my design that supports whatever material we want to image. It needs to be massive or strong enough to support high mass objects that can be placed anywhere in the imaging volume. A fourth support rod would definitely be needed to support the target plate, and I implemented a fourth rod for this purpose that extended beyond the area of each detector and readout. All detectors and the target plate would share three quarter inch stainless steel support rods, and the target plate, made of aluminum 3/8 inch thick, would have a fourth support rod passing only through it to provide the extra support needed.

The primary structural components of our MTS prototype I consisted of a base plate used to support four ¼-20 threaded stainless steel rods, and a target plate. The base plate was made of aluminum and designed with cylinders (also

aluminum) emanating up from where the steel rods screw into it. The steel support rods could screw deeper into the cylinders than the thickness of the base plate would allow, making them more stable. 6061-T6 aluminum alloy was used to machine all components made of aluminum in prototypes I and II. Machinists in our shop recommended the use of this kind of aluminum due to its strength while still being easy to machine. Other components used to mount the detector stacks and target plate follow: ¼ inch washers one inch in diameter (placed underneath readouts to distribute pressure), ¼ inch heavy hex nuts (tightened down on top of the cylinders of the base plate to add stability), 7/8 inch stainless steel coupling nuts (used to support the target plate and the bottom detector assembly of the top detector stack), ½ and ¾ inch nylon spacers (used to quickly and accurately establish desired separation distances between detectors in a stack), and nickel anti-seize lubricant for the aluminum base plate / stainless steel rod interface (used to prevent the aluminum and steel from locking up). Appendix A contains directions for assembly. Following are images of our MTS prototype I, starting with some simulated images made using SolidWorks (fig. 2.1-2) and concluding with various images of the actual prototype (fig. 2.3-7). SolidWorks is a 3D CAD (Computer-Aided Design) design, analysis, and product data management software package developed by Dassault Systèmes SolidWorks Corporation [22]. Both MTS prototypes I and II were modeled using this software during the various phases of their designs to test for feasibility and to make final improvements before production.

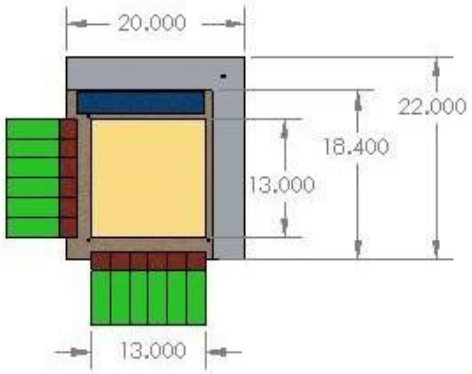

Figure 2.1: Top view of MTS prototype I using SolidWorks. From this perspective, simulated elements of the top detector assembly in the top stack are readily seen including gassiplex cards (green), Panasonic adaptors (red), the section where high voltage is applied (blue), the readout (brown), the GEM detector (gold), and a portion of the target plate (silver). In the portion of the target plate visible, one can see the hole through which the fourth support rod would pass through it. All dimensions shown are in inches.

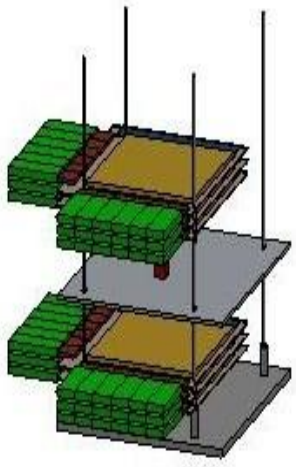

Figure 2.2: Three dimensional view of our MTS prototype I with top and bottom detector stacks using SolidWorks. All main elements of the prototype are visible, along with some material to be imaged on the target plate.

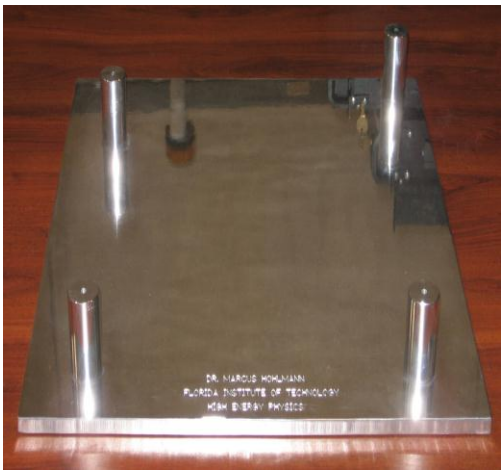

Figure 2.3: Actual base plate used in our MTS prototype I. Its dimensions are 20 in × 22 in × ¾ in. The cylinders have an outer diameter of ¾ in, an inner diameter of ¼ in, and a height of 3.0 in. Steel support rods screw into them 1.5 in deep. The engraving reads "Dr. Marcus Hohlmann / Florida Institute of Technology / High Energy Physics."

Figure 2.4: The target plate used in our MTS prototype I. Its dimensions are 20 in × 22 in × 3/8 in. The engraved square denotes the boundaries of the imaging volume, and the three holes visible by the top left, bottom left, and bottom right corners of the square align with the three fixation holes in each readout. The fourth hole in the target plate used by the fourth support rod which passes through the target plate only is in the upper right hand corner of the image and is hard to make out due to various reflections. All holes are ¼ inch in diameter.

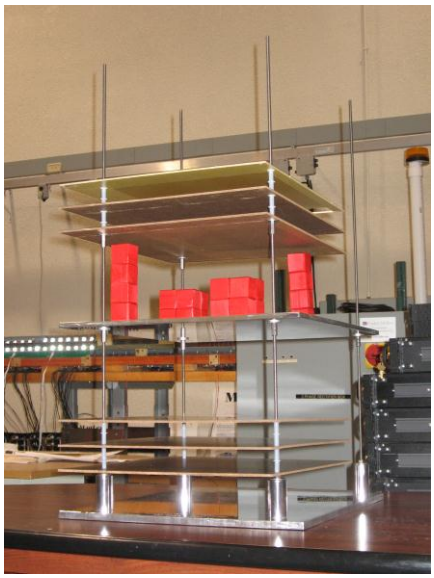

Figure 2.5: MTS prototype I loaded with mock readouts and mock material to be imaged. Nylon spacers can be seen to separate the readouts at uniform distances.

Figure 2.6: MTS prototype I with mock readouts and imaging material from another perspective. The readout at the top of the top stack was an actual readout that had been damaged. One can see the fourth support rod going through the target plate only.

Figure 2.7: Fully commissioned MTS prototype I collecting data at CERN. Note that two GEM detectors are being used in each detector stack, and a small block of lead is being imaged. The damaged readout is able to serve as the target plate here used to image material [23].

2.2 Muon Tomography Station Prototype II

Our MTS prototype I served its purpose well and allowed for the first collection of real data from GEM detectors used to image material. As new detectors were being commissioned and becoming available to use, our focus turned to a prototype II design that would be able to accommodate detectors on four sides of an imaging volume in the form of a cube about a cubic foot in size. During the first several months of 2010, I worked on our prototype II design using SolidWorks, and over the summer I built and commissioned it.

Simulations showed that adding side detector stacks to our prototype II design should dramatically improve the coverage of our imaging station. Coverage is a term that's used to describe the station's ability to effectively image material throughout the entire imaging volume. The better the coverage, the more trackable trajectories of muons pass through each voxel (or small subvolume) of the imaging volume (fig. 2.8) [24]. Recall that muons have to pass through two detector stacks in order for their incoming and outgoing trajectories to be tracked and used to image material.

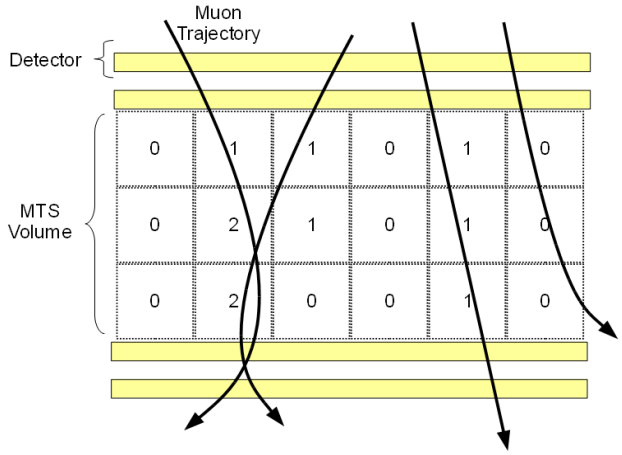

Figure 2.8: Coverage is the imaging station's ability to track muons passing through all subvolumes of the imaging volume. For a muon's track to count (or be measured), it must pass through two detector stacks [24].

With top and bottom detector stacks only, there are many possible ways for a muon to pass through the imaging volume without passing through both top and bottom detector stacks. By adding detector stacks on two more sides of the imaging volume (covering four of six sides of the imaging volume), muons have fewer opportunities to avoid detection. With four sides of the imaging volume covered, muons crossing the top detector stack and either side detector stack can be tracked, and muons crossing either side detector stack and the bottom detector stack can be tracked, in addition to those crossing top and bottom detector stacks. Muons crossing both side detector stacks could also be tracked, but such an event would be less likely. Muons have the highest probability of impacting at an angle of 30° from the vertical at sea level. One might wonder why all six sides of the imaging volume aren't covered to maximize coverage. Two sides of the volume are left uncovered because in the final version, cargo containers must pass through the imaging volume. Sealing off the volume would make impractical the use for which the station was created.

An imaging station with detector stacks on four sides should be a big improvement over the prototype I station, but the design of such a station would have to be very different. Threaded steel rod worked beautifully for a station with top and bottom detector stacks only, but steel rod could not be effectively used to mount side detectors. Since steel rod could not be used, each detector would need its own support plate which would be mounted in a different kind of framework. Detectors would have to be mounted to their support plates via the fixation holes in each detector's readout. Furthermore, support plates would have to be big enough to allow for the space needed by electronics and other various components, such as gas lines, used by each detector. Since the support plates would be larger than the detectors themselves, if they were brought together in such a way as to make four sides of a box, the active area of each GEM detector would not overlap. Active areas of each detector coming together must overlap and define a closed volume to

improve the coverage of the station. This problem was solved by overlapping the detector support plates themselves. Overlapping the support plates would allow the active areas of each GEM detector to overlap and would define a volume closed on four sides by active areas of GEM detectors.

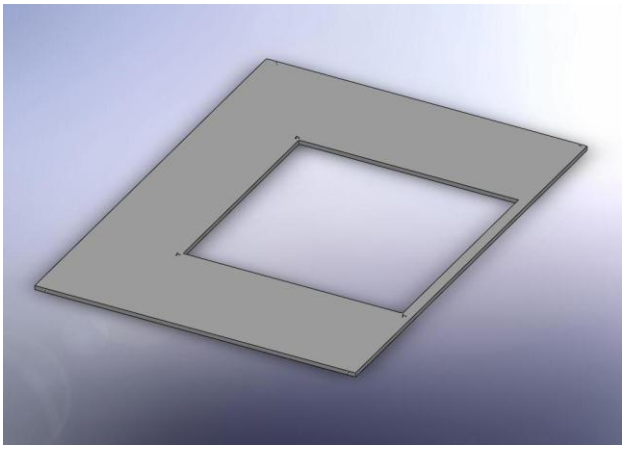

Figure 2.9: PVC plate used to support GEM detectors and their readouts. The support plates have dimensions of ¼ in × 19 in × 26 in. PVC is cut out of the support plate where detectors will be located so that the plate itself does not interfere with a muon's trajectory. The cut-outs are 13 in × 13 in.

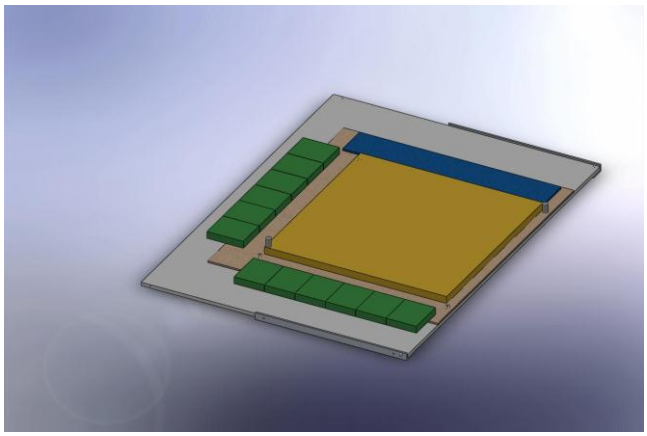

Figure 2.10: Simulated view of a detector assembly mounted to its support plate using SolidWorks. Elements of the detector assembly shown are APV chip hybrid cards (green), the section where high voltage is applied (blue), the readout (brown), the GEM detector (gold), and cylinders representing sites for gas inlet and outlet.

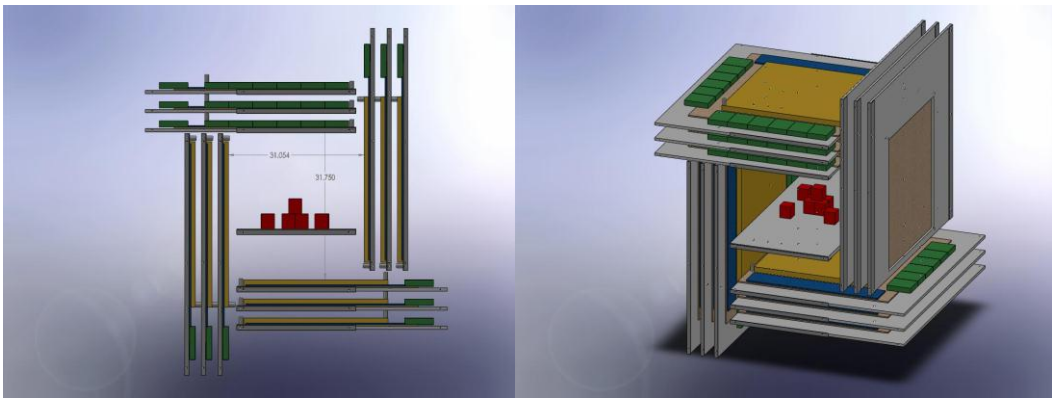

Figure 2.11: Geometry of overlapping detector support plates in such a way as to allow the active areas of each GEM detector to define a closed volume. A simulated target plate with material to be imaged is also shown. The defined imaging volume is about 31 cm^3, or about a cubic foot, and the closest detectors can be brought together is about 1.5 in due to physical limitations.

Once it was determined what the geometry of the support plates must be to maximize coverage, I tried to imagine an imaging station, or framework, built around that geometry. I wanted the design to be a clean and efficient solution to mounting the support plates in their required geometry fixed in space. I had to meet the following specific design requirements, but was given flexibility in how I did so: the detector geometry shown in figure 2.11 had to be accommodated, I had to allow for variable, discrete spacing of detectors in multiples of ¼ inch, PVC support plates had to account for the space required by various hardware components needed to support each detector (fig. 2.9-10), and the station had to be portable (able to be broken down). After working out the problem on paper, I used SolidWorks to test my solution. My prototype II design consisted of extruded angles and T-bars made of 6061-T6 aluminum alloy welded together to make four quadrants (fig. 2.12-2.15). The four quadrants of the framework were bound together by smaller extruded angles screwed into it used to support top and bottom detector stacks, as well as support brackets connected to them using nuts and bolts

for maximum stability. The extruded angles and T-bars used to make each quadrant of the imaging station had holes drilled in them spaced a quarter of an inch apart so that detectors in each stack could be arranged at various separation distances, meeting that design requirement. Following are selected images of the MTS prototype II I designed (fig. 2.16-2.20) and of some of its components. The simulated images were made using SolidWorks. Complete drawings of all the components used to construct both prototypes in PDF and SolidWorks files are available on the FIT T3 Open Science Grid cluster under the account "g4hep": g4hep@uscms1.fltech-grid3.fit.edu; file path geant4/examples/mytestapps/lenny/ MTS Prototypes.

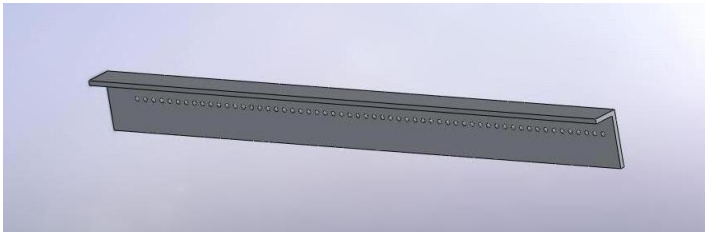

Figure 2.12: An extruded angle used to construct quadrant one of the prototype II imaging station. The L shape is 1.5 in × 0.75 in and is 0.125 in thick, and the angle itself is 15.5 in long. The holes are 0.113 inches in diameter, are 0.25 in apart, and are used to fixate the PVC detector support plates. Another extruded angle is used in quadrant one that is 26.5 in long.

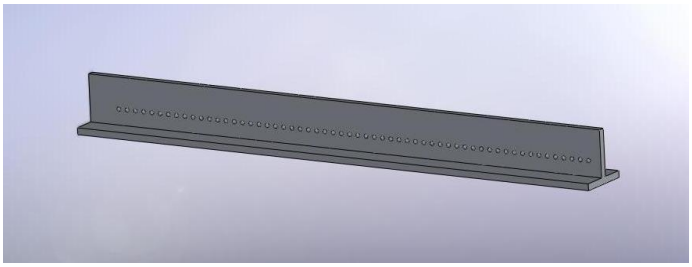

Figure 2.13: A T-bar used to construct quadrant one of the prototype II imaging station. The T shape is 1.5 in × 1.5 in and is 0.188 in thick, and the bar itself is 15.5 inches long. The holes are 0.113 inches in diameter, are 0.25 in apart, and are used to fixate the PVC detector support plates.

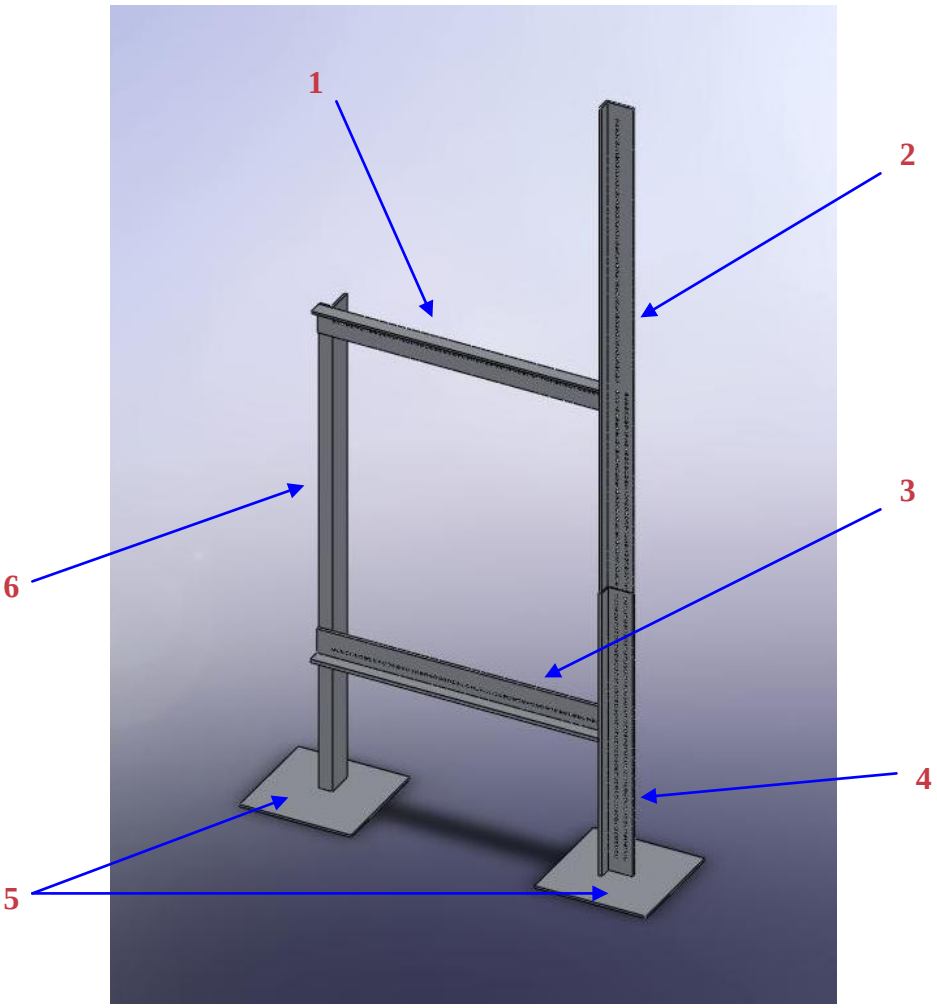

Figure 2.14: Quadrant one of our MTS prototype II imaging station. Elements one and two are referenced in figure 2.12, and elements three and four are like that shown in figure 2.13. Element five is simply an aluminum base plate used for support, and element six is an extruded angle with no holes also used to support the framework. Note that the vertical extruded angle and T-bar have twin sets of holes. One set is used to screw into extruded angles that support detector assemblies in top and bottom detector stacks, and the other set is used to fixate the PVC in those stacks. The sets of twin holes have the same dimensions as those mentioned in the two previous figures and are separated by half an inch. All elements shown are welded together to form a solid and stable assembly.

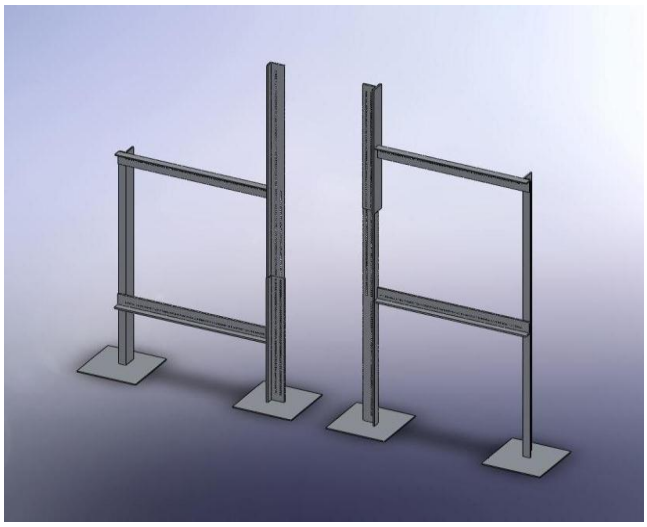

Figure 2.15: Quadrants one and two of our MTS prototype II imaging station. Quadrant two is composed of the same fundamental elements as quadrant one, and they are arranged to accommodate the geometry shown in figure 2.11. In a similar fashion, quadrants three and four are constructed.

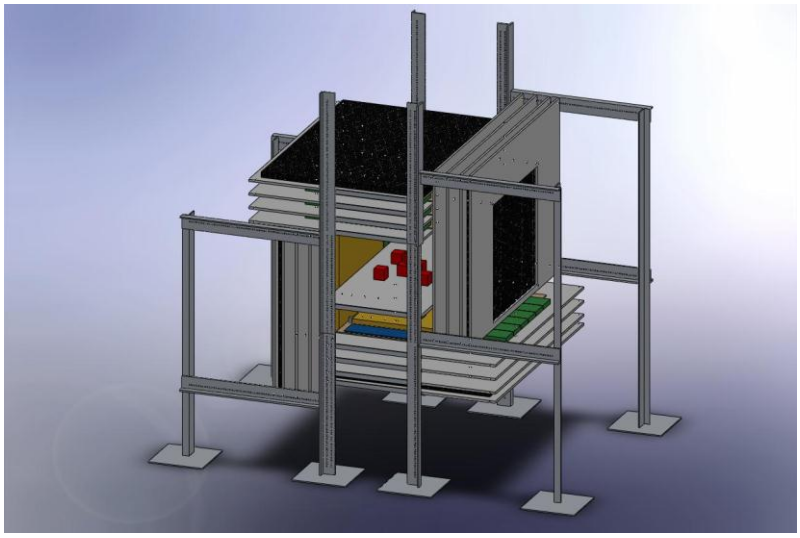

Figure 2.16: Simulated MTS prototype II imaging station complete with all four quadrants, four detector stacks, and target plate with material to be imaged. The black elements represent scintillators used to trigger on trackable muon trajectories, and each detector stack has one. The completed station is approximately 47 inches long by 29 inches wide by 42 inches high.

Figure 2.17: Assembled MTS prototype II in Florida Tech's machine shop shortly after its construction was completed in June 2010. The station is loaded with PVC support plates that will be used to secure GEM detectors and scintillators, along with their supporting electronics.

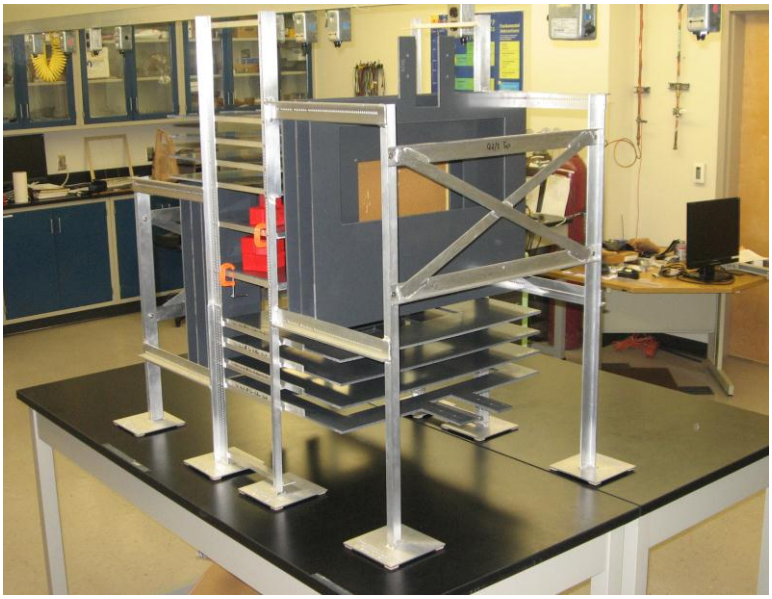

Figure 2.18: Assembled MTS prototype II in Florida Tech's High Energy Physics Lab A. Along with PVC support plates, the station is also loaded with target plates secured by C-clamps and mock material to be imaged.

Figure 2.19: Partially loaded MTS prototype II at CERN. Top and bottom detector stacks are fully loaded, but side detectors have not been mounted yet. A target plate with material to be imaged is also missing.

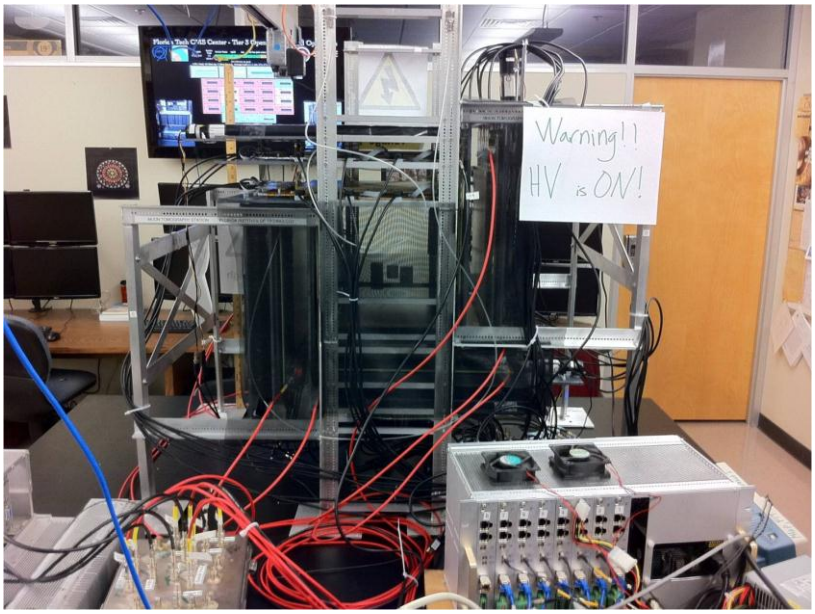

Figure 2.20: Fully loaded MTS prototype II in Florida Tech's High Energy Physics Lab A. Detector stacks are mounted on all four sides, and one can see the material being imaged in the center of the imaging volume.

Chapter 3 MTS Prototype II Simulated Scenarios

3.1 Photon Attenuation Calculation

The primary materials used for nuclear fission weapons are U-235 and Pu-239 [25]. In the simulations that follow in the next section, I chose to test the effectiveness of our imaging station to detect U-235 encased in lead shielding. Current detection systems are designed to detect high energy photons emitted from nuclear contraband. The most probable gamma emitted by U-235 has an energy of 186 keV, and over 92% of all gammas emitted have an energy equal to or less than this value [26]. By looking at the photon mass attenuation length for lead given a photon energy of 186 keV, one can calculate the thickness that a box made of lead would need to have in order to shield 99.9% of all photons with that energy.

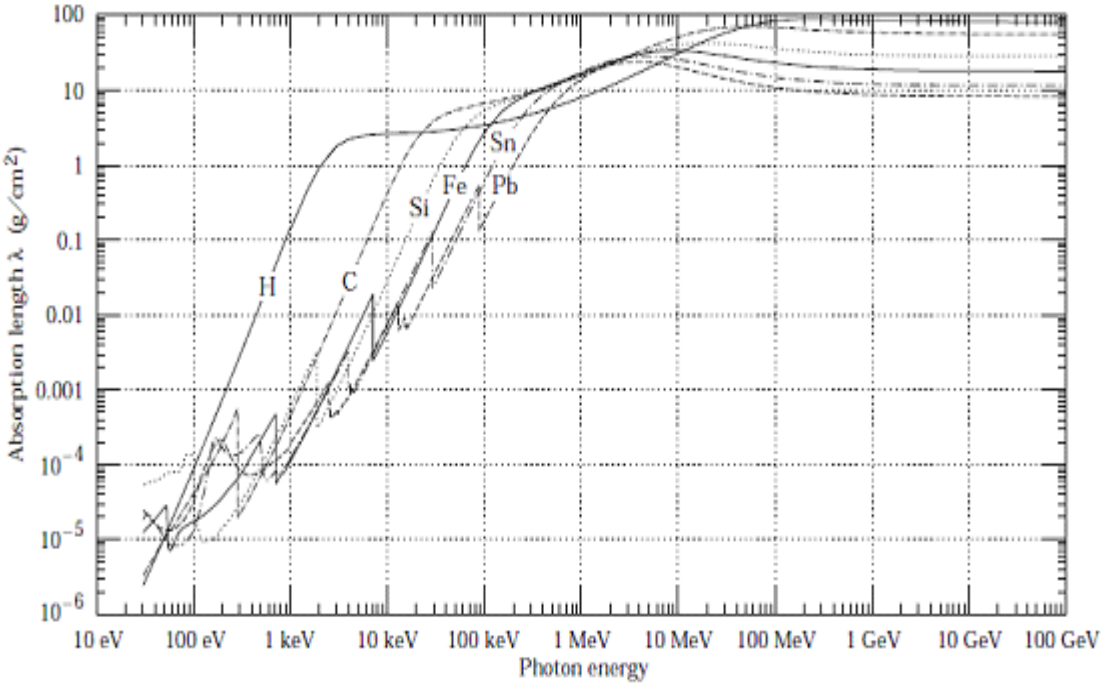

Figure 3.1: The photon mass attenuation length is given for various elements as a function of photon energy [27].

The formula used for such a calculation is as follows:

$$I(x) = I_o e^{\frac{-\rho x}{\lambda}} \qquad [27]$$

where: I(x) is the intensity of the photon remaining after traveling a distance x in cm through the material;

I_o is the initial intensity of the photon;

ρ is the density of the material traversed in g/cm^3;

λ is the photon mass attenuation length, or mean free path, given the material traversed and energy of the photon in g/cm^2.

The density of lead is $\rho = 11.34\ g/cm^3$, and the photon mass attenuation length for a gamma of energy 186 keV traveling through lead is $\lambda = 0.8\ g/cm^2$ (fig. 3.1) [27]. Therefore, to calculate the thickness of lead needed to absorb 99.9% of all gammas with energy 186 keV we have:

$$I(x) = I_o e^{\frac{-\rho x}{\lambda}} \quad \Rightarrow \quad 0.001\, I_o = I_o e^{\frac{-11.34x}{0.8}} \quad \Rightarrow \quad \ln(0.001) = \frac{-11.34x}{0.8}$$

$$\Rightarrow \quad x = \frac{0.8 \ln(0.001)}{-11.34} = 0.487\ cm = 4.87\ mm$$

Therefore, a lead box of thickness 5 mm would be capable of shielding over 99.9% of over 92% of all gammas emitted from U-235. Such a shield would probably be effective at smuggling U-235 given current detection systems. The following section will show that such a shield would not only be ineffective given a muon tomography based detection system, but could in fact make the U-235 stand out even more.

3.2 Analysis of Simulated Scenarios

The scenarios presented in this section were designed to specifically test our Muon Tomography Station Prototype II's ability to detect shielded nuclear contraband. U-235 is chosen for the simulations because it is capable of being used for nuclear fission weapons. The shielding chosen is a lead box of thickness 5 mm completely encasing the uranium and capable of absorbing 99.9% of the most probable gammas emitted from the uranium. The imaging volume of our station in our simulations is 300 mm × 280 mm × 280 mm in the x, y, and z dimensions respectively. The length in the y and z directions is slightly less because detectors occupy that space. The dimensions of the lead boxes used in the simulations are 50 mm × 130 mm × 270 mm or 50 mm × 130 mm × 290 mm, depending on the plane they lie in, and the volume that the uranium occupies within each box is 20 mm × 100 mm × 240 mm or 20 mm × 100 mm × 260 mm, depending on the size of the box it's in. The uranium was designed to spell out the letters "F", "I", and "T", and each letter has a thickness of 20 mm. Pairs of lead boxes are placed in the same plane, as to cover the area of the imaging volume in that plane, and each pair of boxes is 10 mm apart while being spaced 5 mm from the boundary of the imaging volume. Different simulations have the pairs of boxes moving through the imaging volume perpendicular to a coordinate axis. Boxes are initially placed at one boundary of the imaging volume perpendicular to a coordinate axis, then moved to the center of the imaging volume, and then placed at the other boundary of the imaging volume perpendicular to the same axis. I therefore created nine geometries to run simulations on and to analyze, three geometries per coordinate axis, and I chose those geometries because they simulate imaging capability at the boundaries of the imaging volume and at the central region of the imaging volume, where one might expect imaging capability to be most vulnerable and strongest, respectively.

GEANT4 (GEometry ANd Tracking) is a C++ toolkit designed to run particle physics simulations, and the code for the simulations I ran had already been written by other members of my research group [28]. Using my group's code to run the simulations I designed required me to learn how to modify the configuration file responsible for generating the specific material used in each simulation, as well as their geometry. Within the configuration file used for each simulation I also established a 9 m^2 CRY (Cosmic RaY) plane centered above the imaging volume [29], [30]. A CRY plane is a surface from which GEANT4 generates particles, cosmic ray muons in our case. Each cosmic ray muon generated is called an event, and the number of events run, or cosmic ray muons generated, can also be set in the configuration file. Therefore, the simulations are run in event space, and it is important to know how many events correspond to the passage of time in the real world. One important factor to consider in our imaging station is how well it can image material in a given time interval. Transforming from the number of events run in event space to the passage of time in the real world is easily done given the cosmic muon flux at sea level, which is $1x10^4$ events per square meter per minute. The following equation can then be used to determine how many events, or muons generated, correspond to the passage of a specified amount of time.

$$\frac{1x10^4 \text{ events}}{\text{min} \cdot \text{m}^2} \bullet \frac{(\text{time})\,\text{min} \cdot (\text{area})\,\text{m}^2}{1} = \text{number of events}$$

For my simulations, I chose to produce plots for exposure times of 1 minute, 4 minutes, 10 minutes, 60 minutes, and 600 minutes. The number of events that corresponds to the above exposure times is calculated below.

$$\frac{1x10^4 \text{ events}}{\text{min} \cdot \text{m}^2} \bullet \frac{1\,\text{min} \cdot 9\,\text{m}^2}{1} = 90{,}000 \text{ events}$$

$$\frac{1\text{x}10^{4}\ \text{events}}{\text{min}\cdot\text{m}^{2}} \bullet \frac{4\ \text{min}\cdot 9\ \text{m}^{2}}{1} = 360{,}000\ \text{events}$$

$$\frac{1\text{x}10^{4}\ \text{events}}{\text{min}\cdot\text{m}^{2}} \bullet \frac{10\ \text{min}\cdot 9\ \text{m}^{2}}{1} = 900{,}000\ \text{events}$$

$$\frac{1\text{x}10^{4}\ \text{events}}{\text{min}\cdot\text{m}^{2}} \bullet \frac{60\ \text{min}\cdot 9\ \text{m}^{2}}{1} = 5{,}400{,}000\ \text{events}$$

$$\frac{1\text{x}10^{4}\ \text{events}}{\text{min}\cdot\text{m}^{2}} \bullet \frac{600\ \text{min}\cdot 9\ \text{m}^{2}}{1} = 54{,}000{,}000\ \text{events}$$

Each simulation was run with 54,000,000 events, corresponding to an elapsed time of 10 hours, and to help minimize the time required to run a simulation, 50 simulations were run in parallel, each with 1,080,000 events, and their results were concatenated into a single file compiling the results of 54,000,000 events. Running 50 simulations on 50 CPUs in our computing cluster simultaneously went much faster (about 50 times) than running a single simulation on a single CPU with 50 times the number of events. Furthermore, because of the random nature in which GEANT4 generates muons to correspond with reality, concatenating the results of 50 simulations with 1,080,000 events each is statistically equivalent to looking at the results of a single simulation producing 54,000,000 events. The concatenated file for each simulation contained four dimensional data for each trackable event. The data consisted of three spatial coordinates and a scattering angle, denoting the location within the imaging volume that a muon interacted with material and the angle at which it was scattered. Recall that in order for the event to be trackable, the muon has to cross a detector stack before and after interacting with material in the imaging volume. It turned out that for a 9 m^2 CRY plane centered above an imaging volume of approximately a cubic foot, 54,000,000 generated events would

translate to about 657,000 trackable events. That is around 657,000 of 54,000,000 generated events ended up passing through the imaging volume, interacting with material, and passing through two detector stacks. The concatenated files for each of the nine scenarios simulated all contained very close to 657,000 data elements, the average being 657,348. This meant that for a concatenated data file, 657,348 elements would correspond to 10 hours of elapsed time in the real world, and proportionalities could be used given the number of events calculated previously to calculate how many data elements would correspond to the other times. For example, if 90,000 of 54,000,000 events correspond to 1 minute of elapsed time, then 1,096 of 657,348 concatenated data elements would also correspond to 1 minute of elapsed time, etc.

This is important to know because the concatenated data file for each simulation is called by the ROOT configuration file to perform analysis on the results of each simulation [31]. ROOT (Rapid Object-Oriented Technology) is a C++ data analysis framework used to perform analysis by the particle physics community, and the code to perform the analysis of our group's simulations had already been written by other members. However, I modified the code to allow for a variable number of data to be used from the concatenated data file, making it possible to view what different time exposures would look like without having to run more simulations. The desired number of data to be analyzed from the concatenated data file is entered in the ROOT configuration file, along with a range of scattering angles to govern each plot generated. In addition to the lead and uranium included in each scenario, the imaging volume was filled with air, and scattering angles below 3 degrees were not shown, while scattering angles above 8 degrees were shown as 8 degrees. This range was chosen to slightly improve the quality of images produced in the analysis. I used ROOT to analyze the output of my simulations run and to produce images of what our station should be able to produce for a given scenario. In the images of my analysis that follow, all data in

the perpendicular coordinate is collapsed into the plane shown, and degrees shown refer to the scattering angle of muons passing through material. Here images produced given an elapsed time of 10 hours are shown; images for elapsed times of 4 minutes, 10 minutes, and 60 minutes for each scenario are included in appendix E. The configuration files I created for each scenario are included in appendix C, and the code I modified to run my Root analysis is included in appendix D.

I used HepRApp to visualize the geometry of each scenario I created so that any errors could be quickly spotted and then corrected before running my simulations [32]. HepRApp, the original HepRep Data Browsing Application, is a Java application that was developed to let physicists visualize particles interacting with matter (HepRep is a generic interface definition for high energy physics event display representables).

In each simulation, the center of the imaging volume is defined to be at the origin of a Cartesian x-y-z coordinate system. Recall that detector stacks cover four sides of the six-sided volume. The x-axis passes through the open ends of the imaging volume, while the y-axis is perpendicular to two detector stacks, and the z-axis is perpendicular to two detector stacks. The x and y axes are in the horizontal plane (parallel to the surface of the Earth), which makes z the vertical axis. Note that in each simulation there are three detectors in top and bottom detector stacks, and there are two detectors in both side stacks (fig. 3.2). Also note that the simulated resolution in each GEM detector is perfect.

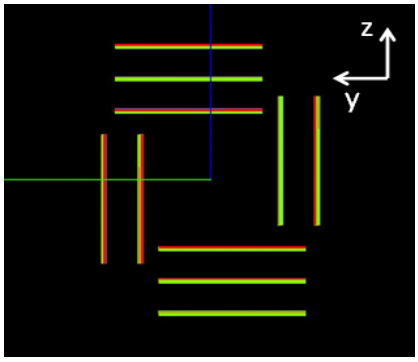

Figure 3.2: Detector geometry and coordinate axes used in each simulation [33].

Each scenario is defined by the plane that the lead boxes with uranium lie in and the value of the third coordinate that corresponds to the location of the geometric center of the boxes. For example, the first series of plots I will present are for my xy scenarios. The first plot described as scenario xy, z = -110 means that the lead boxes are lying in a plane parallel to the plane defined by the x and y axes, and the geometric center of the boxes has its z-coordinate located at -110 mm. All scenarios have uranium letters with vertical elements of width 30 mm. Horizontal elements in the letters "F" and "T" have a width of 20 mm. Recall there is a 10 mm gap between the uranium elements and the lead boxes encasing them, and there is a 10 mm gap between the lead boxes themselves, which are 5 mm thick. Also recall that a Point Of Closest Approach (POCA) reconstruction method is used by our group's code to locate where a muon interacted with matter and to assign a color to that location which depends on the scattering angle. The configuration files for each scenario, as well as the data produced for each scenario, are available on the FIT T3 Open Science Grid cluster under the account "g4hep": g4hep@uscms1.fltech-grid3.fit.edu; file path geant4/examples/mytestapps/lenny.

Following are the geometry and plots for my xy scenarios (fig. 3.3-10). The lead box with uranium in the positive y region has a gap of 30 mm between the letters F-I and I-T at closest distance, and the lead box with uranium in the negative y region has a gap of 20 mm between the letters F-I and I-T at closest distance.

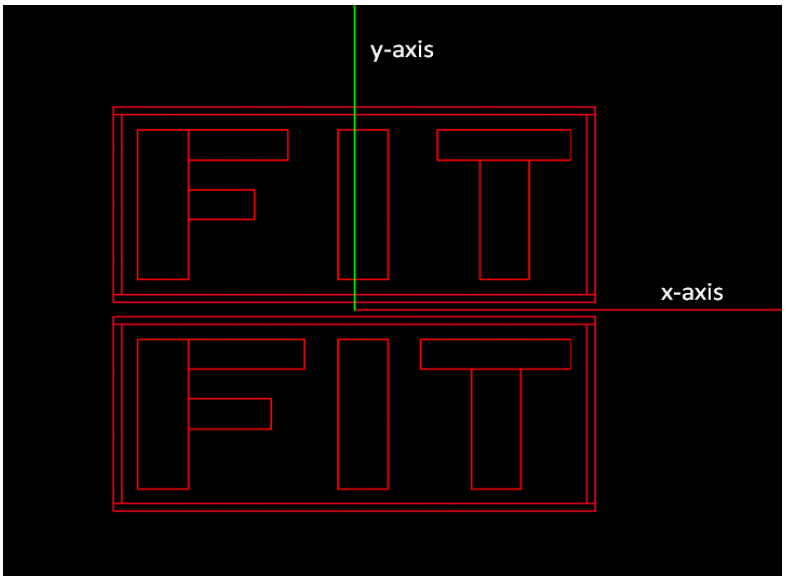

Figure 3.3: Geometry of shielded scenarios xy: z = -110 mm, z = 0 mm, and z = 110 mm viewed in the xy plane. The positive z axis points out of the screen.

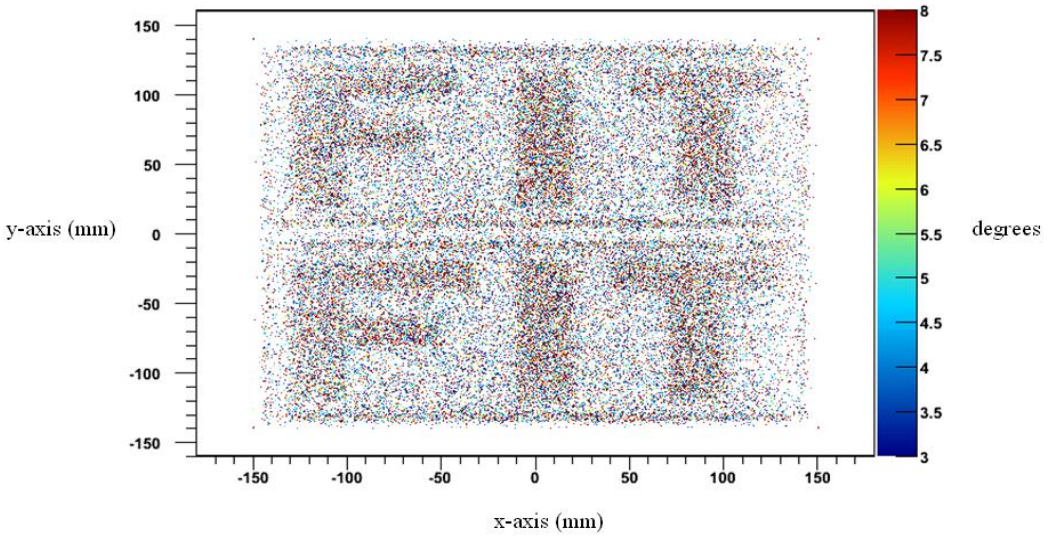

Figure 3.4: Locations of reconstructed scattering points and angles for simulated shielded scenario xy, z = -110 mm, using POCA reconstruction with 600 minutes exposure time viewed in the xy plane. The positive z axis points out of the screen.

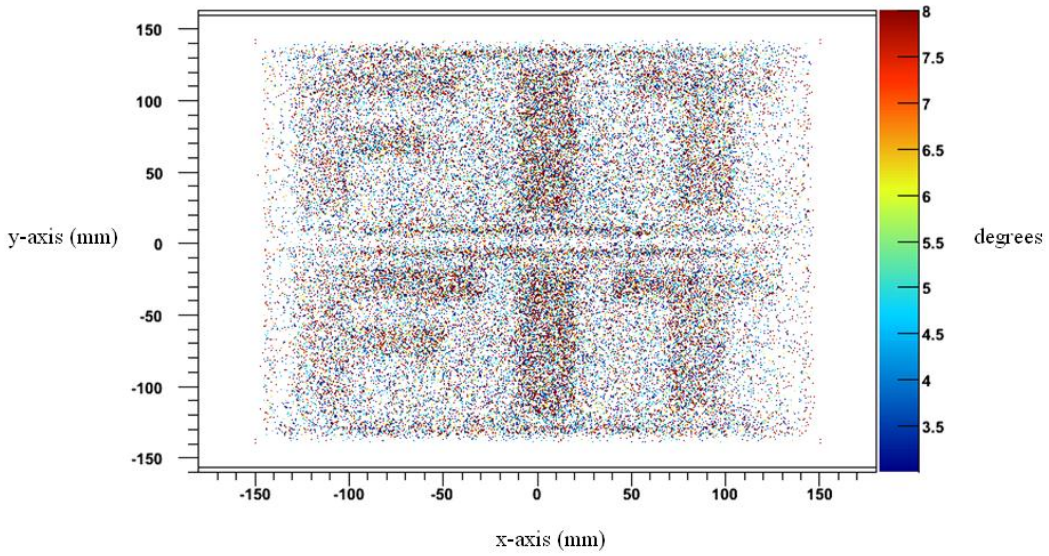

Figure 3.5: Locations of reconstructed scattering points and angles for simulated shielded scenario xy, z = 0 mm, using POCA reconstruction with 600 minutes exposure time viewed in the xy plane. The positive z axis points out of the screen.

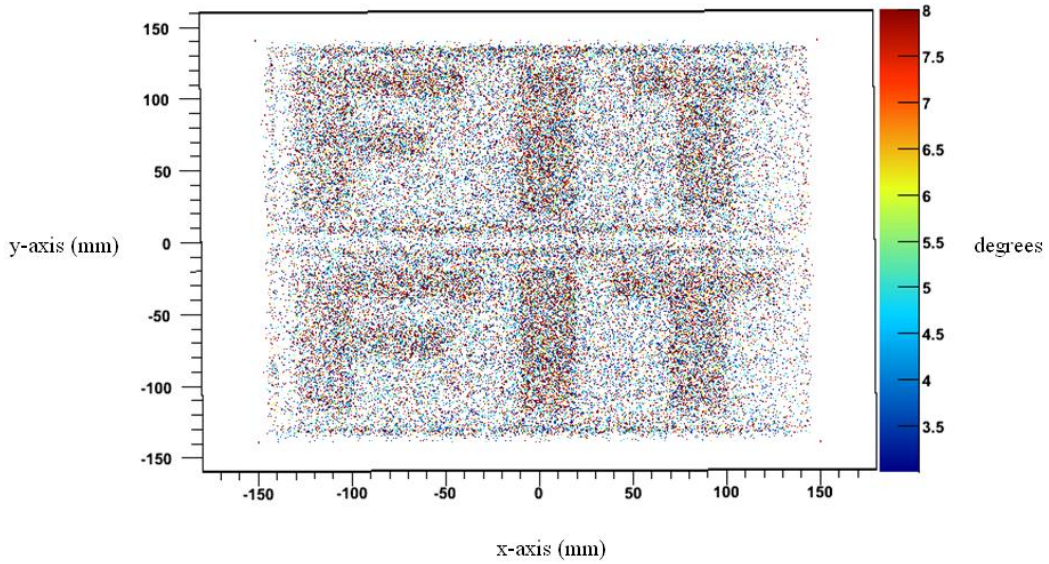

Figure 3.6: Locations of reconstructed scattering points and angles for simulated shielded scenario xy, z = 110 mm, using POCA reconstruction with 600 minutes exposure time viewed in the xy plane. The positive z axis points out of the screen.

Images of the objects at both extremes of the volume perpendicular to the z-axis look very similar, and are much better than those at the boundaries perpendicular to the x or y axes. Uranium shows up very well at the boundaries here, with much better resolution than in the previous two scenarios. The resolution in the x dimension and in the y dimension has been good in the former scenarios, but this is the first time that those dimensions are viewed together, and the combined result is great. These boundaries also have detectors flush up against them, which definitely enhances imaging quality at those locations. Images at the boundaries are actually better than in the center of the volume (z = 0 mm). In the center of the volume, the image starts to fade at both extremes of the x-axis, probably because there are no detectors in yz plane there. In spite of the fading, the edges of the lead boxes can still be seen in those regions and their thickness measured close the actual value of 5 mm. In fact, the thickness of all edges of the lead boxes can be measured close to 5 mm in both dimensions. The 10 mm gap between the lead boxes can be discerned, as well as the 10 mm gap between the uranium and the boxes encasing them. The 30 mm gap between letters F-I and I-T at closest distance can be measured in the positive y region, and the 20 mm gap between letters F-I and I-T at closest distance can be measured in the negative y region. The width of the vertical elements of the uranium letters can be measured close to 30 mm, and the width of the horizontal elements of the uranium letters can be measured close to the actual value of 20 mm. The resolution in both the x and y dimensions from this perspective appears to be close to 5 mm.

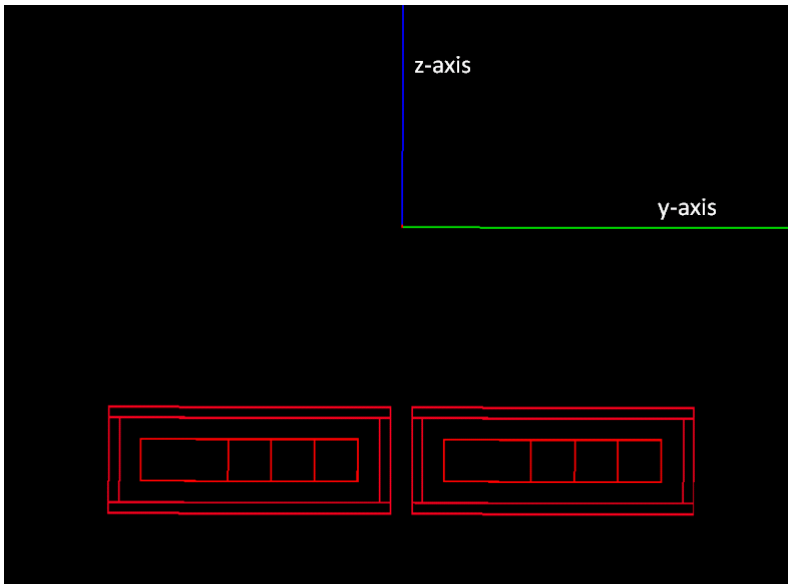

Figure 3.7: Geometry of shielded scenario xy, z = -110 mm, viewed in the yz plane. The positive x axis points out of the screen. The geometry of the other xy scenarios are from this perspective as well, but the boxes are centered at z = 0 mm and z = 110 mm.

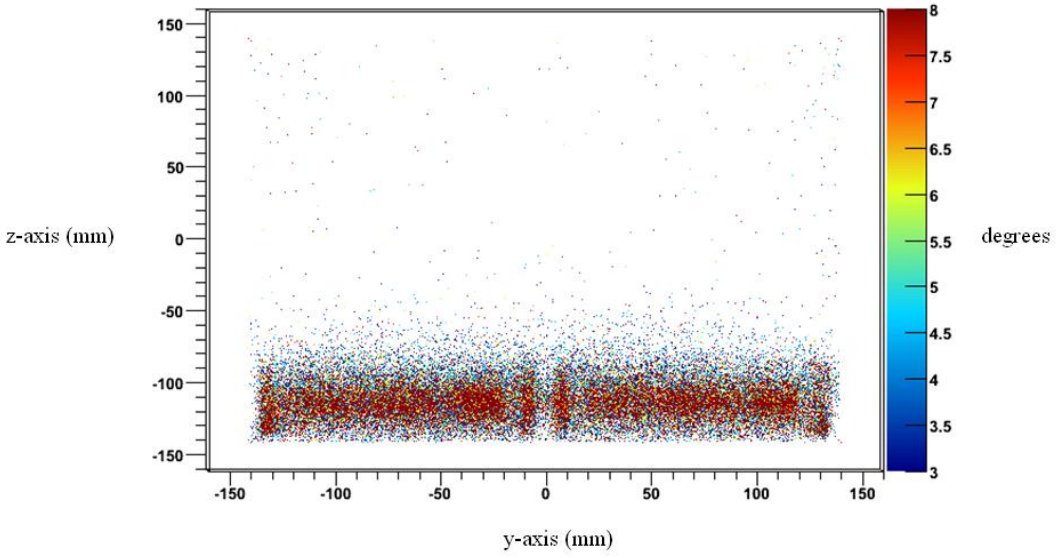

Figure 3.8: Locations of reconstructed scattering points and angles for simulated shielded scenario xy, z = -110 mm, using POCA reconstruction with 600 minutes exposure time viewed in the yz plane. The positive x axis points out of the screen.

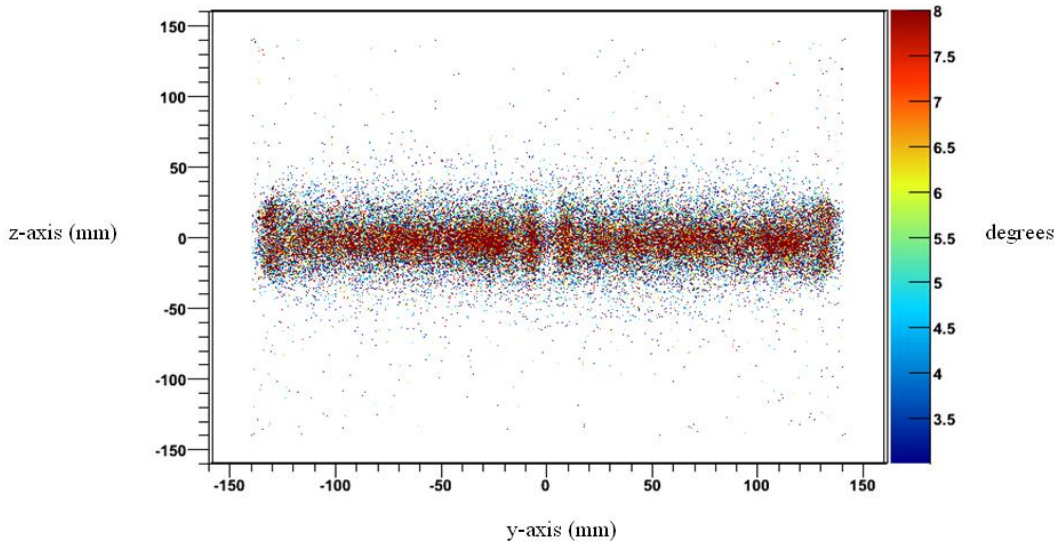

Figure 3.9: Locations of reconstructed scattering points and angles for simulated shielded scenario xy, z = 0 mm, using POCA reconstruction with 600 minutes exposure time viewed in the yz plane. The positive x axis points out of the screen.

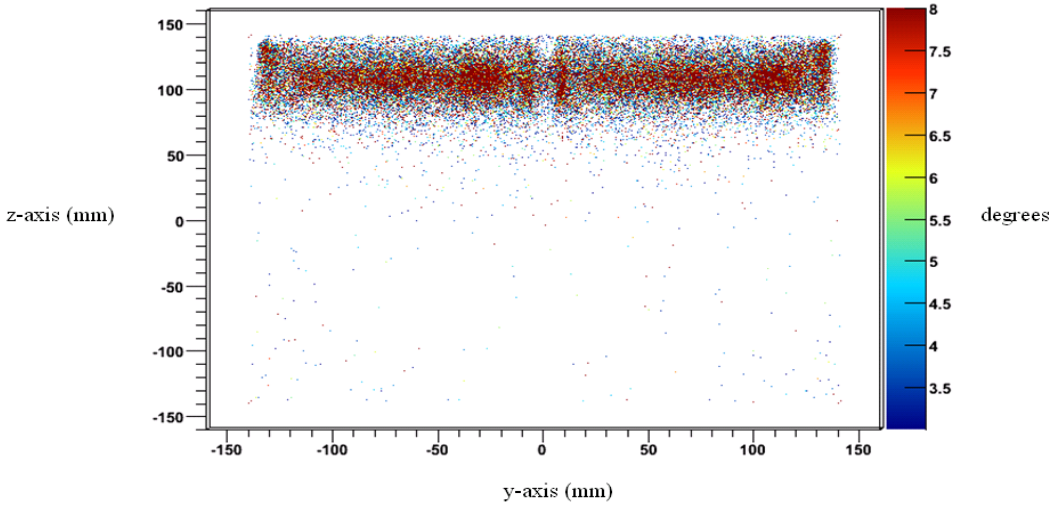

Figure 3.10: Locations of reconstructed scattering points and angles for simulated shielded scenario xy, z = 110 mm, using POCA reconstruction with 600 minutes exposure time viewed in the yz plane. The positive x axis points out of the screen.

All images of the objects (at both extremes of the volume along the z-axis and at the center of the volume) look very similar to one another from this perspective. Shielded uranium is detectable throughout the volume. These images seem hotter than the previous set of results from the same set of scenarios because high-Z material is spread throughout 290 mm in the x direction. From the previous perspective, high-Z material was only spread throughout 50 mm in the z direction. In the y dimension, the thickness of the lead boxes appears to be closer to 10 mm than the actual 5 mm, and the gap between the lead boxes and the uranium can be made out. The length of the uranium letters can be made out close to the actual value of 100 mm, and the length of each lead box can be made out close to the actual value of 130 mm. In the z dimension, the thickness of the lead boxes cannot be made out, and the 10 mm gap between the uranium and the boxes cannot be discerned here. The height of the uranium letters appears to be closer to 30 mm than the actual value of 20 mm, and the height of the lead boxes appears to be closer to 60 mm than the actual value of 50 mm.

Following are the geometry and plots for my yz scenarios (fig. 3.11-18). The lead box with uranium in the positive z region has a gap of 20 mm between the letters F-I and I-T at closest distance, and the lead box with uranium in the negative z region has a gap of 20 mm between the letters F-I and I-T at closest distance.

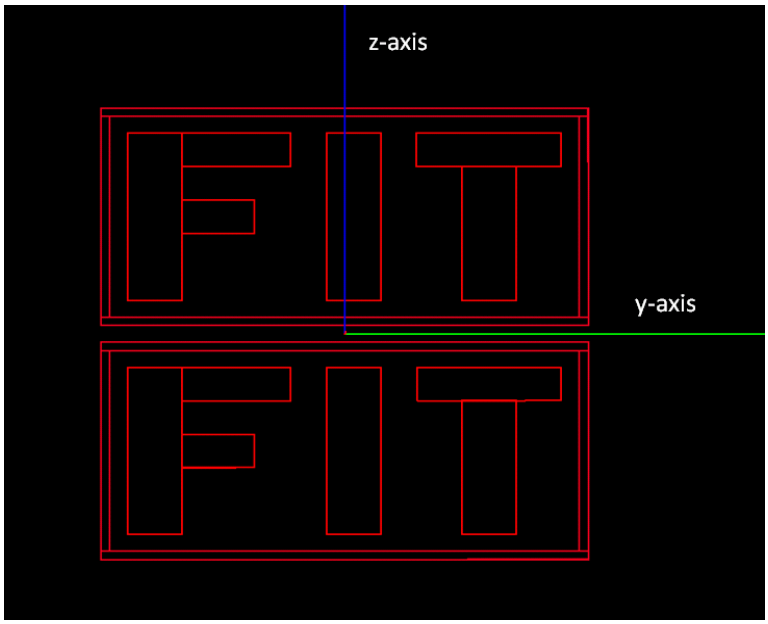

Figure 3.11: Geometry of shielded scenarios yz: x = -110 mm, x = 0 mm, and x = 110 mm viewed in the yz plane. The positive x axis points out of the screen.

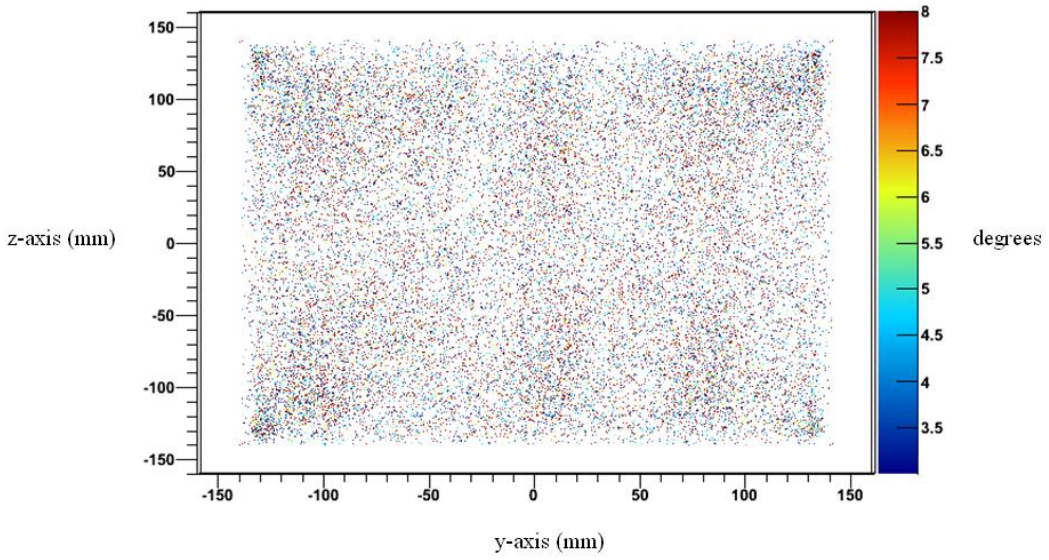

Figure 3.12: Locations of reconstructed scattering points and angles for simulated shielded scenario yz, x = -110 mm, using POCA reconstruction with 600 minutes exposure time viewed in the yz plane. The positive x axis points out of the screen.

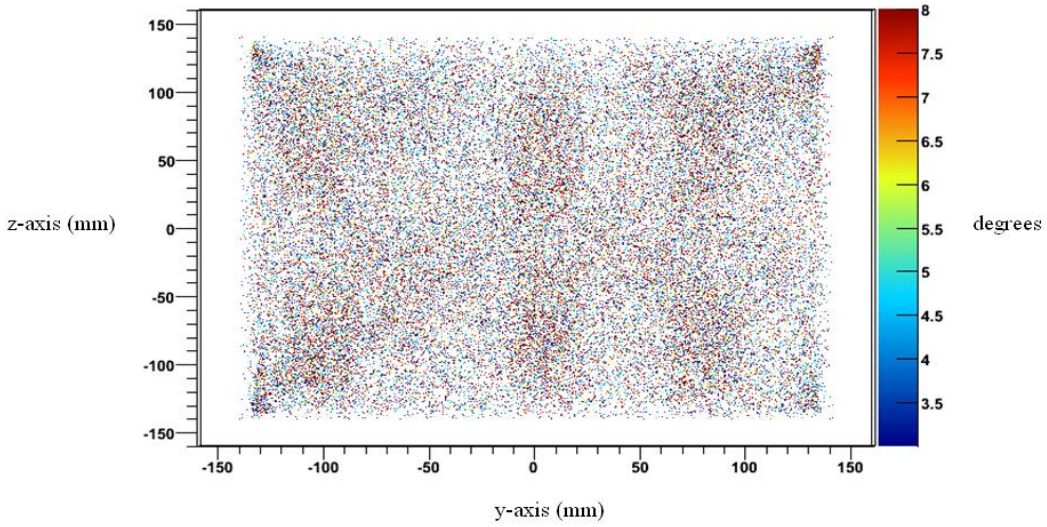

Figure 3.13: Locations of reconstructed scattering points and angles for simulated shielded scenario yz, x = 0 mm, using POCA reconstruction with 600 minutes exposure time viewed in the yz plane. The positive x axis points out of the screen.

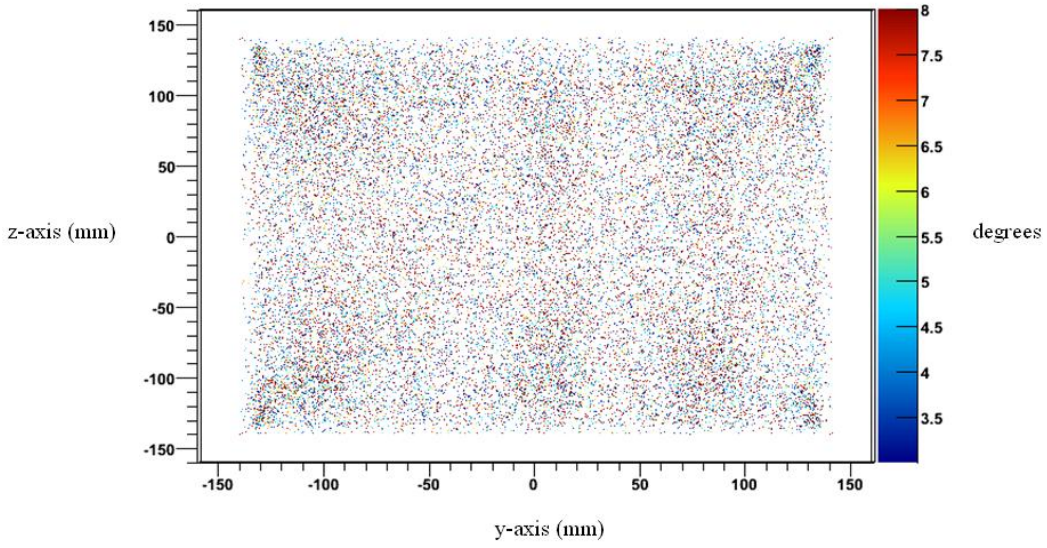

Figure 3.14: Locations of reconstructed scattering points and angles for simulated shielded scenario yz, x = 110 mm, using POCA reconstruction with 600 minutes exposure time viewed in the yz plane. The positive x axis points out of the screen.

In viewing the yz scenarios from the yz plane, images of the objects at both extremes of the volume along the x-axis look very similar, and less measurable scattering occurs at the boundaries than at the center of the volume as one would expect. Uranium is still detectable at the boundaries. At the boundaries, measurable scattering is greatest along the top and bottom sides of each end, probably due to the proximity of these locations to top and bottom detector stacks, respectively. The lack of detectors at these boundaries is probably why the images there are not as clear as one might hope. At the center of the volume (x = 0 mm) where the image is the best, the width of the uranium letter "I" can be made out to be close to 30 mm in the y dimension. The gap between the lead boxes is not measurable, and the height of the uranium letters is difficult to make out but could be put in the neighborhood of 100 mm in the z dimension.

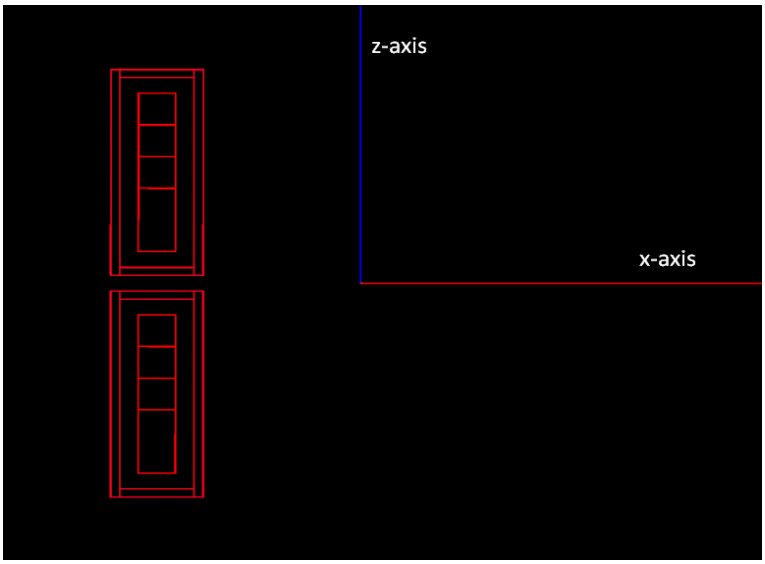

Figure 3.15: Geometry of shielded scenario yz, x = -110 mm, viewed in the xz plane. The negative y axis points out of the screen. The geometry of the other yz scenarios is from this perspective as well, but the boxes are centered at x = 0 mm and x = 110 mm.

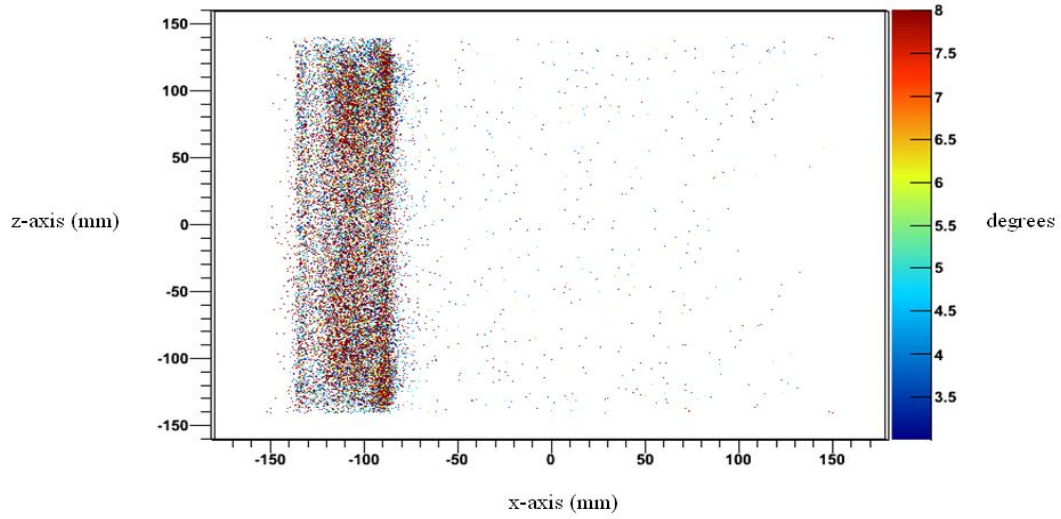

Figure 3.16: Locations of reconstructed scattering points and angles for simulated shielded scenario yz, x = -110 mm, using POCA reconstruction with 600 minutes exposure time viewed in the xz plane. The negative y axis points out of the screen.

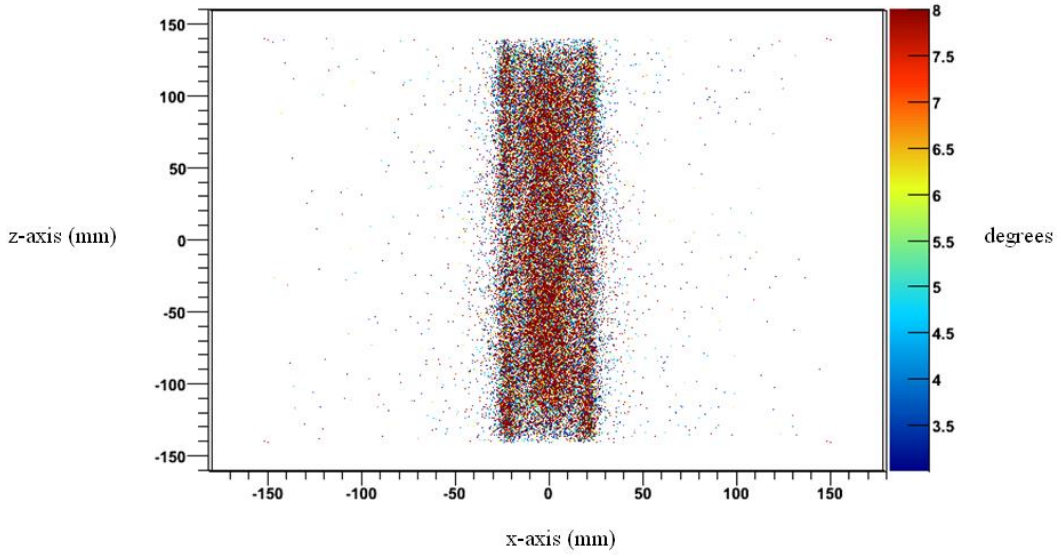

Figure 3.17: Locations of reconstructed scattering points and angles for simulated shielded scenario yz, x = 0 mm, using POCA reconstruction with 600 minutes exposure time viewed in the xz plane. The negative y axis points out of the screen.

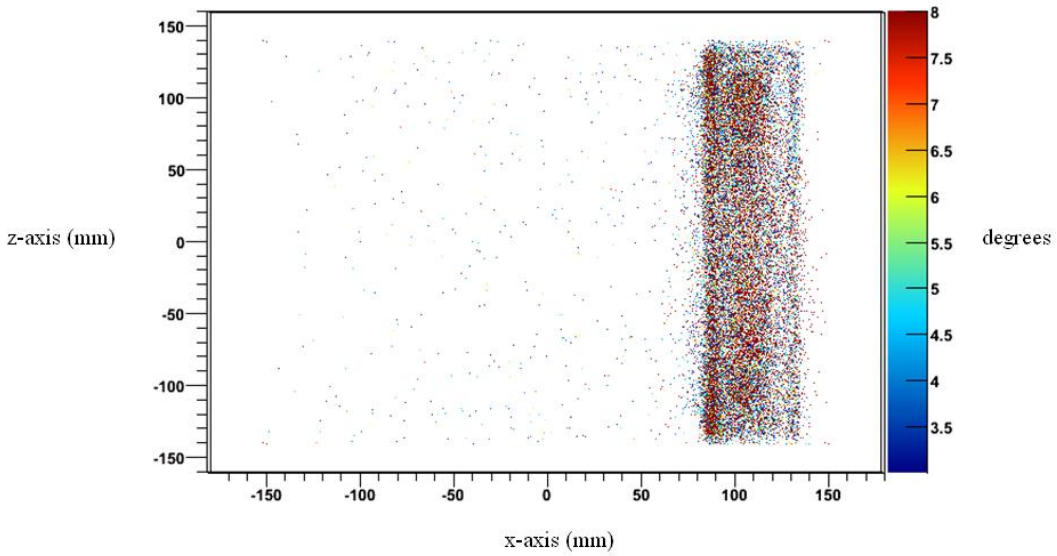

Figure 3.18: Locations of reconstructed scattering points and angles for simulated shielded scenario yz, x = 110 mm, using POCA reconstruction with 600 minutes exposure time viewed in the xz plane. The negative y axis points out of the screen.

In viewing the yz scenarios from the xz plane, the uranium looks very hot. Images of the objects at both extremes of the volume along the x axis look very similar and are basically mirror images of each other, as one would expect. High-Z material is detectable at the boundaries. These images stand out more than the previous set of results from the same set of scenarios because high-Z material is spread throughout 270 mm in the y direction. From the previous perspective, high-Z material was only spread throughout 50 mm in the x direction. In the x dimension, the thickness of the lead boxes appears to be closer to 10 mm than the actual 5 mm, and the gap between the lead boxes and the uranium can be made out. The thickness of the uranium letters appears to be close to the actual value of 20 mm, and the width of the lead boxes appears to be close to the actual value of 50 mm. In the z dimension, the thickness of the lead boxes cannot be made out, and the 10 mm gap between the two boxes cannot be discerned. However, the height of both boxes together, including the gap, can be put close to the actual value of 270 mm. The

combined height of the uranium in both boxes can also be put close to the actual value of 240 mm.

Following are the geometry and plots for my xz scenarios (fig. 3.19-26). The lead box with uranium in the positive z region has a gap of 30 mm between the letters F-I and I-T at closest distance, and the lead box with uranium in the negative z region has a gap of 20 mm between the letters F-I and I-T at closest distance.

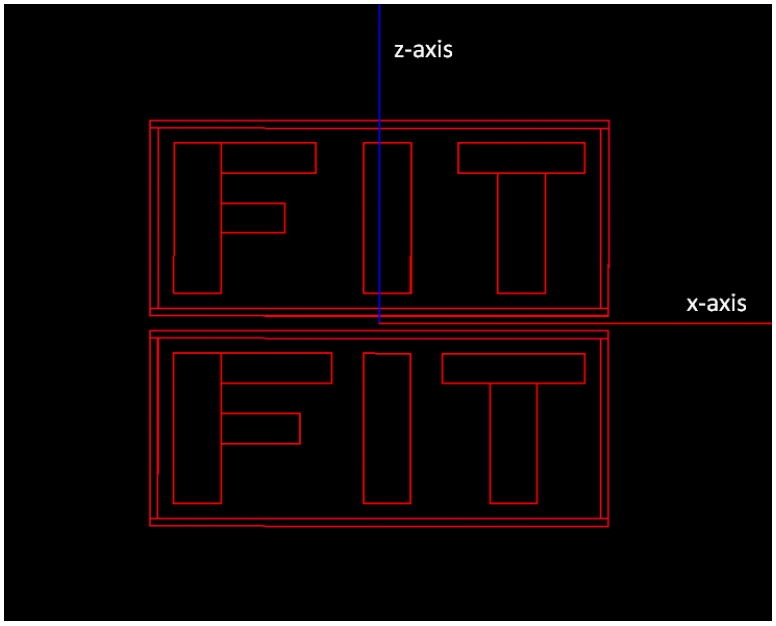

Figure 3.19: Geometry of shielded scenarios xz: y = -110 mm, y = 0 mm, and y = 110 mm viewed in the xz plane. The negative y axis points out of the screen.

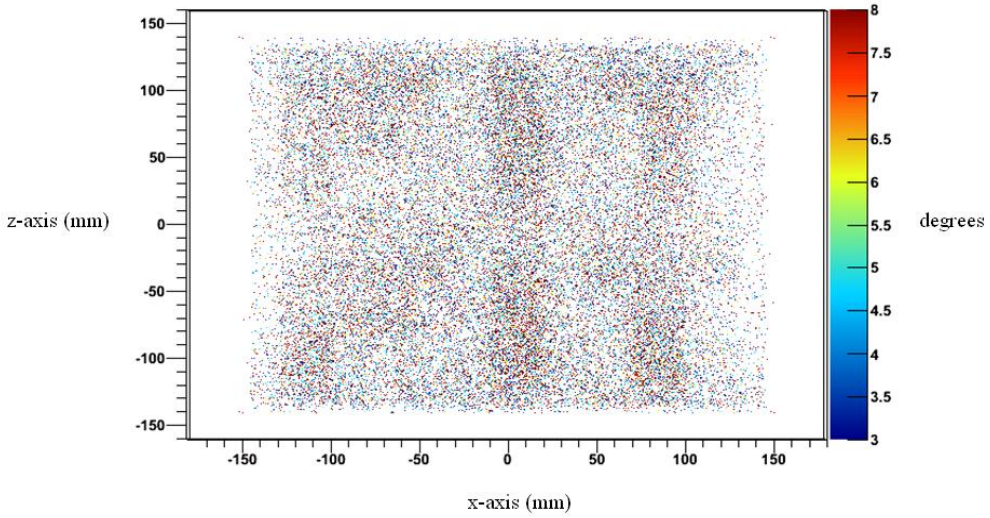

Figure 3.20: Locations of reconstructed scattering points and angles for simulated shielded scenario xz, y = -110 mm, using POCA reconstruction with 600 minutes exposure time viewed in the xz plane. The negative y axis points out of the screen.

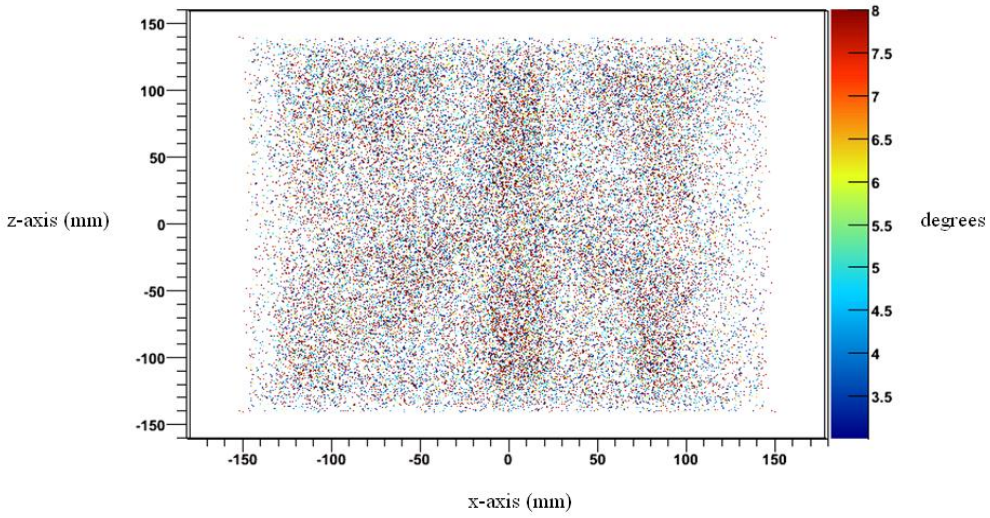

Figure 3.21: Locations of reconstructed scattering points and angles for simulated shielded scenario xz, y = 0 mm, using POCA reconstruction with 600 minutes exposure time viewed in the xz plane. The negative y axis points out of the screen.

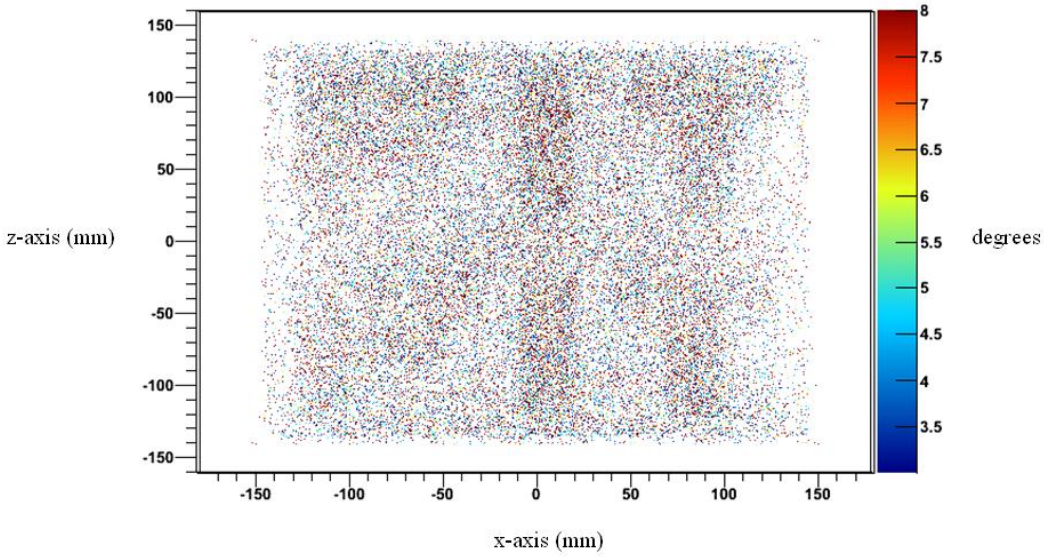

Figure 3.22: Locations of reconstructed scattering points and angles for simulated shielded scenario xz, y = 110 mm, using POCA reconstruction with 600 minutes exposure time viewed in the xz plane. The negative y axis points out of the screen.

In viewing the xz scenarios from the xz plane, images of the objects at both extremes of the volume along the y-axis look very similar, and are much better than those at the extremes perpendicular to the x-axis. The shielded uranium shows up well at the boundaries here. At the boundaries, measurable scattering is much better than in the previous scenario. These boundaries (perpendicular to the y-axis) have detectors flush up against them, which definitely enhances imaging quality at those locations by increasing the number of trackable muons there. The consistency of the images from this perspective is relatively uniform. The width of the uranium letters can be made out to be close to 30 mm in the x dimension. The 10 mm gap between the uranium and the lead boxes can almost be made out in the x dimension. In the z dimension, the 10 mm gap between the lead boxes is not measurable, and the height of the uranium letters is difficult to make out but could be put in the neighborhood of the actual 100 mm.

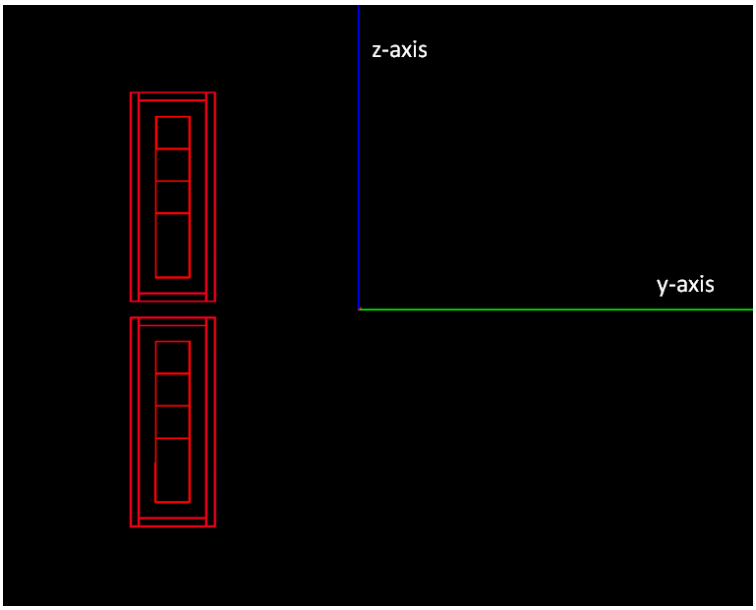

Figure 3.23: Geometry of shielded scenario xz, y = -110 mm, viewed in the yz plane. The positive x axis points out of the screen. The geometry of the other xz scenarios is from this perspective as well, but the boxes are centered at y = 0 mm and y = 110 mm.

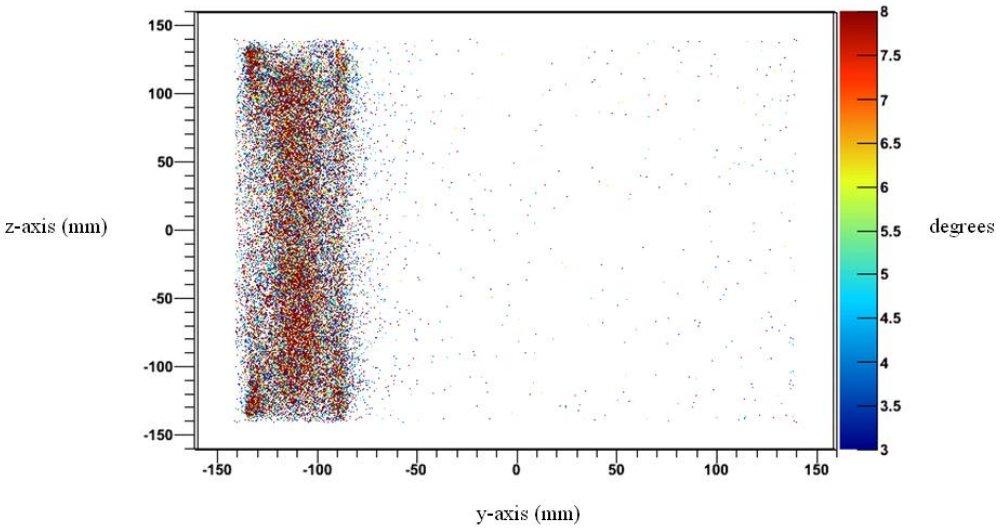

Figure 3.24: Locations of reconstructed scattering points and angles for simulated shielded scenario xz, y = -110 mm, using POCA reconstruction with 600 minutes exposure time viewed in the yz plane. The positive x axis points out of the screen.

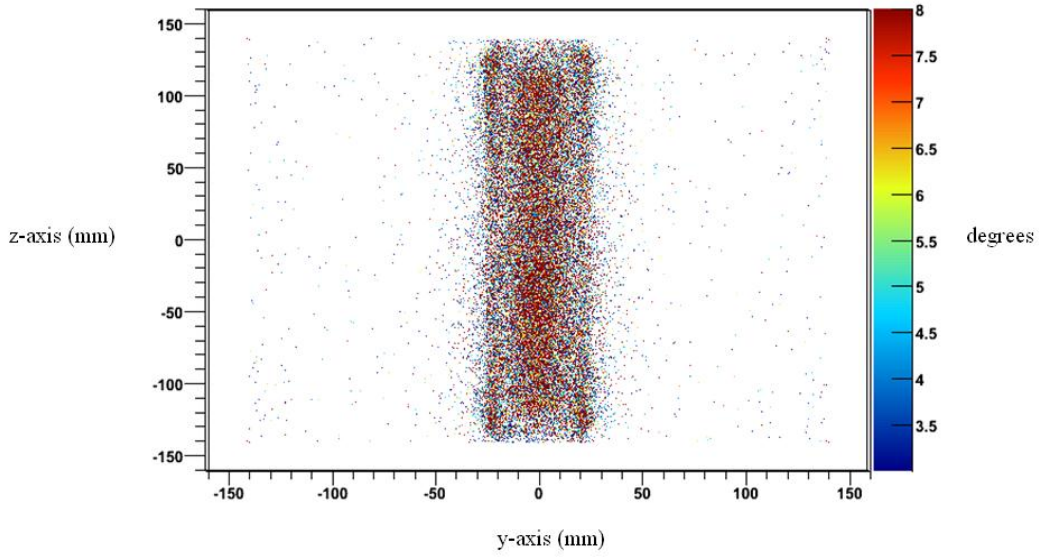

Figure 3.25: Locations of reconstructed scattering points and angles for simulated shielded scenario xz, y = 0 mm, using POCA reconstruction with 600 minutes exposure time viewed in the yz plane. The positive x axis points out of the screen.

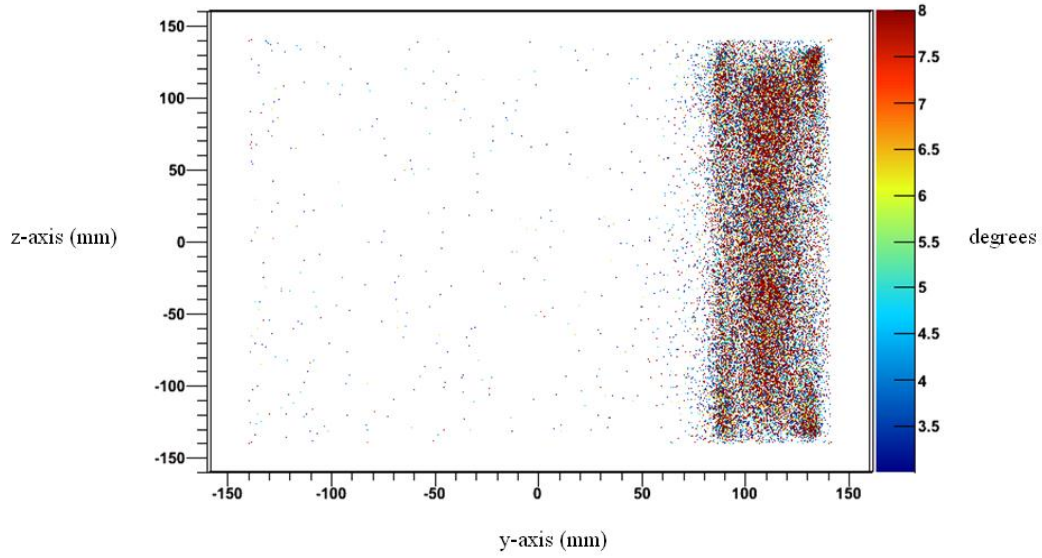

Figure 3.26: Locations of reconstructed scattering points and angles for simulated shielded scenario xz, y = 110 mm, using POCA reconstruction with 600 minutes exposure time viewed in the yz plane. The positive x axis points out of the screen.

In viewing the xz scenarios from the yz plane, images of the objects at both extremes of the volume along the y-axis look very similar to one another and are almost as clear as the image at y = 0 mm. Shielded high-Z material is hot and detectable at the boundaries. Even hotter spots are observed at the four corners of the boundaries, probably because detector stacks come very close to each other there. These images seem hotter than the previous results from the same set of scenarios because high-Z material is spread throughout 290 mm in the x direction. From the previous perspective, high-Z material was only spread throughout 50 mm in the y direction. In the y dimension, the thickness of the lead boxes appears to be closer to 10 mm than the actual 5 mm, but is difficult to make out right at the boundaries. The gap between the lead boxes and the uranium can be made out, but is more difficult to do so at the boundaries. In these instances, the lead box wall closest to the detector stacks at the boundaries is imaged less precisely than the other wall parallel to it and farther from the boundary. The thickness of the uranium letters appears to be close to the actual value of 20 mm, and the width of the lead boxes appears to be close to the actual value of 50 mm. In the z dimension, the thickness of the lead boxes cannot be made out, and the 10 mm gap between the two boxes cannot be discerned. However, the height of both boxes together, including the gap, can be put close to the actual value of 270 mm. The combined height of the uranium in both boxes can also be put close to the actual value of 240 mm.

Finally, I present the results of two scenarios that put shielded and unshielded uranium FIT elements side-by-side lying in the xz plane centered at y = 0 (fig. 3.27-30). In each scenario, the uranium in the positive z region has a gap of 30 mm between letters F-I and I-T at closest distance, and the uranium in the negative z region has a gap of 20 mm between letters F-I and I-T at closest distance. In the first scenario, the uranium in the positive z region is unshielded, while the uranium in the negative z region is shielded, and in the second scenario,

the uranium in the negative z region is unshielded, while the uranium in the positive z region is shielded. I ran scenarios of unshielded and shielded uranium from only one perspective because I simply wanted to compare the difference between the two, not test the imaging capability in different regions of the imaging volume as previously done, and I chose to place the elements in the xz plane centered at y = 0 mm because previous results show that the images from this perspective are neither the best nor the worst overall.

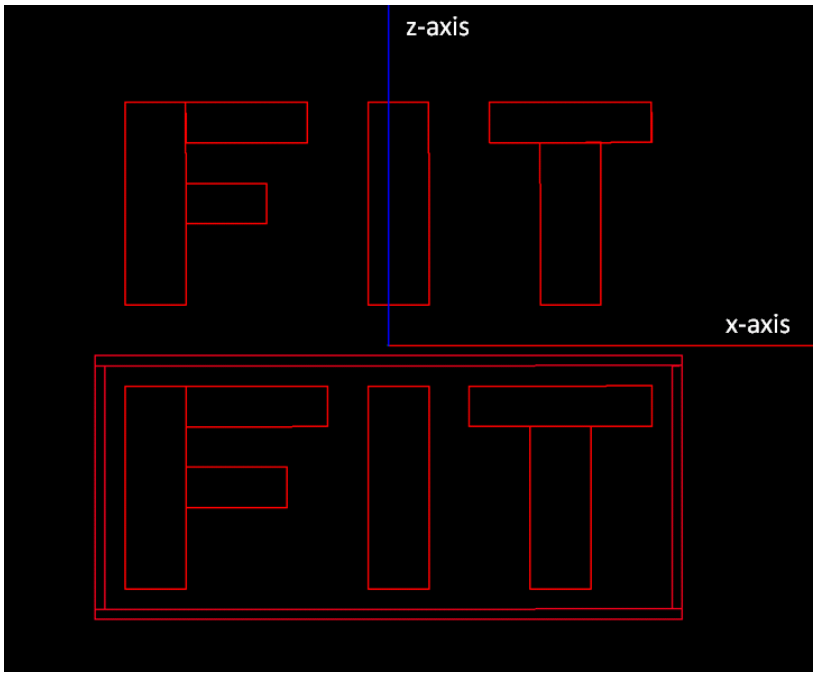

Figure 3.27: Geometry of the first scenario with shielded and unshielded uranium FIT elements. The negative y axis points out of the screen.

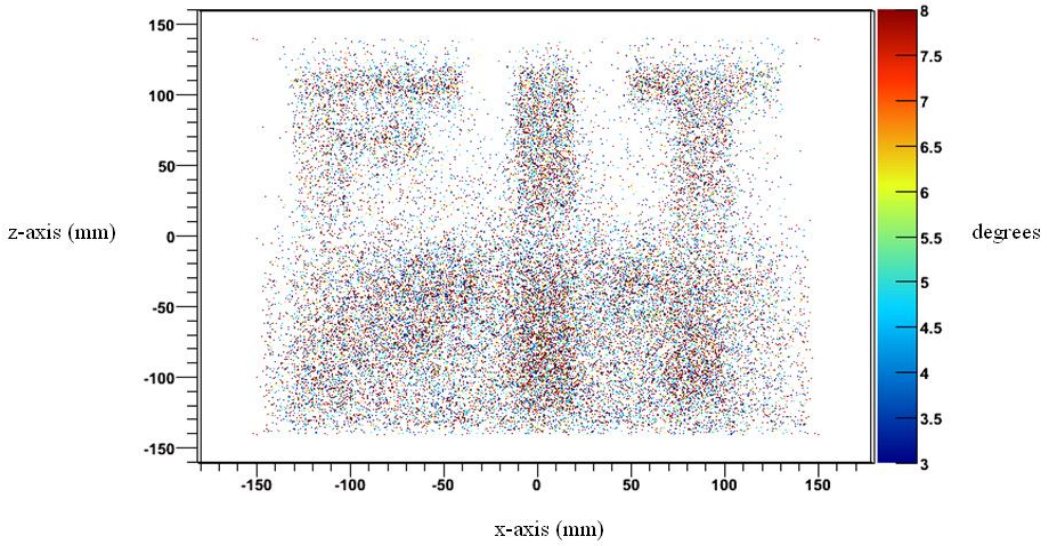

Figure 3.28: Locations of reconstructed scattering points and angles for the first scenario with shielded and unshielded uranium FIT elements using POCA reconstruction with 600 minutes exposure time. The negative y axis points out of the screen.

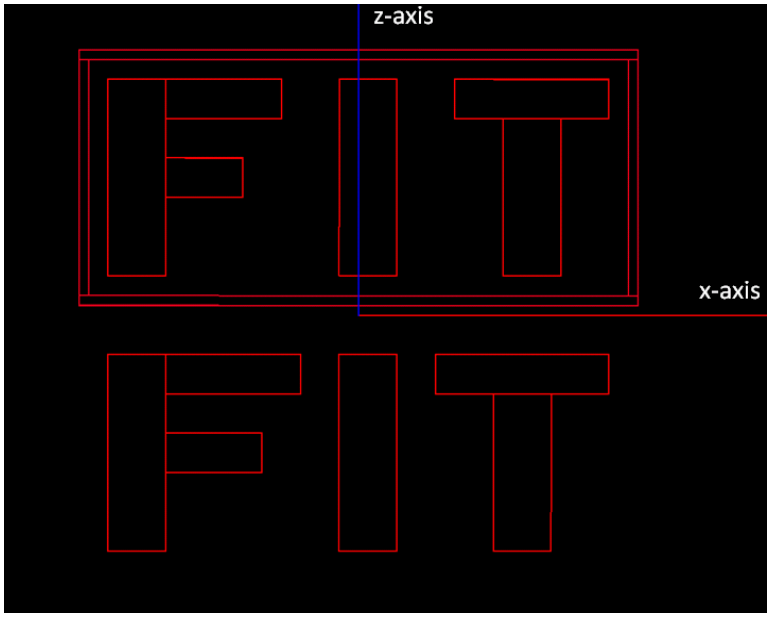

Figure 3.29: Geometry of the second scenario with shielded and unshielded uranium FIT elements. The negative y axis points out of the screen.

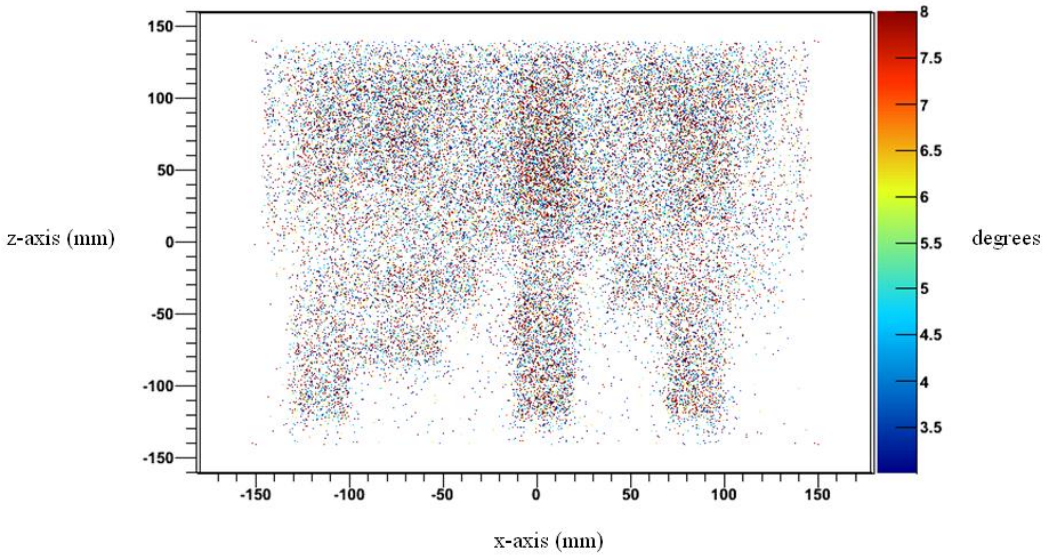

Figure 3.30: Locations of reconstructed scattering points and angles for the second scenario with shielded and unshielded uranium FIT elements using POCA reconstruction with 600 minutes exposure time. The negative y axis points out of the screen.

The results of the unshielded scenarios are very interesting because they show just how effective a muon tomography based imaging system is at detecting shielded nuclear material. In fact, with a muon tomography based system it appears that attempting to shield nuclear material has the opposite effect. These results show that shielded uranium actually looks slightly hotter than unshielded uranium! This phenomenon must be the result of the multiple scattering that occurs first with the lead at one side of the box, then with the uranium, and then again with the lead on the other side of the box. It appears all of that scattering must result, on average, in greater angles of deflection when POCA calculations are made leading to the reconstruction of hotter images than if there were no shielding. While the shielded uranium may appear a little hotter than the unshielded uranium, resolution for the unshielded uranium is better. The increase in multiple scattering that makes the shielded uranium appear slightly hotter also reduces the resolution of the images

there. If, however, we are only interested in quickly identifying regions within the imaging volume where scattering is commensurate with that of nuclear contraband, the loss in resolution that accompanies shielding really doesn't matter. All of the features of the unshielded uranium can be made out close to their actual values, even in the z dimension, where the gap between the horizontal elements of the letter "F" can be made out close to 20 mm, and the height of the letters can be made out close to 100 mm. In the x dimension, the difference in spacing between the letters F-I and I-T at closest distance in the positive and negative z regions can be made out in the unshielded uranium and measured close to the actual values of 30 mm and 20 mm respectively, and the width of the letters can be measured close to the actual value of 30 mm.

Analysis of the scenarios presented in this section shows that our muon tomography station prototype II should be very effective at detecting shielded nuclear material throughout its imaging volume. In fact, a lead shield capable of shielding 99.9% of the most probable gammas emitted from U-235 makes the uranium burn a little brighter in our images than unshielded uranium. Of the three planes cutting through our imaging volume (xy, yz, and xz), images in the yz plane are less clear than those in the other two. This is probably due to the fact that there are no detector stacks at the boundaries of the imaging volume parallel to this plane. Resolution in the z dimension appears to be less than resolution in the x and y dimensions in the shielded scenarios. In these instances, details in z smaller that 20 mm cannot be made out, while details in x and y between 5 mm and 10 mm can be. Since the simulations occur in an ideal, abstract space, the most probable angle of an incident muon (30° degrees from the vertical at sea level) and physical properties of real detectors in the vertical position should not be factors in determining resolution in z as they might otherwise be. This leads me to believe that it may be possible to improve our POCA reconstruction method to eliminate some of the smearing in z observed in the shielded scenarios. Images in the xy

plane were the best overall. The features of shielded uranium in that plane were as clear as the unshielded uranium in the xz plane. Besides possibly improving our reconstruction method, improvements could be made to the imaging station itself to enhance its overall effectiveness. Improving future prototype efficiency will be important, because in practice exposure time will be limited. All images shown in this section were produced from 10 hours of simulated exposure time. Images produced from 4 minutes, 10 minutes, and 60 minutes of simulated exposure time can be seen in appendix E. In order to fully replace current detection systems, our system may need to make better images in shorter periods of time. In any case, our detection system could be used in parallel with current ones as a secondary check for cargo flagged as needing a more thorough scan. In the final chapter, I make some suggestions for prototype III improvements.

Chapter 4 Conclusion

4.1 Suggestions for Prototype III Improvements

In the next generation prototype, support brackets that may be used to mount detectors in top and bottom detector stacks could be inverted, but this would require drilling holes in the framework differently than is currently done. Future generation prototypes will have larger GEM detectors, and inverted support brackets may be able to bear a larger load better.

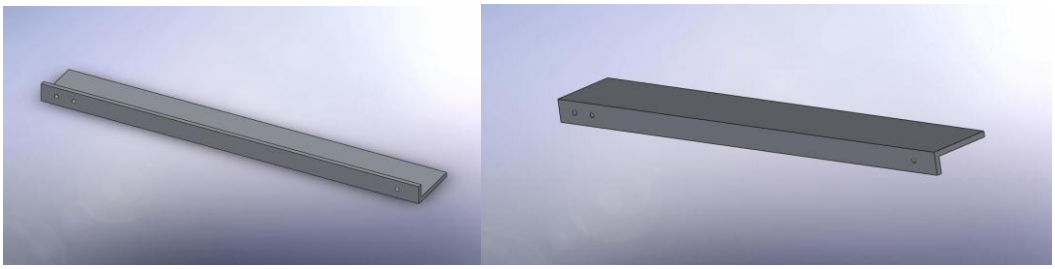

Figure 4.1: Images of current (left) and inverted (right) support brackets for detectors in top and bottom detector stacks.

The image on the left in figure 4.1 shows how support brackets for detectors in top and bottom detector stacks are currently oriented when screwed into the main framework. The hole on the far right is screwed into the framework, along with the right hole in the pair to the left. The hole farthest to the left (left hole in pair to the left) is used to fixate the PVC support plate. All holes are in the same plane. The image to the right in the same figure shows an inverted support bracket, however changes would have to be made to the holes in the bracket and to the framework for it to be functional. The hole farthest to the left shouldn't be there. The hole used to fixate the support plate would exist in the framework only, and the two holes used to fixate the inverted support bracket would not be in the same plane as the hole in the framework used to fixate the support plate.

The next generation prototype could explore using a phenolic material or garolite to support detectors within the new framework, instead of the PVC detector support that is currently used. A phenolic material or garolite would be more rigid and less massive than PVC. Garolite is the material that many circuit boards are made of (usually green) and would require special permission and caution when machining. It would also need to be thick enough for a fine screw to go through so it could be secured in place.

After our muon tomography prototype II station had been built, I realized that solid T-stock could have been used for main vertical elements in each quadrant. This would have eliminated a total of four welds, kept the framework more precise, and probably would have made it more sturdy.

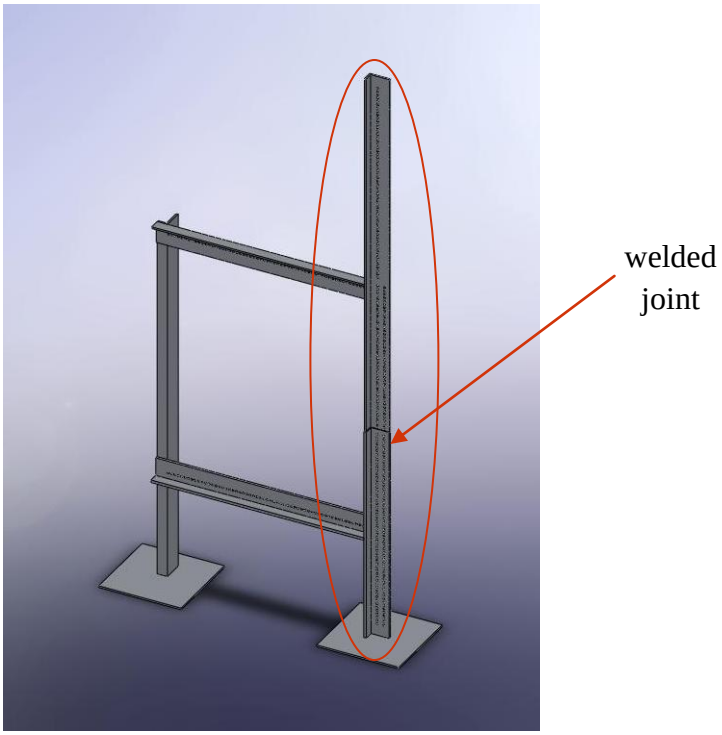

Figure 4.2: Image of a quadrant of our MTS prototype II highlighting a welded joint that could be eliminated.

Within the oval in figure 4.2 is what I describe as the main vertical element of the quadrant. Currently, it is composed of T-stock (bottom) and extruded angle (top) welded together at the location pointed out by the arrow. Solid T-stock could have been used all the way through, and the top part of the "T" in the stock that would have been in the way (where the extruded angle is now) could have been easily cut away with a band saw. Future generation prototypes could eliminate welds and make their framework sturdier by employing solid T-stock as described above where appropriate.

Finally, changes could be made to improve the coverage of the next generation prototype by adding detector stacks to our current station or by changing the geometry of current detectors [20]. While it may be possible to modify our current station to accommodate certain changes in detector geometry, other changes would require a new framework to support the modified geometry. Figures 4.3 and 4.4 show the current geometry of detectors in our MTS prototype II station and a coverage plot for that geometry, respectively. Subsequently, suggestions are made that could improve the coverage and efficiency of future prototypes.

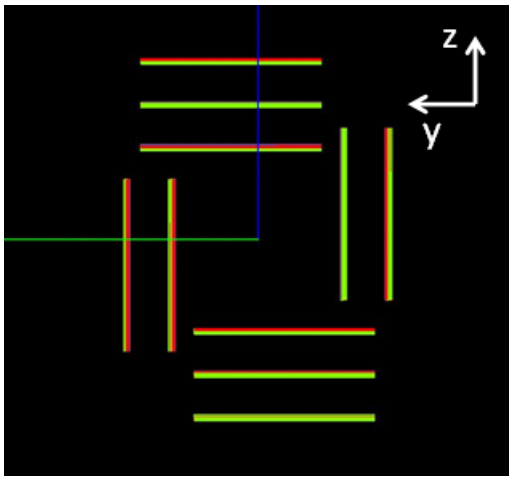

Figure 4.3: Current geometry of detectors in our muon tomography station prototype II [33].

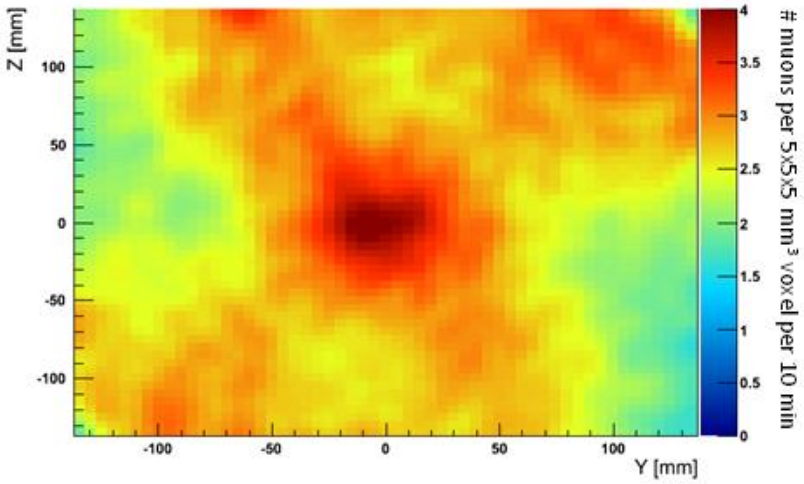

Figure 4.4: Coverage plot for the imaging volume given the current geometry of detectors in our station [33].

Adding bottom detector stacks to both sides of the volume with no side detectors at the boundary there helps to compensate for the lack of side detectors at those sites by allowing some muons passing through the open ends to be tracked. Prototype I stations could be used to easily mount the extra bottom detector stacks. This type of geometry has been labeled as "Extended MTS" by our group and is an idea that I came up with. Figures 4.5 and 4.6 show the geometry and the resulting coverage.

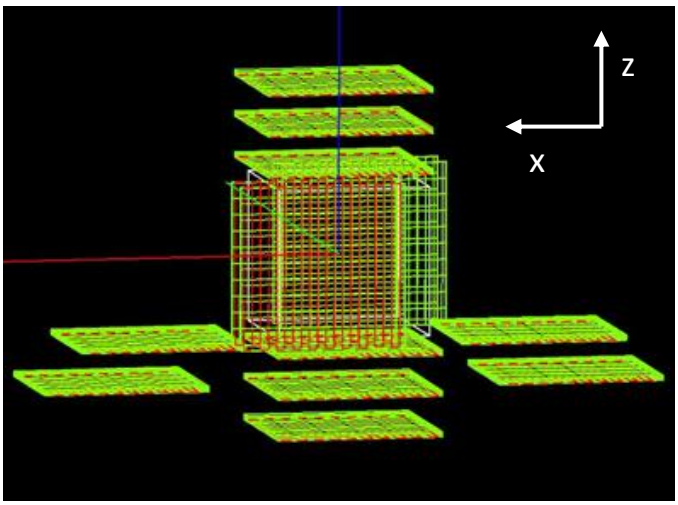

Figure 4.5: Image of an "Extended MTS" detector geometry [33].

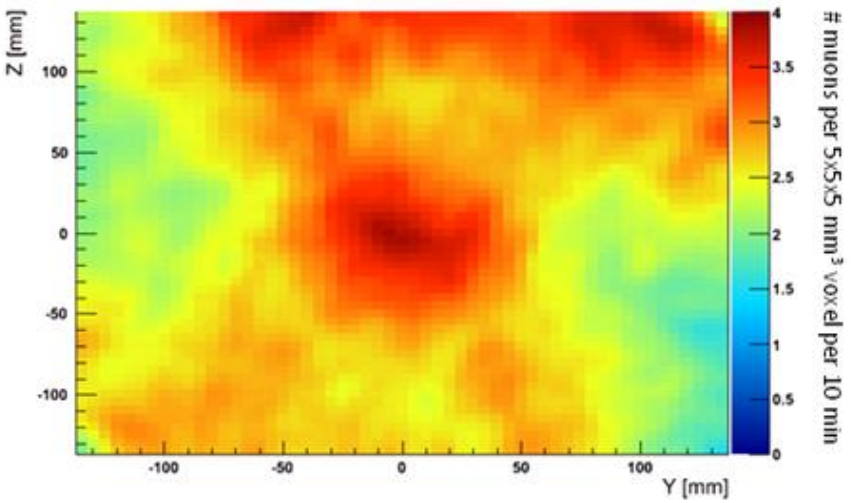

Figure 4.6: Coverage plot for the imaging volume given an "Extended MTS" detector geometry [33].

Orienting top detector stacks so that they are normal to the highest probable angle of incidence (30° from the vertical) should increase the flux of muons crossing the plane of the detectors, and having two top detector stacks instead of one in general should help to increase coverage of the imaging volume. This type of geometry has been labeled as "Pavilion Geometry" by our group. Figures 4.7 and 4.8 show the geometry and the resulting coverage.

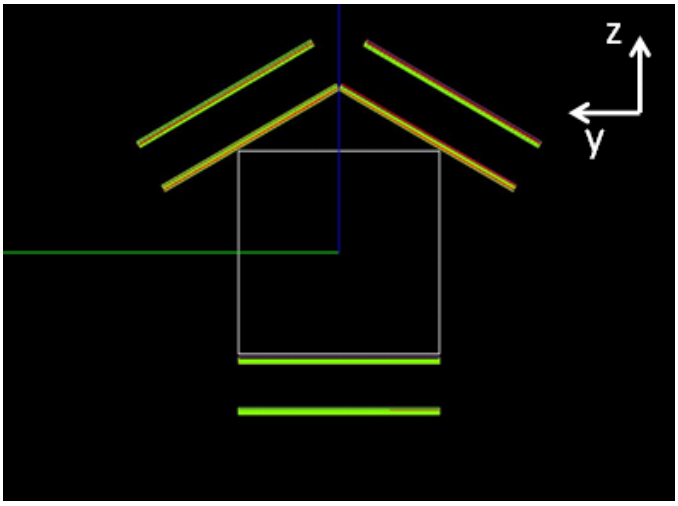

Figure 4.7: Image of a "Pavilion Geometry" detector geometry [33].

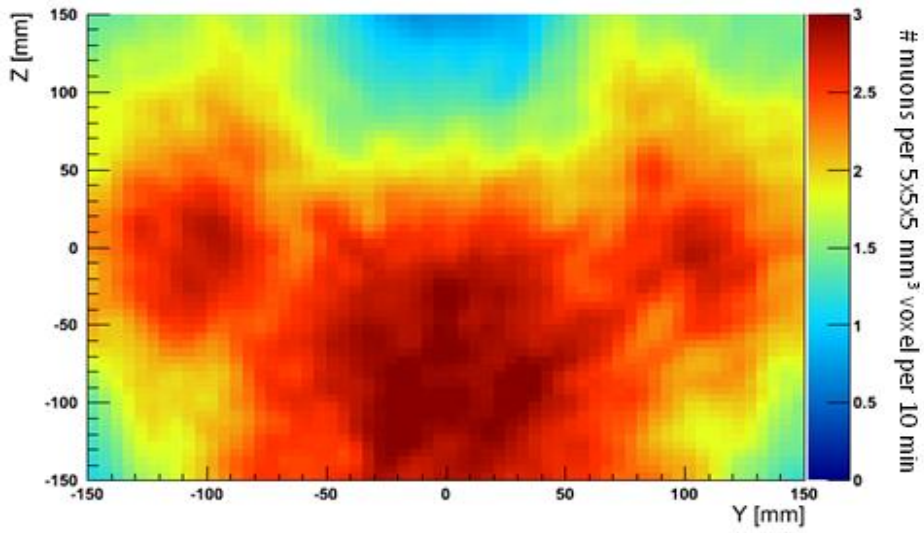

Figure 4.8: Coverage plot for the imaging volume given a "Pavilion Geometry" detector geometry [33].

Adding bottom detector stacks as presented in the Extended MTS geometry clearly increased the coverage in the top half of the imaging volume, and the Pavilion Geometry clearly increased coverage in the bottom half of the imaging volume. Perhaps a combination of the two could be even more effective. Part of the current research and analysis being performed in our group is focused on determining the optimal next generation geometry of detector stacks. The results of this analysis will determine the next generation framework required of our muon tomography station prototype III.

4.2 Summary

The discovery of the muon can be traced back to the era spanning 1930 to 1950 when Yukawa proposed the first significant theory of the strong nuclear force, a number of systematic studies of cosmic radiation were underway, and the theory of quantum electrodynamics was being developed. For many, it was Street and

Stevenson's group that first provided the most convincing evidence for the existence of the muon through a striking photograph they took. The muon turned out not to be what Yukawa was looking for in his quest to explore the strong nuclear force, but it did help to support and validate quantum electrodynamics.

In the 1960's, Luis Alvarez found one of the first ways to apply muons in experimental physics by using them to develop an imaging technique called shadow radiography. The technique exploits the high penetrating nature of muons and uses detectors to compare the number of incident muons in certain areas against others. Discrepancies in average muon counts can yield important information about the material they have passed through, and it was in this way that Alvarez searched for hidden chambers in the ancient Egyptian pyramid of Chephren. Muon tomography is a very different imaging technique than shadow radiography, but also exploits the free supply of cosmic ray muons passing through us all the time. Muon tomography was developed by Christopher Morris at Los Alamos National Lab in 2001 and uses detectors to track the path of a muon through a volume to image material in it. Muons interact with matter via Coulomb scattering and are scattered more by atoms with large atomic numbers than those with smaller atomic numbers. Detectors employed in muon tomography can be used to measure the angle of deflection of muons passing through material in the imaging volume, and this information can in turn be used to create images of the material present, as well as its density. Drift tubes and gas electron multiplier detectors have been used in this imaging technique involving muons.

Our research group is the first to use gas electron multiplier (GEM) detectors for muon tomography, and each GEM detector has five basic components: a honeycomb frame, a drift cathode, foils (referred to as GEM foils), a readout, and a gas mixture which fills the volume of each sealed detector. The location that a muon crosses a detector is given when a muon ionizes the gas in the detector resulting in an electron avalanche produced by the GEM foils within the

detector. The number of electrons reaching the readout produces a large enough current to generate a signal revealing where the muon crossed the detector. Stacks of detectors can be used to generate incoming and outgoing trajectories of muons, and reconstruction algorithms can take that information and locate where a muon interacted with material in the imaging volume and how dense the material was. Our group uses a Point Of Closest Approach (POCA) reconstruction algorithm, and we are testing how effective a muon tomography based imaging system would be at detecting shielded nuclear material.

In order to conduct any tests, an imaging station needed to be designed to mount detectors in a given geometry and to define an imaging volume. I designed our group's muon tomography station prototypes I and II. Our MTS prototype I was designed to accommodate top and bottom detector stacks only, defining an imaging volume of about a cubic foot. Our MTS prototype II was designed to accommodate two side detector stacks, in addition to top and bottom detector stacks, surrounding the cubic foot imaging volume on four of six sides and thereby increasing our imaging station's coverage.

I then designed and implemented various scenarios to simulate our prototype II station's ability to detect shielded nuclear contraband. Our research group receives funding from the Department of Homeland Security, and the goal of our research is to improve the detection of shielded nuclear material (SNM) at our nation's ports and borders. Muon Tomography (MT) offers advantages over current detection systems through its ability to discriminate high-Z material from a lower-Z background. It is based on the scattering of muons, not on the detection of high energy photons emitted from nuclear material as is currently done. It may be possible to smuggle SNM past current systems, and we hope to show that such a shield would be useless given a MT based system. Since uranium 235 is a primary material used for nuclear fission weapons, I calculated how thick a lead shield would have to be to absorb 99.9% of the most probable gamma rays emitted from

U-235. It turns out that a box of lead 5 mm thick would do the trick, so I simulated what uranium encased in 5 mm thick boxes of lead would look like imaged in our MTS prototype II. The results were impressive. Not only was shielded uranium detectable everywhere in the imaging volume, shielded uranium was shown to stand out more than unshielded uranium! Because our images are reconstructed from scattered muons, a dense shield increases the amount of scattering on average and causes the SNM to burn slightly brighter than if there were no shielding. The results of my simulations showed that a muon tomography based detection system can detect SNM that may slip past current systems. All images shown in the body of the thesis using POCA reconstruction were produced from 10 hours of simulated exposure time. Images produced from 4 minutes, 10 minutes, and 60 minutes of simulated exposure time can be seen in appendix E. In order to fully replace current detection systems, our system may need to make better images in shorter periods of time because in practice, exposure time will be limited. The conclusion is that our detection system could at least be used in parallel with current ones as a secondary check for cargo flagged as needing a more thorough scan, thereby improving national security.

Finally, after designing and building both MTS prototypes for our group, I thought about possible improvements that could be implemented in future prototypes. They included the use of inverted support brackets that may be able to bear a larger load associated with larger detectors better, the use of lighter, stronger material to support detectors in the imaging station, the use of solid T-stock where applicable to reduce welds and increase the structural integrity of the station, and the implementation of a modified detector geometry to increase the coverage and efficiency of the station.

References

[1] D. Griffiths, "Introduction to Elementary Particles," Wiley-VCH Verlag GmbH & Co. KGaA, second edition, 2008.

[2] P. Galison, "The Discovery of the Muon and the Failed Revolution against Quantum Electrodynamics," *Centaurus*, vol. 50, pp. 105-159, 2008.

[3] Contemporary Physics Education Project (CPEP) web page: http://www.cpepweb.org/.

[4] C. F. Powell, "Properties of the π- and μ-mesons of cosmic radiation," *Research* (London), pp. 83-98, 1949.

[5] F. Close, M. Marten, and C. Sutton, "The Particle Odyssey: A Journey to the Heart of Matter," Oxford University Press, 2002.

[6] C. A. Wohl, "Scientist as Detective: Luis Alvarez and the Pyramid Burial Chambers, the JFK Assassination, and the End of the Dinosaurs," *American Journal of Physics*, 75 no. 11, pp. 968-977, 2007.

[7] L. J. Schultz, "Cosmic Ray Muon Radiography," Ph.D. thesis, Dept. Elect. Comput. Eng., Portland State Univ., Portland, OR, 2003.

[8] G. E. Hogan, *et al.*, "Detection of High-Z Objects Using Multiple Scattering of Cosmic Ray Muons," *AIP Conf. Proc.*, vol. 698, pp. 755-758, 2004.

[9] L. J. Schultz, *et al.*, "Image Reconstruction and Material Discrimination via Cosmic Ray Muon Radiography," *Nucl. Instrum. Meth. A*, vol. 519, pp. 687-694, 2004.

[10] L. J. Schultz, *et al.*, "Statistical Reconstruction for Cosmic Ray Muon Tomography," *IEEE Trans. Image Process.*, vol. 16, no. 8, pp. 1985-1993, Aug. 2007.

[11] J. A. Green, *et al.*, "Optimizing the Tracking Efficiency for Cosmic Ray Muon Tomography," Los Alamos National Lab., NM, Tech. Rep. UCRL-TM-229452, 2007.

[12] IEEE Global History Network web page: http://www.ieeeghn.org/wiki/index.php/Milestones:CERN_Experimental_Instrumentation,_1968.

[13] F. Sauli, "GEM: A New Concept for Electron Amplification in Gas Detectors," *Nucl. Instrum. Meth. A*, vol. 386, pp. 531-534, 1997.

[14] CERN Gas Detectors Development (GDD) web page: http://gdd.web.cern.ch/GDD, 2011.

[15] L. Cox, *et al.*, "Detector Requirements for a Cosmic Ray Muon Scattering Tomography System," *Proc. IEEE Nucl. Sci. Symp.*, pp. 706-710, 2008.

[16] M. Hohlmann, *et al.*, "GEANT4 Simulation of a Cosmic Ray Muon Tomography System with Micro-Pattern Gas Detectors for the Detection of High-Z Materials," *IEEE Trans. Nucl. Sci.*, vol. 56, no. 3, pp. 1356-1363, 2009.

[17] Dr. Marcus Hohlmann, private communications, presentations at weekly meetings of High Energy Physics Research Group A, Florida Institute of Technology, 2008.

[18] B. Benson, "Thermal Stretching of GEM Foils and Characterization of Triple-GEM Detectors for Uses in Astronomy," Thesis, Florida Institute of Technology, 2011.

[19] F. Murtas, "Development of a Gaseous Detector Based on Gas Electron Multiplier (GEM) Technology," http://www.lnf.infn.it/seminars/talks/murtas_28_11_02.pdf, 2002.

[20] A. Quintero, "Construction and Performance of Gas Electron Multiplier Detectors for Nuclear Contraband Detection Using Muon Tomography," Thesis, Florida Institute of Technology, 2010.

[21] C. Altunbas, *et al.*, "Construction, Test and Commissioning of the Triple-GEM Tracking Detector for COMPASS," *Nucl. Instrum. Meth. A*, vol 490, pp. 177-203, 2002.

[22] SolidWorks Home Page: http://www.solidworks.com/

[23] K. Gnanvo, *et al.*, "Imaging of High-Z Material for Nuclear Contraband Detection with a Minimal Prototype of a Muon Tomography Station based on GEM Detectors," *Nucl. Instrum. Meth. A*, vol. 652, pp. 16-20, 2011.

[24] J. B. Locke, Fall 2009 Summary of Research, High Energy Physics Research Group A, Florida Institute of Technology, 2009.

[25] Federation of American Scientists web page: http://www.fas.org/nuke/intro/nuke/design.htm.

[26] Lawrence Berkeley National Laboratory web page: http://ie.lbl.gov/toi/radSearch.asp.

[27] National Institute of Standards and Technology web page: http://www.nist.gov/pml/data/index.cfm.

[28] J. B. Locke, "Software Development for MTS Alignment, GEM Spatial Resolution, and GEANT4 Simulation," Undergraduate Research Report, High Energy Physics Research Group A, Florida Institute of Technology, fall 2011.

[29] D. Wright, *et al.*, "Monte Carlo Simulation of Proton-induced Cosmic-ray Cascades in the Atmosphere," Cosmic-ray Physics Team, Lawrence Livermore National Lab., CA, Tech. Rep. LA-UR-06-8497, 2006.

[30] C. Hagmann, D. Lange, and D. Wright, "Cosmic-ray Shower Generator (CRY) for Monte Carlo Transport Codes," *Proc. IEEE Nucl. Sci. Symp.*, vol. 2, pp. 1143-1146, 2007.

[31] R. Brun and F. Rademakers, "ROOT – An Object Oriented Data Analysis Framework," *Nucl. Instrum. Meth. A*, vol. 389, pp. 81-86, 1997.

[32] Stanford Linear Accelerator Center, HepRApp Users Home Page: http://www.slac.stanford.edu/BFROOT/www/Computing/Graphics/Wired/

[33] Nathan Mertins, private communications, presentations at weekly meetings of High Energy Physics Research Group A, Florida Institute of Technology, spring 2012.

Appendix A: Directions to Assemble MTS Prototype I

1. Screw in a heavy hex nut by hand about two inches from the end of a threaded rod going into the base plate.

2. Slide two washers in from the same end so they rest against the nut.

3. Apply a light coat of anti-seize lubricant (nickel based) to the end of the threaded rod going into the base plate.

4. Screw the threaded rod into one of the cylinders welded into the base plate.

5. After the rod is screwed in all the way, tighten the heavy hex nut by hand. Over tightening the nut using a wrench could damage the system.

6. Repeat steps 1-5 for the remaining rods and cylinders.

7. Lower the first detector so that it rests on the heavy hex nuts.

8. Use the appropriate kind and number of spacers to achieve the desired detector gap.

9. Repeat steps 7-8 until the bottom detector stack is complete.

10. Lower coupling nuts on each rod by screwing them down by hand until they are at the desired height for the target plate. This may take a few minutes (four minutes max per rod) and patience should be exercised. When screwing the

coupling nuts down, keep the steel rods as straight as possible. Hastily lowering the nuts and generating sway in the rods could damage the system.

11. Drop two washers onto the coupling nuts and lower the target plate into place. Verify that the target plate is parallel to the base plate by using a level.

12. For added support, lower a heavy hex nut on each rod and tighten by hand onto the target plate.

13. Lower coupling nuts on the three rods supporting the detectors to the desired height and drop two washers onto each nut. Lower the bottom detector of the top stack and make sure it is level.

14. Use the appropriate kind and number of spacers to achieve the desired detector gap and lower the next detector.

15. Repeat until the top detector stack is complete.

16. Place the material to be imaged within the etched square on the target plate and begin taking data.

Appendix B: Directions to Assemble MTS Prototype II

Contents and Supplies

1. Four main quadrants of station.
2. Two main support brackets for framework, one joining quadrants one and four and the other joining quadrants two and three.
3. Three PVC plates for detector support in bottom stack.
4. Three PVC plates for detector support in top stack.
5. Two PVC plates for detector support in side stack joining quadrants one and four.
6. Two PVC plates for detector support in side stack joining quadrants two and three.
7. Scintillator and PVC support for bottom stack.
8. Scintillator and PVC support for top stack.
9. Scintillator and PVC support for side stack joining quadrants one and four.
10. Scintillator and PVC support for side stack joining quadrants two and three.
11. Four aluminum spacers for all PVC support in bottom stack.
12. Ten extruded angles for PVC detector support joining quadrants one and two.
13. Ten extruded angles for PVC detector support joining quadrants three and four.
14. Two extruded angles for target plate(s) joining quadrants one and two.
15. Two extruded angles for target plate(s) joining quadrants three and four.
16. Phillips screw drivers with large and small heads.
17. 7/16 wrench.
18. C-clamps for target plate(s).
19. 6-32 1/2 inch bolts to attach all extruded angles to framework.
20. 1/4-20 bolts for main support brackets for framework.

21. 1/4-20 jam nuts for 1/4-20 bolts.
22. 6-32 1¼ inch bolts for bottom stack PVC support.
23. 6-32 5/8 inch bolts for both side stack PVC supports.
24. 6-32 1 inch bolts for top stack PVC support.
25. 1/4-20 bolts to fixate detectors (readout) to PVC support.

Assembly Instructions

As you proceed, make sure you use the correct bolt to fixate each part as described above and marked on labels of the bags containing the bolts. Bolts fixating PVC support plates should not be over-tightened.

1. Arrange aluminum quadrants in the correct order (counterclockwise) starting with quadrant one.

2. * Link quadrants one and two with aluminum angles placed in the top-most and bottom-most notches. Leave the holes closest to the T-bars empty, as bolts to fixate the PVC support will go through them. Repeat the process linking quadrants three and four. Read the warning on the following page and make sure bolts are tightened.

3. * Link quadrants one and four together with the appropriately marked bracket. Repeat process linking quadrants two and three. Make sure all bolts are tightened.

* **Be mindful of how the station is aligning during steps two and three as not to damage a part during assembly by applying an unwanted torque.**

4. Install the angles for the bottom detector stack. The angles closest to the imaging volume can be installed six notches down from the volume. Subsequent angles are put in eight notches below the previous. Tighten all bolts. Note: One could calculate the position of the bottom-most angles (supporting the scintillator) and install them first and then fixate the scintillator immediately afterwards. Angles and detectors could then be installed and fixated working your way up to the imaging volume. Installing the scintillator and detectors as you go is easier than trying to install them after all angles are in place (true for bottom stack only / this is recommended). Use aluminum spacers in bottom stack for all PVC support. Spacers are placed on side of quadrant two.

5. Install angles for the top detector stack. The angles closest to the imaging volume can be placed in the lowest notches (those closest to the imaging volume). Subsequent angles are installed eight notches above the previous ones. Tighten all bolts.

6. Install angles for the target plate(s). Choose positions for the angles that best suit the desired experiments to be run.

7. If not already done, fixate the scintillator and detectors in the bottom stack to the frame. Use aluminum spacers in bottom stack for all PVC support. Spacers are placed on side of quadrant two.

8. Insert target plate(s) and clamp them to their angles using c-clamps.

9. Fixate the detectors and scintillator in the side stack joining quadrants one and four to the frame. Make sure the detectors are facing the imaging volume and that the short side of the readout is upward.

10. Fixate the detectors and scintillator in the side stack joining quadrants two and three to the frame. Make sure the detectors are facing the imaging volume and that the short side of the readout is downward.

11. Fixate the detectors and scintillator in the top stack to the frame.

Appendix C: Configuration Files for Simulated Scenarios

 # Configuration file for all scenarios with uranium and lead boxes in the yz
 # plane. Desired elements to appear in a simulation are uncommented. For
 # example, elements are uncommented to run scenario yz, x = -110 mm now.
 # To run another yz scenario, simply comment out the elements located at x =
 # -110 and uncomment the desired elements. In the Platform and Target
 # section, lines starting with ### can be uncommented. Lines beginning with #
 # are permanent comments, as they describe specific elements being acted on.
#

```
#### Cry Settings
/control/verbose 0
/run/verbose 0
/event/verbose 0
/tracking/verbose 0
/CRY/input returnMuons 1
/CRY/input returnGammas 0
/CRY/input returnNeutrons 0
/CRY/input returnElectrons 0
/CRY/input returnPions 0
/CRY/input returnProtons 0
/CRY/input date 2012.5
/CRY/input latitude 90.0
/CRY/input altitude 0
/CRY/input subboxLength 3
#/CRY/input returnGammas 2
#/CRY/input
/CRY/update

#### Visualization Settings
/vis/verbose 1
/vis/scene/create
#/vis/open OGLIX
/vis/open HepRepFile
/vis/heprep/useSolids 0
/vis/drawVolume
/vis/viewer/zoom 1.
/vis/scene/add/axes 0 0 0 1000 mm
/vis/viewer/set/upVector  0 0 1
/vis/viewer/set/viewpointThetaPhi 100 -65 deg
```

```
/vis/scene/add/hits
#/vis/scene/add/logo
#/vis/scene/add/trajectories
/vis/viewer/flush
#/vis/viewer/set/style wireframe
/vis/viewer/set/style surface
/vis/scene/endOfEventAction accumulate 1000

#### Output Settings
/mydet/simulationOutput          pocaReconstruction
#/mydet/simulationOutput           coverage
/myanalysis/setOutputPocaFileName  n0

#### Detector geometry
/mydet/setExpHallSize              4000 mm
/mydet/setExpHallMat               G4_AIR
/mydet/setTheLateralDetectors      yes
/mydet/setGapSubDetectorLayers     20 mm
/mydet/setNumberOfSubDetectorLayers 3
/mydet/setMTSSize                  300 mm
/mydet/setMTSHeight                300 mm
/mydet/setVoxelSize                20 mm

#### Platform and Target    MATERIAL  SHAPE MOTHER    SIZE(XYZ)
THICK  POSITION(XYZ)
#/mydet/setShieldParameters  Lead     box   container 250 250 50       2    0  0  36
#/mydet/setShieldParameters  Lead     box   container 250 250 50       2    0  0  -36
#
#  Main F Negative Z X=0
###/mydet/setShieldParameters  Uranium  box  container  20  30 100  2  0 -105 -70
#
#  Mid F Negative Z X=0
###/mydet/setShieldParameters  Uranium box  container  20  40  20   2  0  -70  -70
#
#  Top F Negative Z X=0
###/mydet/setShieldParameters  Uranium  box  container  20  60  20   2   0  -60 -30
#
#  Main I Negative Z X=0
###/mydet/setShieldParameters  Uranium  box  container  20  30 100   2   0   5   -70
#
#  Top T Negative Z X=0
###/mydet/setShieldParameters  Uranium box container  20  80  20     2   0  80   -30
```

```
#
#  Main T Negative Z X=0
###/mydet/setShieldParameters  Uranium  box  container  20  30  80   2   0   80  -80
#
#  Left Box Negative Z X=0
###/mydet/setShieldParameters  Lead  box  container  40  5   120   2  0  -132.5  -70
#
#  Right Box Negative Z X=0
###/mydet/setShieldParameters  Lead  box   container  40  5  120   2   0 132.5   -70
#
#  Up Box Negative Z X=0
###/mydet/setShieldParameters  Lead  box  container  40   270   5    2   0   0   -7.5
#
#  Down Box Negative Z X=0
###/mydet/setShieldParameters  Lead  box  container  40   270   5   2    0   0  -132.5
#
#  Top Box Negative Z X=0
###/mydet/setShieldParameters  Lead box  container  5   270  130   2   22.5  0    -70
#
#  Bottom Box Negative Z X=0
###/mydet/setShieldParameters  Lead  box  container  5  270 130  2  -22.5  0    -70
#
#/mydet/setShieldParameters  Uranium  box  container 100 100 100   2   0   0      0


#  Main F Positive Z X=0
###/mydet/setShieldParameters  Uranium box  container  20  30 100   2  0  -105  70
#
#  Mid F Positive Z X=0
###/mydet/setShieldParameters  Uranium box  container  20  40  20   2   0  -70   70
#
#  Top F Positive Z X=0
###/mydet/setShieldParameters  Uranium box container  20  60  20   2   0  -60   110
#
#  Main I Positive Z X=0
###/mydet/setShieldParameters  Uranium  box  container  20  30 100   2   0   5   70
#
#  Top T Positive Z X=0
###/mydet/setShieldParameters  Uranium box  container  20  80  20   2  0   80   110
#
#  Main T Positive Z X=0
###/mydet/setShieldParameters  Uranium box container  20  30 80   2   0   80    60
```

```
#
#  Left Box Positive Z X=0
###/mydet/setShieldParameters  Lead  box  container  40  5.00  120  2  0 -132.5  70
#
#  Right Box Positive Z X=0
###/mydet/setShieldParameters  Lead box  container  40  5.00  120   2  0  132.5  70
#
#  Up Box Positive Z X=0
###/mydet/setShieldParameters  Lead box  container  40  270   5     2   0   0   132.5
#
#  Down Box Positive Z X=0
###/mydet/setShieldParameters  Lead  box  container  40  270   5    2    0   0     7.5
#
#  Top Box Positive Z X=0
###/mydet/setShieldParameters  Lead  box  container  5   270  130   2   22.5   0   70
#
#  Bottom Box Positive Z X=0
###/mydet/setShieldParameters  Lead  box  container  5   270   130  2   -22.5   0  70
#
#/mydet/setShieldParameters  Uranium box  container 100 100   100    2   0    0    0


#  Main F Negative Z X=-110
/mydet/setShieldParameters  Uranium box container  20  30  100  2  -110  -105  -70
#
#  Mid F Negative Z X=-110
/mydet/setShieldParameters  Uranium box container  20  40  20    2  -110  -70   -70
#
#  Top F Negative Z X=-110
/mydet/setShieldParameters  Uranium box container  20  60  20    2   -110  -60  -30
#
#  Main I Negative Z X=-110
/mydet/setShieldParameters  Uranium box  container  20  30  100   2   -110  5   -70
#
#  Top T Negative Z X=-110
/mydet/setShieldParameters  Uranium box container  20  80  20    2  -110   80   -30
#
#  Main T Negative Z X=-110
/mydet/setShieldParameters  Uranium box container  20  30  80   2   -110   80   -80
#
#  Left Box Negative Z X=-110
/mydet/setShieldParameters  Lead box container  40  5.00  120  2  -110  -132.5  -70
```

```
#
#  Right Box Negative Z X=-110
/mydet/setShieldParameters  Lead box container  40  5.00  120   2   -110  132.5  -70
#
#  Up Box Negative Z X=-110
/mydet/setShieldParameters  Lead box container  40  270   5     2    -110   0       -7.5
#
#  Down Box Negative Z X=-110
/mydet/setShieldParameters  Lead box container  40  270   5     2    -110   0   -132.5
#
#  Top Box Negative Z X=-110
/mydet/setShieldParameters  Lead box container  5   270   130   2   -87.5    0       -70
#
#  Bottom Box Negative Z X=-110
/mydet/setShieldParameters  Lead box container  5   270   130   2   -132.5   0      -70
#
#/mydet/setShieldParameters  Uranium box container 100 100   100      2   0    0    0


#  Main F Positive Z X=-110
/mydet/setShieldParameters  Uranium box container  20  30 100   2  -110  -105   70
#
#  Mid F Positive Z X=-110
/mydet/setShieldParameters  Uranium box container  20  40  20   2  -110    -70    70
#
#  Top F Positive Z X=-110
/mydet/setShieldParameters  Uranium box container  20  60  20   2  -110  -60    110
#
#  Main I Positive Z X=-110
/mydet/setShieldParameters  Uranium box container  20  30  100  2   -110   5      70
#
#  Top T Positive Z X=-110
/mydet/setShieldParameters  Uranium box  container  20  80  20   2   -110  80    110
#
#  Main T Positive Z X=-110
/mydet/setShieldParameters  Uranium box container  20  30  80   2   -110   80      60
#
#  Left Box Positive Z X=-110
/mydet/setShieldParameters  Lead box container  40  5.00  120   2   -110  -132.5  70
#
#  Right Box Positive Z X=-110
/mydet/setShieldParameters  Lead box container  40  5.00  120    2   -110  132.5  70
```

```
#
#  Up Box Positive Z X=-110
/mydet/setShieldParameters  Lead box container  40  270   5      2   -110  0      132.5
#
#  Down Box Positive Z X=-110
/mydet/setShieldParameters  Lead box container  40  270   5      2    -110   0      7.5
#
#  Top Box Positive Z X=-110
/mydet/setShieldParameters  Lead box container  5   270   130    2    -87.5   0      70
#
#  Bottom Box Positive Z X=-110
/mydet/setShieldParameters  Lead box container  5   270   130    2    -132.5  0      70
#
#/mydet/setShieldParameters  Uranium box container 100 100   100      2   0    0    0


#  Main F Negative Z X=110
###/mydet/setShieldParameters Uranium box container  20  30 100  2 110 -105 -70
#
#  Mid F Negative Z X=110
###/mydet/setShieldParameters  Uranium box container  20  40  20  2 110  -70  -70
#
#  Top F Negative Z X=110
###/mydet/setShieldParameters  Uranium box container  20  60  20  2  110 -60  -30
#
#  Main I Negative Z X=110
###/mydet/setShieldParameters  Uranium box container  20  30  100  2  110  5   -70
#
#  Top T Negative Z X=110
###/mydet/setShieldParameters  Uranium box container  20  80  20  2  110  80   -30
#
#  Main T Negative Z X=110
###/mydet/setShieldParameters  Uranium box container  20  30 80  2  110   80   -80
#
#  Left Box Negative Z X=110
###/mydet/setShieldParameters Lead box container  40 5.00  120  2 110  -132.5 -70
#
#  Right Box Negative Z X=110
###/mydet/setShieldParameters Lead box container  40  5.00  120  2  110 132.5 -70
#
#  Up Box Negative Z X=110
###/mydet/setShieldParameters Lead box container  40  270   5    2  110    0      -7.5
```

```
#
#  Down Box Negative Z X=110
###/mydet/setShieldParameters Lead  box  container  40  270   5   2  110  0   -132.5
#
#  Top Box Negative Z X=110
###/mydet/setShieldParameters Lead box container  5   270   130   2  132.5 0     -70
#
#  Bottom Box Negative Z X=110
###/mydet/setShieldParameters Lead box container  5   270   130  2    87.5  0     -70
#
#/mydet/setShieldParameters Uranium box container 100 100   100    2   0    0       0


#  Main F Positive Z X=110
###/mydet/setShieldParameters Uranium box container  20  30 100  2 110 -105   70
#
#  Mid F Positive Z X=110
###/mydet/setShieldParameters Uranium box  container  20  40  20  2 110  -70    70
#
#  Top F Positive Z X=110
###/mydet/setShieldParameters Uranium box container  20  60  20   2 110  -60  110
#
#  Main I Positive Z X=110
###/mydet/setShieldParameters Uranium box container  20  30  100  2 110  5      70
#
#  Top T Positive Z X=110
###/mydet/setShieldParameters Uranium box container  20  80  20  2  110  80   110
#
#  Main T Positive Z X=110
###/mydet/setShieldParameters Uranium box container  20  30  80  2  110 80     60
#
#  Left Box Positive Z X=110
###/mydet/setShieldParameters Lead box container  40  5.00 120  2  110  -132.5 70
#
#  Right Box Positive Z X=110
###/mydet/setShieldParameters Lead box container  40  5.00 120  2  110 132.5   70
#
#  Up Box Positive Z X=110
###/mydet/setShieldParameters Lead  box  container  40  270  5   2  110   0    132.5
#
#  Down Box Positive Z X=110
###/mydet/setShieldParameters Lead box container  40  270  5   2   110     0       7.5
```

```
#
#  Top Box Positive Z X=110
###/mydet/setShieldParameters Lead box container  5  270   130  2   132.5    0    70
#
#  Bottom Box Positive Z X=110
###/mydet/setShieldParameters Lead box container  5   270   130  2  87.5    0      70
#
#/mydet/setShieldParameters Uranium box  container 100 100   100   2   0     0     0


/mydet/update
#/run/beamOn 14400000
/run/beamOn 30
```

 # Configuration file for all scenarios with uranium and lead boxes in the xz
 # plane. Desired elements to appear in a simulation are uncommented. For
 # example, elements are uncommented to run the xz scenario in which
 # uranium is unshielded in the positive z region and shielded in the negative z
 # region at y = 0 mm. To run another xz scenario, simply comment out the
 # elements located at y = 0 and uncomment the desired elements. In the
 # Platform and Target section, lines starting with ### can be uncommented.
 # Lines beginning with # are permanent comments, as they describe specific
 # elements being acted on.
#
Cry Settings
/control/verbose 0
/run/verbose 0
/event/verbose 0
/tracking/verbose 0
/CRY/input returnMuons 1
/CRY/input returnGammas 0
/CRY/input returnNeutrons 0
/CRY/input returnElectrons 0
/CRY/input returnPions 0
/CRY/input returnProtons 0
/CRY/input date 2012.5
/CRY/input latitude 90.0
/CRY/input altitude 0
/CRY/input subboxLength 3
#/CRY/input returnGammas 2
#/CRY/input
/CRY/update

Visualization Settings
/vis/verbose 1
/vis/scene/create
#/vis/open OGLIX
/vis/open HepRepFile
/vis/heprep/useSolids 0
/vis/drawVolume
/vis/viewer/zoom 1.
/vis/scene/add/axes 0 0 0 1000 mm
/vis/viewer/set/upVector 0 0 1
/vis/viewer/set/viewpointThetaPhi 100 -65 deg
/vis/scene/add/hits
#/vis/scene/add/logo

```
#/vis/scene/add/trajectories
/vis/viewer/flush
#/vis/viewer/set/style wireframe
/vis/viewer/set/style surface
/vis/scene/endOfEventAction accumulate 1000

#### Output Settings
/mydet/simulationOutput          pocaReconstruction
#/mydet/simulationOutput          coverage
/myanalysis/setOutputPocaFileName  n0

#### Detector geometry
/mydet/setExpHallSize             4000 mm
/mydet/setExpHallMat              G4_AIR
/mydet/setTheLateralDetectors      yes
/mydet/setGapSubDetectorLayers     20 mm
/mydet/setNumberOfSubDetectorLayers 3
/mydet/setMTSSize                 300 mm
/mydet/setMTSHeight               300 mm
/mydet/setVoxelSize               20 mm

#### Platform and Target    MATERIAL  SHAPE MOTHER    SIZE(XYZ)
THICK  POSITION(XYZ)
#/mydet/setShieldParameters Lead  box   container 250 250 50          2     0  0   36
#/mydet/setShieldParameters Lead  box   container 250 250 50          2     0  0  -36
#
#  Main F Negative Z Y=0
/mydet/setShieldParameters Uranium box container  30 20  100     2   -115   0   -70
#
#  Mid F Negative Z Y=0
/mydet/setShieldParameters Uranium box  container  50  20 20       2    -75   0  -70
#
#  Top F Negative Z Y=0
/mydet/setShieldParameters Uranium box  container  70  20 20       2    -65   0  -30
#
#  Main I Negative Z Y=0
/mydet/setShieldParameters Uranium box  container  30 20  100      2     5    0  -70
#
#  Top T Negative Z Y=0
/mydet/setShieldParameters Uranium  box  container  90  20 20       2     85   0  -30
#
#  Main T Negative Z Y=0
```

```
/mydet/setShieldParameters Uranium box container  30 20  80        2     85   0  -80
#
#  Left Box Negative Z Y=0
/mydet/setShieldParameters Lead box container  5.00  40  120     2    -142.5  0  -70
#
#  Right Box Negative Z Y=0
/mydet/setShieldParameters Lead box container  5.00  40  120     2     142.5  0  -70
#
#  Up Box Negative Z Y=0
/mydet/setShieldParameters Lead box container  290   40  5       2     0      0  -7.5
#
#  Down Box Negative Z Y=0
/mydet/setShieldParameters Lead box container  290   40  5       2     0      0  -132.5
#
#  Top Box Negative Z Y=0
/mydet/setShieldParameters Lead box container  290   5  130      2     0      22.5  -70
#
#  Bottom Box Negative Z Y=0
/mydet/setShieldParameters Lead box container  290   5  130      2     0     -22.5  -70
#
#/mydet/setShieldParameters Uranium box container 100 100 100     2    0     0     0


#  Main F Positive Z Y=0
/mydet/setShieldParameters Uranium box container  30 20  100      2    -115  0  70
#
#  Mid F Positive Z Y=0
/mydet/setShieldParameters Uranium box container  40  20 20       2    -80   0  70
#
#  Top F Positive Z Y=0
/mydet/setShieldParameters Uranium box container  60  20 20       2    -70   0  110
#
#  Main I Positive Z Y=0
/mydet/setShieldParameters Uranium box container  30 20  100       2     5    0  70
#
#  Top T Positive Z Y=0
/mydet/setShieldParameters Uranium box container  80  20 20       2     90   0  110
#
#  Main T Positive Z Y=0
/mydet/setShieldParameters Uranium box container  30 20  80        2     90   0  60
#
#  Left Box Positive Z Y=0
```

```
###/mydet/setShieldParameters Lead box container  5.00  40  120   2   -142.5  0  70
#
#  Right Box Positive Z Y=0
###/mydet/setShieldParameters Lead box container  5.00  40  120   2    142.5  0  70
#
#  Up Box Positive Z Y=0
###/mydet/setShieldParameters Lead box container  290   40  5     2    0      0  132.5
#
#  Down Box Positive Z Y=0
###/mydet/setShieldParameters Lead box container  290   40  5       2      0      0  7.5
#
#  Top Box Positive Z Y=0
###/mydet/setShieldParameters Lead box container  290   5  130     2    0    22.5  70
#
#  Bottom Box Positive Z Y=0
###/mydet/setShieldParameters Lead box container  290   5  130    2   0     -22.5  70
#
#/mydet/setShieldParameters Uranium box container 100 100 100      2    0     0     0


#  Main F Negative Z Y=-110
###/mydet/setShieldParameters Uranium box container 30 20 100  2  -115 -110 -70
#
#  Mid F Negative Z Y=-110
###/mydet/setShieldParameters Uranium box container  50  20 20  2   -75  -110 -70
#
#  Top F Negative Z Y=-110
###/mydet/setShieldParameters Uranium box container  70  20 20   2  -65  -110 -30
#
#  Main I Negative Z Y=-110
###/mydet/setShieldParameters Uranium box container  30 20  100  2  5   -110  -70
#
#  Top T Negative Z Y=-110
###/mydet/setShieldParameters Uranium box container  90  20 20    2  85 -110  -30
#
#  Main T Negative Z Y=-110
###/mydet/setShieldParameters Uranium box container  30  20 80    2  85  -110 -80
#
#  Left Box Negative Z Y=-110
###/mydet/setShieldParameters Lead box container  5.00 40 120  2 -142.5 -110 -70
#
#  Right Box Negative Z Y=-110
```

```
###/mydet/setShieldParameters Lead box container 5.00  40  120  2  142.5 -110 -70
#
#  Up Box Negative Z Y=-110
###/mydet/setShieldParameters Lead box container  290  40  5    2    0      -110  -7.5
#
#  Down Box Negative Z Y=-110
###/mydet/setShieldParameters Lead box container  290   40  5   2   0   -110  -132.5
#
#  Top Box Negative Z Y=-110
###/mydet/setShieldParameters Lead box container  290   5  130 2    0     -87.5  -70
#
#  Bottom Box Negative Z Y=-110
###/mydet/setShieldParameters Lead box container  290   5  130  2   0    -132.5  -70
#
#/mydet/setShieldParameters Uranium box container 100 100 100      2    0     0     0


#  Main F Positive Z Y=-110
###/mydet/setShieldParameters Uranium box container  30 20  100  2 -115 -110 70
#
#  Mid F Positive Z Y=-110
###/mydet/setShieldParameters Uranium box container  40  20 20  2  -80   -110  70
#
#  Top F Positive Z Y=-110
###/mydet/setShieldParameters Uranium box container  60  20 20  2  -70 -110  110
#
#  Main I Positive Z Y=-110
###/mydet/setShieldParameters Uranium box container  30 20  100  2   5    -110  70
#
#  Top T Positive Z Y=-110
###/mydet/setShieldParameters Uranium box container  80  20 20    2  90 -110  110
#
#  Main T Positive Z Y=-110
###/mydet/setShieldParameters Uranium box container  30 20  80   2    90  -110  60
#
#  Left Box Positive Z Y=-110
###/mydet/setShieldParameters Lead box container  5.00  40  120  2 -142.5 -110 70
#
#  Right Box Positive Z Y=-110
###/mydet/setShieldParameters Lead box container  5.00  40  120  2 142.5 -110  70
#
#  Up Box Positive Z Y=-110
```

```
###/mydet/setShieldParameters Lead box container  290   40  5   2   0    -110  132.5
#
#  Down Box Positive Z Y=-110
###/mydet/setShieldParameters Lead box  container  290   40  5   2    0     -110  7.5
#
#  Top Box Positive Z Y=-110
###/mydet/setShieldParameters Lead box container  290   5  130   2   0     -87.5  70
#
#  Bottom Box Positive Z Y=-110
###/mydet/setShieldParameters Lead box container  290   5  130   2   0    -132.5  70
#
#/mydet/setShieldParameters Uranium box container 100 100 100      2    0     0     0


#  Main F Negative Z Y=110
###/mydet/setShieldParameters Uranium box container  30 20 100  2  -115 110 -70
#
#  Mid F Negative Z Y=110
###/mydet/setShieldParameters Uranium box container  50  20 20   2  -75  110  -70
#
#  Top F Negative Z Y=110
###/mydet/setShieldParameters Uranium box container  70  20 20   2   -65 110  -30
#
#  Main I Negative Z Y=110
###/mydet/setShieldParameters Uranium box container  30 20  100  2    5   110  -70
#
#  Top T Negative Z Y=110
###/mydet/setShieldParameters Uranium box container  90  20 20    2   85  110  -30
#
#  Main T Negative Z Y=110
###/mydet/setShieldParameters Uranium box container  30 20  80    2   85  110  -80
#
#  Left Box Negative Z Y=110
###/mydet/setShieldParameters Lead box container  5.00  40  120  2 -142.5 110 -70
#
#  Right Box Negative Z Y=110
###/mydet/setShieldParameters Lead box container  5.00  40  120  2  142.5 110 -70
#
#  Up Box Negative Z Y=110
###/mydet/setShieldParameters Lead box container  290   40  5     2    0    110  -7.5
#
#  Down Box Negative Z Y=110
```

```
###/mydet/setShieldParameters Lead box container  290   40  5    2    0  110  -132.5
#
#  Top Box Negative Z Y=110
###/mydet/setShieldParameters Lead box container  290   5  130  2    0   132.5  -70
#
#  Bottom Box Negative Z Y=110
###/mydet/setShieldParameters Lead box container  290   5  130  2    0      87.5  -70
#
#/mydet/setShieldParameters Uranium box container 100 100 100     2    0     0      0


#  Main F Positive Z Y=110
###/mydet/setShieldParameters Uranium box container  30 20  100  2   -115 110 70
#
#  Mid F Positive Z Y=110
###/mydet/setShieldParameters Uranium box container  40  20 20    2   -80  110  70
#
#  Top F Positive Z Y=110
###/mydet/setShieldParameters Uranium box container  60  20 20    2  -70  110 110
#
#  Main I Positive Z Y=110
###/mydet/setShieldParameters Uranium box container  30 20  100   2   5    110  70
#
#  Top T Positive Z Y=110
###/mydet/setShieldParameters Uranium box container  80  20 20    2   90  110 110
#
#  Main T Positive Z Y=110
###/mydet/setShieldParameters Uranium box container  30 20  80    2   90   110  60
#
#  Left Box Positive Z Y=110
###/mydet/setShieldParameters Lead box container  5.00  40  120 2  -142.5  110 70
#
#  Right Box Positive Z Y=110
###/mydet/setShieldParameters Lead box container  5.00  40  120  2  142.5  110 70
#
#  Up Box Positive Z Y=110
###/mydet/setShieldParameters Lead box container  290   40  5    2   0    110  132.5
#
#  Down Box Positive Z Y=110
###/mydet/setShieldParameters Lead box container  290   40  5     2    0      110  7.5
#
#  Top Box Positive Z Y=110
```

```
###/mydet/setShieldParameters Lead box container  290   5  130   2    0   132.5  70
#
#  Bottom Box Positive Z Y=110
###/mydet/setShieldParameters Lead box container  290   5  130   2    0     87.5  70
#
#/mydet/setShieldParameters Uranium box container 100 100 100       2    0     0    0


/mydet/update
#/run/beamOn 14400000
/run/beamOn 30
```

 # Configuration file for all scenarios with uranium and lead boxes in the xy
 # plane. Desired elements to appear in a simulation are uncommented. For
 # example, elements are uncommented to run scenario xy, z = -110 mm now.
 # To run another xy scenario, simply comment out the elements located at z =
 # -110 and uncomment the desired elements. In the Platform and Target
 # section, lines starting with ### can be uncommented. Lines beginning with #
 # are permanent comments, as they describe specific elements being acted on.
#
Cry Settings
/control/verbose 0
/run/verbose 0
/event/verbose 0
/tracking/verbose 0
/CRY/input returnMuons 1
/CRY/input returnGammas 0
/CRY/input returnNeutrons 0
/CRY/input returnElectrons 0
/CRY/input returnPions 0
/CRY/input returnProtons 0
/CRY/input date 2012.5
/CRY/input latitude 90.0
/CRY/input altitude 0
/CRY/input subboxLength 3
#/CRY/input returnGammas 2
#/CRY/input
/CRY/update

Visualization Settings
/vis/verbose 1
/vis/scene/create
#/vis/open OGLIX
/vis/open HepRepFile
/vis/heprep/useSolids 0
/vis/drawVolume
/vis/viewer/zoom 1.
/vis/scene/add/axes 0 0 0 1000 mm
/vis/viewer/set/upVector 0 0 1
/vis/viewer/set/viewpointThetaPhi 100 -65 deg
/vis/scene/add/hits
#/vis/scene/add/logo
#/vis/scene/add/trajectories
/vis/viewer/flush

```
#/vis/viewer/set/style wireframe
/vis/viewer/set/style surface
/vis/scene/endOfEventAction accumulate 1000


#### Output Settings
/mydet/simulationOutput          pocaReconstruction
#/mydet/simulationOutput           coverage
/myanalysis/setOutputPocaFileName  n0


#### Detector geometry
/mydet/setExpHallSize             4000 mm
/mydet/setExpHallMat              G4_AIR
/mydet/setTheLateralDetectors       yes
/mydet/setGapSubDetectorLayers      20 mm
/mydet/setNumberOfSubDetectorLayers 3
/mydet/setMTSSize                 300 mm
/mydet/setMTSHeight               300 mm
/mydet/setVoxelSize               20 mm

#### Platform and Target    MATERIAL  SHAPE MOTHER    SIZE(XYZ)
THICK  POSITION(XYZ)
#/mydet/setShieldParameters Lead box container 250 250 50            2      0  0  36
#/mydet/setShieldParameters Lead box container 250 250 50            2      0  0  -36
#
#  Main F Negative Y Z=0
###/mydet/setShieldParameters Uranium box container  30 100 20   2  -115  -70   0
#
#  Mid F Negative Y Z=0
###/mydet/setShieldParameters Uranium box container  50  20 20     2  -75  -70    0
#
#  Top F Negative Y Z=0
###/mydet/setShieldParameters Uranium box container  70  20 20      2   -65  -30  0
#
#  Main I Negative Y Z=0
###/mydet/setShieldParameters Uranium box container  30 100 20     2    5  -70    0
#
#  Top T Negative Y Z=0
###/mydet/setShieldParameters Uranium box container  90  20 20      2    85   -30  0
#
#  Main T Negative Y Z=0
```

```
###/mydet/setShieldParameters Uranium box container  30 80 20    2     85   -80    0
#
#  Left Box Negative Y Z=0
###/mydet/setShieldParameters Lead box container  5.00  120  40   2  -142.5  -70  0
#
#  Right Box Negative Y Z=0
###/mydet/setShieldParameters Lead box container  5.00  120  40    2  142.5  -70  0
#
#  Up Box Negative Y Z=0
###/mydet/setShieldParameters Lead box container  290   5    40    2   0      -7.5    0
#
#  Down Box Negative Y Z=0
###/mydet/setShieldParameters Lead box container  290   5    40     2   0    -132.5  0
#
#  Top Box Negative Y Z=0
###/mydet/setShieldParameters Lead box container  290   130   5    2    0  -70   22.5
#
#  Bottom Box Negative Y Z=0
###/mydet/setShieldParameters Lead box container  290   130   5    2    0  -70  -22.5
#
#/mydet/setShieldParameters Uranium box container 100 100 100   2     0     0       0


#  Main F Positive Y Z=0
###/mydet/setShieldParameters Uranium box container  30 100 20   2  -115  70     0
#
#  Mid F Positive Y Z=0
###/mydet/setShieldParameters Uranium box container  40  20 20    2   -80   70     0
#
#  Top F Positive Y Z=0
###/mydet/setShieldParameters Uranium box container  60  20 20    2  -70   110    0
#
#  Main I Positive Y Z=0
###/mydet/setShieldParameters Uranium box container  30 100 20    2    5    70     0
#
#  Top T Positive Y Z=0
###/mydet/setShieldParameters Uranium box container  80  20 20     2   90  110    0
#
#  Main T Positive Y Z=0
###/mydet/setShieldParameters  Uranium box container  30 80 20     2   90  60      0
#
#  Left Box Positive Y Z=0
```

```
###/mydet/setShieldParameters Lead box container  5.00  120  40  2  -142.5  70    0
#
#  Right Box Positive Y Z=0
###/mydet/setShieldParameters Lead box container  5.00  120  40  2   142.5  70    0
#
#  Up Box Positive Y Z=0
###/mydet/setShieldParameters Lead box container  290   5    40   2    0     132.5   0
#
#  Down Box Positive Y Z=0
###/mydet/setShieldParameters Lead box container  290   5    40   2    0      7.5     0
#
#  Top Box Positive Y Z=0
###/mydet/setShieldParameters Lead box container  290   130   5    2    0   70   22.5
#
#  Bottom Box Positive Y Z=0
###/mydet/setShieldParameters Lead box container  290   130   5    2    0   70  -22.5
#
#/mydet/setShieldParameters Uranium box container 100 100 100    2    0     0      0


#  Main F Negative Y Z=-110
/mydet/setShieldParameters Uranium box container  30 100 20   2  -115  -70    -110
#
#  Mid F Negative Y Z=-110
/mydet/setShieldParameters Uranium box container  50  20 20    2   -75   -70    -110
#
#  Top F Negative Y Z=-110
/mydet/setShieldParameters Uranium box container  70  20 20     2   -65  -30    -110
#
#  Main I Negative Y Z=-110
/mydet/setShieldParameters Uranium box container  30 100 20    2    5    -70    -110
#
#  Top T Negative Y Z=-110
/mydet/setShieldParameters Uranium box container  90  20 20     2   85   -30    -110
#
#  Main T Negative Y Z=-110
/mydet/setShieldParameters  Uranium box container  30 80 20     2   85   -80    -110
#
#  Left Box Negative Y Z=-110
/mydet/setShieldParameters Lead box container  5.00  120  40   2  -142.5  -70  -110
#
#  Right Box Negative Y Z=-110
```

```
/mydet/setShieldParameters Lead box container  5.00  120  40   2   142.5  -70   -110
#
#  Up Box Negative Y Z=-110
/mydet/setShieldParameters Lead box container  290   5    40   2    0     -7.5   -110
#
#  Down Box Negative Y Z=-110
/mydet/setShieldParameters Lead box container  290   5    40   2    0    -132.5  -110
#
#  Top Box Negative Y Z=-110
/mydet/setShieldParameters Lead box container  290   130   5   2    0     -70    -87.5
#
#  Bottom Box Negative Y Z=-110
/mydet/setShieldParameters Lead box container  290   130   5   2    0    -70    -132.5
#
#/mydet/setShieldParameters Uranium box container 100 100 100    2    0    0    0


#  Main F Positive Y Z=-110
/mydet/setShieldParameters Uranium box container  30 100 20    2  -115  70    -110
#
#  Mid F Positive Y Z=-110
/mydet/setShieldParameters Uranium box container  40  20 20    2   -80   70    -110
#
#  Top F Positive Y Z=-110
/mydet/setShieldParameters Uranium box container  60  20 20     2  -70  110   -110
#
#  Main I Positive Y Z=-110
/mydet/setShieldParameters Uranium box container  30 100 20     2    5    70    -110
#
#  Top T Positive Y Z=-110
/mydet/setShieldParameters Uranium box container  80  20 20       2   90  110  -110
#
#  Main T Positive Y Z=-110
/mydet/setShieldParameters Uranium box container  30 80 20        2    90  60   -110
#
#  Left Box Positive Y Z=-110
/mydet/setShieldParameters Lead box container  5.00  120  40    2  -142.5  70  -110
#
#  Right Box Positive Y Z=-110
/mydet/setShieldParameters Lead box container  5.00  120  40     2  142.5  70  -110
#
#  Up Box Positive Y Z=-110
```

```
/mydet/setShieldParameters Lead box container  290   5    40    2     0    132.5   -110
#
#  Down Box Positive Y Z=-110
/mydet/setShieldParameters Lead box container  290   5    40     2     0     7.5     -110
#
#  Top Box Positive Y Z=-110
/mydet/setShieldParameters Lead box container  290   130   5     2     0    70     -87.5
#
#  Bottom Box Positive Y Z=-110
/mydet/setShieldParameters Lead box container  290   130   5      2     0    70  -132.5
#
#/mydet/setShieldParameters Uranium box container 100 100 100       2    0     0    0


#  Main F Negative Y Z=110
###/mydet/setShieldParameters Uranium box container  30 100 20  2  -115 -70 110
#
#  Mid F Negative Y Z=110
###/mydet/setShieldParameters Uranium box container  50  20 20   2  -75 -70   110
#
#  Top F Negative Y Z=110
###/mydet/setShieldParameters Uranium box container  70  20 20    2  -65  -30 110
#
#  Main I Negative Y Z=110
###/mydet/setShieldParameters Uranium box container  30 100 20    2   5  -70   110
#
#  Top T Negative Y Z=110
###/mydet/setShieldParameters Uranium box container  90  20 20     2  85 -30   110
#
#  Main T Negative Y Z=110
###/mydet/setShieldParameters Uranium box container  30 80 20   2    85   -80  110
#
#  Left Box Negative Y Z=110
###/mydet/setShieldParameters Lead box container  5.00  120  40  2 -142.5 -70 110
#
#  Right Box Negative Y Z=110
###/mydet/setShieldParameters Lead box container  5.00  120  40  2  142.5 -70 110
#
#  Up Box Negative Y Z=110
###/mydet/setShieldParameters Lead box container  290   5    40   2   0    -7.5    110
#
#  Down Box Negative Y Z=110
```

```
###/mydet/setShieldParameters Lead box container  290   5    40  2  0   -132.5  110
#
#  Top Box Negative Y Z=110
###/mydet/setShieldParameters Lead box container  290   130   5  2  0   -70    132.5
#
#  Bottom Box Negative Y Z=110
###/mydet/setShieldParameters Lead box container  290   130   5   2  0   -70     87.5
#
#/mydet/setShieldParameters Uranium box container 100 100 100     2    0     0      0


#  Main F Positive Y Z=110
###/mydet/setShieldParameters Uranium box container  30 100 20   2  -115 70  110
#
#  Mid F Positive Y Z=110
###/mydet/setShieldParameters Uranium box container  40  20 20    2  -80 70    110
#
#  Top F Positive Y Z=110
###/mydet/setShieldParameters Uranium box container  60  20 20   2  -70 110   110
#
#  Main I Positive Y Z=110
###/mydet/setShieldParameters Uranium box container  30 100 20   2   5  70     110
#
#  Top T Positive Y Z=110
###/mydet/setShieldParameters Uranium box container  80  20 20    2   90 110  110
#
#  Main T Positive Y Z=110
###/mydet/setShieldParameters Uranium box container  30 80 20     2   90 60    110
#
#  Left Box Positive Y Z=110
###/mydet/setShieldParameters Lead box container  5.00  120  40  2 -142.5  70 110
#
#  Right Box Positive Y Z=110
###/mydet/setShieldParameters Lead  box container  5.00  120  40  2 142.5  70 110
#
#  Up Box Positive Y Z=110
###/mydet/setShieldParameters Lead box container  290   5    40    2  0  132.5  110
#
#  Down Box Positive Y Z=110
###/mydet/setShieldParameters Lead box container  290   5    40    2   0   7.5    110
#
#  Top Box Positive Y Z=110
```

```
###/mydet/setShieldParameters Lead box container  290   130   5   2   0   70   132.5
#
#  Bottom Box Positive Y Z=110
###/mydet/setShieldParameters Lead box container  290   130   5   2   0   70    87.5
#
#/mydet/setShieldParameters Uranium box container 100 100 100   2   0     0     0


/mydet/update
#/run/beamOn 14400000
/run/beamOn 30
```

Appendix D: Modified Code to Run ROOT Analysis

```
//void analysisMTS(TString configurationFile = "coverage.txt") {
//void analysisMTS(TString configurationFile = "pocaSlices2D.txt") {
void analysisMTS(TString configurationFile = "pocaPoints3D.txt") {
//void analysisMTS(TString configurationFile = "pocaAnalysis.txt") {

  getStyle() ;
  getStyle() ;

  TString firstString, secondString, sim1, sim2, output, expo, slicePlane, reco,
saved3dPlot, fileFormat ;
  TString sizeXStr, sizeYStr, sizeZStr, binSizeStr, offsetStr, maxDocaStr,
maxValueStr, cutStr, minValueStr, cutMuonsStr, binContentStr ;
  Int_t sizeX, sizeY, sizeZ, binSize, offset, binContent ;
  Float_t maxValue, cut, maxDoca, minValue ;
  Int_t numberOfEvents;

  TString configFile = gSystem->UnixPathName(TCint::GetCurrentMacroName());
  configFile.ReplaceAll("analysisMTS.C","");
  configFile.ReplaceAll("/./","/");
  configFile.Append(configurationFile) ;
  ifstream configStream;
  configStream.open(configFile.Data());

  while (1) {
    configStream >> firstString >> secondString ;
    if(firstString == "sim1")       sim1 = secondString ;
    if(firstString == "sim2")       sim2 = secondString ;
    if(firstString == "reco")       reco = secondString ;
    if(firstString == "expo")       expo = secondString;
    if(firstString == "output")     output = secondString ;
    if(firstString == "fileFormat")  fileFormat = secondString ;
    if(firstString == "slicePlane")  slicePlane = secondString ;
    if(firstString == "saved3dPlot") saved3dPlot = secondString ;
    if(firstString == "cutMuons")    cutMuonsStr = secondString ;
    if(firstString == "sizeX")      sizeXStr = secondString ;
    if(firstString == "sizeY")      sizeYStr = secondString ;
    if(firstString == "sizeZ")      sizeZStr = secondString ;
    if(firstString == "offset")     offsetStr = secondString ;
```

```
   if(firstString == "binSize")     binSizeStr = secondString ;
   if(firstString == "maxDoca")     maxDocaStr = secondString ;
   if(firstString == "maxValue")    maxValueStr = secondString ;
   if(firstString == "cut")         cutStr = secondString ;
   if(firstString == "minValue")    minValueStr = secondString ;
   if(firstString == "binContent")  binContentStr = secondString ;
   if(firstString == "numberOfEvents") numberOfEvents = atoi
(secondString.Data());
   if (!configStream.good())       break ;
  }

  sizeX      = atoi(sizeXStr.Data()) ;
  sizeY      = atoi(sizeYStr.Data()) ;
  sizeZ      = atoi(sizeZStr.Data()) ;
  offset     = atoi(offsetStr.Data()) ;
  binSize    = atoi(binSizeStr.Data()) ;
  cutMuons   = atoi(cutMuonsStr.Data()) ;
  cut        = atof(cutStr.Data()) ;
  maxDoca    = atof(maxDocaStr.Data()) ;
  maxValue   = atof(maxValueStr.Data()) ;
  minValue   = atof(minValueStr.Data()) ;
  binContent = atoi(binContentStr.Data()) ;

  printf("sim1        %s\n",sim1.Data());
  printf("sim2        %s\n",sim2.Data());
  printf("reco        %s\n",reco.Data());
  printf("expo        %s\n",expo.Data());
  printf("output      %s\n",output.Data());
  printf("fileFormat  %s\n",fileFormat.Data());
  printf("slicePlane  %s\n",slicePlane.Data());
  printf("saved3dPlot %s\n",saved3dPlot.Data());
  printf("cutMuons    %d\n",cutMuons);
  printf("sizeX       %d\n",sizeX);
  printf("sizeY       %d\n",sizeY);
  printf("sizeZ       %d\n",sizeZ);
  printf("binContent  %d\n",binContent);
  printf("offset      %d\n",offset);
  printf("binSize     %d\n",binSize);
  printf("cut         %f\n",cut);
  printf("maxDoca     %f\n",maxDoca);
  printf("maxValue    %f\n",maxValue);
  printf("minValue    %f\n",minValue);
```

```
  TFile *f = new TFile(Form("%s.root",sim1.Data()),"RECREATE");

  Int_t nbinx = sizeX/binSize;
  Int_t nbiny = sizeY/binSize;
  Int_t nbinz = sizeZ/binSize;
  Int_t total1,  total2 ;
  Float_t norm = 1 ;
  Int_t  maximum = maxValue ;

  if(output == "pocaAnalysis") {
    getPocaRecoAnalysis(sim1,output,reco,fileFormat,sizeX,sizeY,sizeZ,binSize) ;
    getPocaRecoAnalysis(sim2,output,reco,fileFormat,sizeX,sizeY,sizeZ,binSize) ;
  }

  if(output == "coverage3d") {
    if (output == "coverage3d") maximum = getCoverageMax(sim1,sim2) ;

get3dPlots(sim1,expo,output,reco,fileFormat,maximum,cut,0,sizeX,sizeY,sizeZ,bin
Size,cutMuons,binContent,saved3dPlot) ;

get3dPlots(sim2,expo,output,reco,fileFormat,maximum,cut,0,sizeX,sizeY,sizeZ,bin
Size,cutMuons,binContent,saved3dPlot) ;
  }

  if(output == "pocaPoints3d") {
    total1 = getExpoTime(sim1,expo,output,fileFormat) ;
    total2 = getExpoTime(sim2,expo,output,fileFormat) ;

get3dPlots(sim1,expo,output,reco,fileFormat,maximum,cut,total1,sizeX,sizeY,size
Z,binSize,cutMuons,binContent,saved3dPlot,numberOfEvents) ;

get3dPlots(sim2,expo,output,reco,fileFormat,maximum,cut,total1,sizeX,sizeY,size
Z,binSize,cutMuons,binContent,saved3dPlot,numberOfEvents) ;
  }

  if(output == "coverage2d") {
    norm = getCoverageMax(sim1,sim2) ;
    printf(" max= %d\n",maximum);

get2DSlicedHists(sim1,sim2,slicePlane,expo,output,reco,fileFormat,0,0,norm,size
X,sizeY,sizeZ,binSize,offset,maxValue,cut,minValue,cutMuons) ;
   }
```

```
  if(output == "poca2dSlices"){

get2DSlicedHists(sim1,sim2,slicePlane,expo,output,reco,fileFormat,total1,total2,no
rm,sizeX,sizeY,sizeZ,binSize,offset,maxValue,cut,minValue,cutMuons) ;
  }

  configStream.close() ;
  f->Write();
}

void getStyle() {
  gROOT->Reset();
  gStyle->SetOptStat(0);
  gStyle->SetCanvasColor(0) ;
  gStyle->SetCanvasBorderMode(0) ;

  gStyle->SetLabelFont(62,"xyz");
  gStyle->SetLabelSize(0.03,"xyz");
  gStyle->SetLabelColor(1,"xyz");
  gStyle->SetTitleBorderSize(0) ;
  gStyle->SetTitleFillColor(0) ;
  gStyle->SetTitleSize(0.075,"xyz");
  gStyle->SetTitleOffset(4.5,"xyz");
  gStyle->SetPalette(1);

  const Int_t NRGBs = 5;
  const Int_t NCont = 255;
  Double_t stops[NRGBs] = { 0.00, 0.34, 0.61, 0.84, 1.00 };
  Double_t red[NRGBs]   = { 0.00, 0.00, 0.87, 1.00, 0.51 };
  Double_t green[NRGBs] = { 0.00, 0.81, 1.00, 0.20, 0.00 };
  Double_t blue[NRGBs]  = { 0.51, 1.00, 0.12, 0.00, 0.00 };
  TColor::CreateGradientColorTable(NRGBs, stops, red, green, blue, NCont);
  gStyle->SetNumberContours(NCont);
}

Int_t getExpoTime(TString sim, TString expo, TString output, TString fileFormat)
{

  TString dir = gSystem->UnixPathName(TCint::GetCurrentMacroName());
  dir.ReplaceAll("analysisMTS.C","");
  dir.ReplaceAll("/./","/");
  dir.Append(sim) ;
```

```
  ifstream in;
  in.open(Form("%s.txt",dir.Data()));

  Float_t x, y, z, meanAngle, lambda, doca;
  Int_t nTotal = 0;

  while (1) {
    if(fileFormat == "angle")          in >> x >> y >> z >> meanAngle ;
    if(fileFormat == "angleLambda")    in >> x >> y >> z >> meanAngle >> lambda
;
    if(fileFormat == "angleLambdaDoca") in >> x >> y >> z >> meanAngle >>
lambda >> doca ;
    if (!in.good()) break ;
    nTotal++ ;
  }

  if(expo == "4Min") nTotal = (Int_t) (nTotal/2.5) ;
  if(expo == "1Min") nTotal = (Int_t) (nTotal/10) ;

  printf("%d muons in the MTS for %s exposure time\n",nTotal,expo.Data());
  in.close() ;
  return nTotal ;
}

Int_t getCoverageMax(TString sim1, TString sim2) {

  TString dir1 = gSystem->UnixPathName(TCint::GetCurrentMacroName());
  dir1.ReplaceAll("analysisMTS.C","");
  dir1.ReplaceAll("/./","/");
  dir1.Append(sim1) ;
  ifstream in1;
  in1.open(Form("%s.txt",dir1.Data()));

  TString dir2 = gSystem->UnixPathName(TCint::GetCurrentMacroName());
  dir2.ReplaceAll("analysisMTS.C","");
  dir2.ReplaceAll("/./","/");
  dir2.Append(sim2) ;
  ifstream in2;
  in2.open(Form("%s.txt",dir2.Data()));

  Float_t x, y, z ;
  Int_t nlines, coverage, max1, max2, max ;
```

```
  while (1) {
    in1 >> x >> y >> z >> coverage ;
    if (!in1.good()) break ;
    if (coverage > max1) max1 = coverage ;
    nlines++ ;
  }
  printf(" found %d points, max1 value: %d\n",nlines,max1) ;
  in1.close() ;
  nlines = 0 ;

  while (1) {
    in2 >> x >> y >> z >> coverage ;
    if (!in2.good()) break ;
    if (coverage > max2) max2 = coverage ;
    nlines++ ;
  }
  printf(" found %d points, max2 value: %d\n",nlines,max2) ;
  in2.close() ;
  nlines = 0 ;
  if (max1>max2) max = max1 ;
  else           max = max2 ;
  return max ;
}

void getPocaRecoAnalysis(TString sim, TString output, TString reco, TString
fileFormat, Int_t sizeX, Int_t sizeY, Int_t sizeZ, Int_t binSize){

  TString dir = gSystem->UnixPathName(TCint::GetCurrentMacroName());
  dir.ReplaceAll("analysisMTS.C","");
  dir.ReplaceAll("/./","/");
  dir.Append(sim) ;
  ifstream in;
  in.open(Form("%s.txt",dir.Data()));

  Int_t nbinx = sizeX/binSize ;
  Int_t nbiny = sizeY/binSize ;
  Int_t nbinz = sizeZ/binSize ;

  Float_t x, y, z, meanAngle, lambda, parameter, doca, docaReco;
  Int_t nlines, coverage;
```

```
  //  h3d = new TH3F("3dPoca","3dPoca", nbinx,-sizeX/2,sizeX/2,nbiny,-
sizeY/2,sizeY/2,nbinz,-sizeZ/2,sizeZ/2);
  h1d     = new TH1F("1dPoca","1dPoca", nbinx,-sizeX/2,sizeX/2);
  h1dNorm = new TH1F("1dPocaNorm","1dPocaNorm", nbinx,-sizeX/2,sizeX/2);

  while (1) {
    if(fileFormat == "coverage")        in >> x >> y >> z >> coverage ;
    if(fileFormat == "angle")           in >> x >> y >> z >> meanAngle ;
    if(fileFormat == "angleLambda")     in >> x >> y >> z >> meanAngle >> lambda
;
    if(fileFormat == "angleLambdaDoca") in >> x >> y >> z >> meanAngle >>
lambda >> doca ;
    if (!in.good()) break;

    if((x>=-sizeX/2) && (x<=sizeX/2) && (y>=-sizeY/2) && (y<=sizeY/2) &&
(z>=-sizeZ/2) && (z<=sizeZ/2)) {
      if(fileFormat == "coverage")                    parameter = coverage ;
      if(fileFormat == "angle")                      parameter = meanAngle ;
      if((fileFormat == "angleLambda") && (reco == "lambda"))       parameter =
lambda ;
      if((fileFormat == "angleLambda") && (reco == "meanAngle"))    parameter =
meanAngleileFormat  angleLambdaDoca
 ;
      if((fileFormat == "angleLambdaDoca") && (reco == "doca"))     parameter =
doca ;
      if((fileFormat == "angleLambdaDoca") && (reco == "lambda"))   parameter =
lambda ;
      if((fileFormat == "angleLambdaDoca") && (reco == "meanAngle")) parameter
= meanAngle ;
      if((fileFormat == "angleLambdaDoca") && (reco == "docaReco"))  parameter
= lambda/doca ;
      h1d->Fill(x,parameter) ;
      h1dNorm->Fill(x) ;
      nlines++ ;
    }
  }
  h1d->Divide(h1dNorm) ;
}

void get3dPlots(TString sim, TString expo, TString output, TString reco, TString
fileFormat, Float_t maxValue, Float_t cut, Int_t total, Int_t sizeX, Int_t sizeY, Int_t
```

```
sizeZ, Int_t binSize, Int_t nbMuonCut, Int_t binContent, TString saved3dPlot, Int_t
numberOfEvents) {

  TString dir = gSystem->UnixPathName(TCint::GetCurrentMacroName());
  dir.ReplaceAll("analysisMTS.C","");
  dir.ReplaceAll("/./","/");
  dir.Append(sim) ;
  ifstream in;
  in.open(Form("%s.txt",dir.Data()));
  dir.ReplaceAll("10Min",expo.Data());

  Int_t nbinx = sizeX/binSize ;
  Int_t nbiny = sizeY/binSize ;
  Int_t nbinz = sizeZ/binSize ;

  Float_t x, y, z, meanAngle, lambda, parameter, doca, docaReco;
  Int_t nlines, coverage;

  TNtuple *ntuple = new TNtuple(Form("ntuple %s",sim.Data()),"data from ascii
file","x:y:z:parameter");

  Int_t numberOfEventsCounter = 0;

  while (1) {
    if(fileFormat == "coverage")       in >> x >> y >> z >> coverage ;
    if(fileFormat == "angle")          in >> x >> y >> z >> meanAngle ;
    if(fileFormat == "angleLambda")    in >> x >> y >> z >> meanAngle >> lambda
;
    if(fileFormat == "angleLambdaDoca") in >> x >> y >> z >> meanAngle >>
lambda >> doca ;
    if (!in.good() || numberOfEventsCounter >= numberOfEvents) break;
    numberOfEventsCounter++;

    if((x>=-sizeX/2) && (x<=sizeX/2) && (y>=-sizeY/2) && (y<=sizeY/2) &&
(z>=-sizeZ/2) && (z<=sizeZ/2)) {

      if(fileFormat == "coverage")                    parameter = coverage ;
      if(fileFormat == "angle")                       parameter = meanAngle ;
      if((fileFormat == "angleLambda") && (reco == "lambda"))       parameter =
lambda ;
      if((fileFormat == "angleLambda") && (reco == "meanAngle"))    parameter =
meanAngle ;
```

```
    if((fileFormat == "angleLambdaDoca") && (reco == "doca"))      parameter =
doca ;
    if((fileFormat == "angleLambdaDoca") && (reco == "lambda"))    parameter =
lambda ;
    if((fileFormat == "angleLambdaDoca") && (reco == "meanAngle")) parameter
= meanAngle ;
    if((fileFormat == "angleLambdaDoca") && (reco == "docaReco"))  parameter
= lambda/doca ;

    if(output != "coverage3d") {
        if(parameter > cut) {
          if(parameter > maxValue) parameter = maxValue ;
          ntuple->Fill(x,y,z,parameter) ;
        }
    }

    Float_t xMean = 0.0 ;
    Float_t yMean = 0.0 ;
    Float_t zMean = 0.0 ;

    Int_t ii = 0 ;
    Int_t jj = 0 ;
    Int_t kk = 0 ;
    Int_t increment = Int_t (binSize/binContent) ;

    if(output == "coverage3d") {
        for(ii=0; ii<binContent; ii++) {
          for(jj=0; jj<binContent; jj++) {
            for(kk=0; kk<binContent; kk++) {
              xMean = x -0.5*binSize + ii*increment ;
              yMean = y -0.5*binSize + jj*increment ;
              zMean = z -0.5*binSize + kk*increment ;
              ntuple->Fill(xMean,yMean,zMean,parameter) ;
            }
          }
        }
    }
    nlines++ ;
    if(nlines == total) break ;
  }
 }
 printf(" found %d points for histograms\n",nlines);
```

```
  if((output == "pocaPoints3d") || (output == "coverage3d")) {
    ntuple->Fill(-sizeX/2,-sizeY/2,-sizeZ/2,maxValue) ;
    ntuple->Fill(-sizeX/2,-sizeY/2,sizeZ/2,maxValue) ;
    ntuple->Fill(-sizeX/2,sizeY/2,-sizeZ/2,maxValue) ;
    ntuple->Fill(-sizeX/2,sizeY/2,sizeZ/2,maxValue) ;
    ntuple->Fill(sizeX/2,-sizeY/2,-sizeZ/2,maxValue) ;
    ntuple->Fill(sizeX/2,-sizeY/2,sizeZ/2,maxValue) ;
    ntuple->Fill(sizeX/2,sizeY/2,-sizeZ/2,maxValue) ;
    ntuple->Fill(sizeX/2,sizeY/2,sizeZ/2,maxValue) ;

    if(reco == "doca")        ntuple->SetTitle("3d poca-doca");
    if(reco == "lambda")      ntuple->SetTitle("3d poca-lambda");
    if(reco == "meanAngle")   ntuple->SetTitle("3d poca-meanAngle");
    if(reco == "coverage3d")  ntuple->SetTitle("3d coverage");

    if(saved3dPlot == "yes") {
      TString pictureName = image3DFileName(sim, output, cut, maxValue,
"3D.png")  ;
      TCanvas c("3D plots","3D em-plots",80,80,1000,600);
      c.cd();
      ntuple->Draw("z:y:x:parameter","","colz") ;
      ntuple->UseCurrentStyle();
      c.SaveAs(pictureName);
    }

    else {
      ntuple->Draw("z:y:x:parameter","","colz") ;
      ntuple->UseCurrentStyle();
    }
  }

  in.close();
}



void get2DSlicedHists(TString sim1,TString sim2,TString slicePlane,TString
expo,TString output,TString reco,TString fileFormat,Int_t total1,Int_t total2,Int_t
norm,Int_t sizeX,Int_t sizeY,Int_t sizeZ,Float_t binSize,Int_t offset,Float_t
maxValue,Float_t cut,Float_t minValue,Int_t nbMuonCut) {

  TString dir1 = gSystem->UnixPathName(TCint::GetCurrentMacroName());
```

```
dir1.ReplaceAll("analysisMTS.C","");
dir1.ReplaceAll("/./","/");
dir1.Append(sim1) ;

TString dir2 = gSystem->UnixPathName(TCint::GetCurrentMacroName());
dir2.ReplaceAll("analysisMTS.C","");
dir2.ReplaceAll("/./","/");
dir2.Append(sim2) ;

ifstream in1, in2;
in1.open(Form("%s.txt",dir1.Data()));
in2.open(Form("%s.txt",dir2.Data()));

dir1.ReplaceAll("10Min",expo.Data());
dir2.ReplaceAll("10Min",expo.Data());

Int_t size1 = sizeX ;
Int_t size2 = sizeY ;
Int_t size3 = sizeZ ;

Int_t nbin1 = sizeX/binSize ;
Int_t nbin2 = sizeY/binSize ;
Int_t nbin3 = sizeZ/binSize ;
TString histTitle1 = "h1xy2d" ;
TString histTitle2 = "h2xy2d" ;

if(slicePlane == "XZ") {
  nbin1 = sizeX/binSize ;
  nbin2 = sizeZ/binSize ;
  nbin3 = sizeY/binSize ;

  size1 = sizeX ;
  size2 = sizeZ ;
  size3 = sizeY ;

  histTitle1 = "h1xz2d" ;
  histTitle2 = "h2xz2d" ;
}

if(slicePlane == "YZ") {
  nbin1 = sizeY/binSize ;
  nbin2 = sizeZ/binSize ;
```

```
   nbin3 = sizeX/binSize ;

   size1 = sizeY ;
   size2 = sizeZ ;
   size3 = sizeX ;

   histTitle1 = "h1yz2d" ;
   histTitle2 = "h2yz2d" ;
  }

  Float_t x, y, z, coverage, meanAngle, lambda, doca, parameter;
  Int_t nlines = 0;

  TH2F *h2d1[200];
  TH2F *h2d1N[200];
  TH2F *h2d2[200];
  TH2F *h2d2N[200];
  TH2F *h2dratio[200];
  TH2F *hdoca1[200];
  TH2F *hdoca2[200];

  for(int k=0; k<200; k++) {

    TString title2d1Hist  = histTitle1.Append(sim1) ;
    TString title2d2Hist  = histTitle2.Append(sim2) ;

    h2d1[k] = new
TH2F(title2d1Hist.Append(Form("%d",k)),title2d1Hist.Append(Form("%d",k)),
nbin1,-size1/2,size1/2,nbin2,-size2/2,size2/2);
    h2d1N[k] = new TH2F(Form("1%d",k),Form("1%d",k), nbin1,-
size1/2,size1/2,nbin2,-size2/2,size2/2);

    h2d2[k] = new
TH2F(title2d2Hist.Append(Form("%d",k)),title2d2Hist.Append(Form("%d",k)),
nbin1,-size1/2,size1/2,nbin2,-size2/2,size2/2);
    h2d2N[k] = new TH2F(Form("2%d",k),Form("2%d",k), nbin1,-
size1/2,size1/2,nbin2,-size2/2,size2/2);

    hdoca1[k] = new
TH2F(title2d1Hist.Append(Form("doca1%d",k)),title2d1Hist.Append(Form("doca
1%d",k)),nbin1,-size1/2,size1/2,nbin2,-size2/2,size2/2);
```

```
   hdoca2[k] = new
TH2F(title2d1Hist.Append(Form("doca2%d",k)),title2d1Hist.Append(Form("doca
2%d",k)),nbin1,-size1/2,size1/2,nbin2,-size2/2,size2/2);
   if(output =="coverage2d")  h2dratio[k] = new TH2F(Form("ratio
%d",k),Form("ratio %d",k), nbin1,-size1/2,size1/2,nbin2,-size2/2,size2/2);
  }

  while (1) {
   if(fileFormat == "coverage")       in1 >> x >> y >> z >> coverage ;
   if(fileFormat == "angle")          in1 >> x >> y >> z >> meanAngle ;
   if(fileFormat == "angleLambda")    in1 >> x >> y >> z >> meanAngle >>
lambda ;
   if(fileFormat == "angleLambdaDoca") in1 >> x >> y >> z >> meanAngle >>
lambda >> doca ;
   if (!in1.good()) break;
   if(fileFormat == "coverage")                    parameter = coverage ;
   if(fileFormat == "angle")                      parameter = meanAngle ;
   if((fileFormat == "angleLambda") && (reco == "lambda"))       parameter =
lambda ;
   if((fileFormat == "angleLambda") && (reco == "meanAngle"))    parameter =
meanAngle ;
   if((fileFormat == "angleLambdaDoca") && (reco == "doca"))     parameter =
doca ;
   if((fileFormat == "angleLambdaDoca") && (reco == "lambda"))   parameter =
lambda ;
   if((fileFormat == "angleLambdaDoca") && (reco == "meanAngle")) parameter
= meanAngle ;
   if((fileFormat == "angleLambdaDoca") && (reco == "docaReco"))  parameter =
lambda/doca ;

   if(slicePlane == "XY") {
     if((x>=-sizeX/2)&&(x<=sizeX/2)&&(y>=-
sizeY/2)&&(y<=sizeY/2)&&(z>=(offset-sizeZ/2))&&(z<=(offset+sizeZ/2))) {
          Int_t j = (Int_t) ((size3/2 + offset - z)/binSize) + 1  ;
          Int_t k = nbin3 - j ;
          if(k<0) k=0 ;
          h2d1[k]->Fill(x,y,parameter) ;
          hdoca1[k]->Fill(x,y,doca) ;
          h2d1N[k]->Fill(x,y) ;
          if(output =="coverage2d")  h2dratio[k]->Fill(x,y,parameter) ;
     }
   }
```

```
   if(slicePlane == "XZ") {
     if((x>=-sizeX/2)&&(x<=sizeX/2)&&(y>=(offset-
sizeY/2))&&(y<=(offset+sizeY/2))&&(z>=-sizeZ/2)&&(z<=sizeZ/2)) {
          Int_t j = (Int_t) ((size3/2 + offset - y)/binSize) + 1 ;
          Int_t k = nbin3 - j ;
          if(k<0) k=0 ;
          h2d1[k]->Fill(x,z,parameter) ;
          hdoca1[k]->Fill(x,z,doca) ;
          h2d1N[k]->Fill(x,z) ;
          if(output =="coverage2d")  h2dratio[k]->Fill(x,z,parameter) ;
     }
   }

   if(slicePlane == "YZ") {
     if((x>=(offset-sizeX/2))&&(x<=(offset+sizeX/2))&&(y>=-
sizeY/2)&&(y<=sizeY/2)&&(z>=-sizeZ/2)&&(z<=sizeZ/2)) {
          Int_t j = (Int_t) ((size3/2 + offset - x)/binSize) + 1 ;
          Int_t k = nbin3 - j ;
          if(k<0) k=0 ;
          h2d1[k]->Fill(y,z,parameter) ;
          hdoca1[k]->Fill(x,y,doca) ;
          h2d1N[k]->Fill(y,z) ;
          if(output =="coverage2d")  h2dratio[k]->Fill(y,z,parameter) ;
     }
   }
   nlines++;
   if(nlines == total1) break ;
  }

  nlines = 0 ;
  while (1) {

   if(fileFormat == "coverage")       in2 >> x >> y >> z >> coverage ;
   if(fileFormat == "angle")          in2 >> x >> y >> z >> meanAngle ;
   if(fileFormat == "angleLambda")    in2 >> x >> y >> z >> meanAngle >>
lambda ;
   if(fileFormat == "angleLambdaDoca") in2 >> x >> y >> z >> meanAngle >>
lambda >> doca ;
   if (!in2.good()) break;
   if(fileFormat == "coverage")                          parameter = coverage ;
   if(fileFormat == "angle")                            parameter = meanAngle ;
```

```
   if((fileFormat == "angleLambda") && (reco == "lambda"))        parameter =
lambda ;
   if((fileFormat == "angleLambda") && (reco == "meanAngle"))     parameter =
meanAngle ;
   if((fileFormat == "angleLambdaDoca") && (reco == "doca"))      parameter =
doca ;
   if((fileFormat == "angleLambdaDoca") && (reco == "lambda"))    parameter =
lambda ;
   if((fileFormat == "angleLambdaDoca") && (reco == "meanAngle")) parameter
= meanAngle ;
   if((fileFormat == "angleLambdaDoca") && (reco == "docaReco"))  parameter =
lambda/doca ;

   if(slicePlane == "XY") {
     if((x>=-sizeX/2)&&(x<=sizeX/2)&&(y>=-
sizeY/2)&&(y<=sizeY/2)&&(z>=(offset-sizeZ/2))&&(z<=(offset+sizeZ/2))) {
          Int_t j = (Int_t) ((size3/2 + offset - z)/binSize) + 1 ;
          Int_t k = nbin3 - j ;
          if(k<0) k=0 ;
          h2d2[k]->Fill(x,y,parameter) ;
          hdoca2[k]->Fill(x,y,doca) ;
          h2d2N[k]->Fill(x,y) ;
     }
   }
   if(slicePlane == "XZ") {
     if((x>=-sizeX/2)&&(x<=sizeX/2)&&(y>=(offset-
sizeY/2))&&(y<=(offset+sizeY/2))&&(z>=-sizeZ/2)&&(z<=sizeZ/2)) {
          Int_t j = (Int_t) ((size3/2 + offset - y)/binSize) + 1 ;
          Int_t k = nbin3 - j ;
          if(k<0) k=0 ;
          h2d2[k]->Fill(x,z,parameter) ;
          hdoca2[k]->Fill(x,z,doca) ;
          h2d2N[k]->Fill(x,z) ;
     }
   }

   if(slicePlane == "YZ") {
     if((x>=(offset-sizeX/2))&&(x<=(offset+sizeX/2))&&(y>=-
sizeY/2)&&(y<=sizeY/2)&&(z>=-sizeZ/2)&&(z<=sizeZ/2)) {
          Int_t j = (Int_t) ((size3/2 + offset - x)/binSize) + 1 ;
          Int_t k = nbin3 - j ;
          if(k<0) k=0 ;
```

```
          h2d2[k]->Fill(y,z,parameter) ;
          hdoca2[k]->Fill(y,z,doca) ;
          h2d2N[k]->Fill(y,z) ;
     }
    }

    nlines++;
    if(nlines == total2) break ;
   }

   for(int k=0; k<nbin3; k++) {
    Int_t voxel = -size3/2 + offset + (k+0.5)*binSize ;
    Float_t maxVal = 1.0 ;
    if(output == "coverage2d") {
     maxVal = 1 ;
     h2dratio[k]->Divide(h2d2[k]) ;

save2dSlicedHists(h2d1[k],sim1,slicePlane,output,"",norm,voxel,k,maxVal,minVal
ue) ;

save2dSlicedHists(h2d2[k],sim2,slicePlane,output,"",norm,voxel,k,maxVal,minVal
ue) ;
     save2dSlicedHists(h2dratio[k],"ratio",slicePlane,output,"",1,voxel,k,2,0) ;
    }
    else {
     maxVal = maxValue ;
     if(reco == "docaReco") {
          h2d1[k]->Divide(hdoca1[k]) ;
          h2d2[k]->Divide(hdoca2[k]) ;
     }
     else {
          h2d1[k]->Divide(h2d1N[k]) ;
          h2d2[k]->Divide(h2d2N[k]) ;
     }

     for(int i=0; i<nbin1; i++) {
          for(int j=0; j<nbin2; j++) {

            Int_t nbMuons1 = h2d1N[k]->GetBinContent(i,j) ;
            Int_t nbMuons2 = h2d2N[k]->GetBinContent(i,j) ;
            Float_t param1 = h2d1[k]->GetBinContent(i,j) ;
        Float_t param2 = h2d2[k]->GetBinContent(i,j) ;
```

```
          if((nbMuons1 < nbMuonCut) || (param1 < cut)) {
            h2d1[k]->SetBinContent(i,j,0) ;
         h2d1N[k]->SetBinContent(i,j,0) ;
          }

        if((nbMuons2 < nbMuonCut) || (param1 < cut)) {
            h2d2[k]->SetBinContent(i,j,0) ;
         h2d2N[k]->SetBinContent(i,j,0) ;
          }
        }
    }

save2dSlicedHists(h2d1[k],sim1,slicePlane,output,reco,norm,voxel,k,maxVal,min
Value) ;

save2dSlicedHists(h2d2[k],sim2,slicePlane,output,reco,norm,voxel,k,maxVal,min
Value) ;
   }
 }

 in1.close();
 in2.close();
}

void save2dSlicedHists(TH2F *h2d, TString input, TString slicePlane, TString
output, TString reco, Float_t norm, Int_t sliceCut, Int_t number, Float_t maxVal,
Float_t minVal) {

 TString title       =
image2DFileName(input,reco,slicePlane,norm,sliceCut,number,"")  ;
 TString pictureName =
image2DFileName(input,reco,slicePlane,0.0,sliceCut,number,".png")  ;

 if(output == "coverage2d") {
  h2d->Scale(1/norm) ;
  h2d->Smooth();
 }

 if(slicePlane == "XY") {
  h2d->GetXaxis()->SetTitle("X [mm]");
  h2d->GetYaxis()->SetTitle("Y [mm]");
 }
```

```
  if(slicePlane == "XZ") {
    h2d->GetXaxis()->SetTitle("X [mm]");
    h2d->GetYaxis()->SetTitle("Z [mm]");
  }
  if(slicePlane == "YZ") {
    h2d->GetXaxis()->SetTitle("Y [mm]");
    h2d->GetYaxis()->SetTitle("Z [mm]");
  }

//  h2d->Draw("lego2");
  h2d->Draw("colz");
  h2d->UseCurrentStyle();
  h2d->GetXaxis()->SetTitleOffset(0.95);
  h2d->GetXaxis()->SetTitleSize(0.04);
  h2d->GetXaxis()->SetLabelOffset(0.01);
  h2d->GetXaxis()->SetLabelSize(0.03);
  h2d->GetYaxis()->SetTitleOffset(1.15);
  h2d->GetYaxis()->SetTitleSize(0.04);
  h2d->GetYaxis()->SetLabelOffset(0.01);
  h2d->GetYaxis()->SetLabelSize(0.03);
  h2d->SetMinimum(minVal);
  h2d->SetMaximum(maxVal);
  h2d->SetTitle(title);
  TImage *img = TImage::Create();
  img->FromPad(c1);
  img->WriteImage(pictureName);
  delete img;
  c1->Close();
}

TString image3DFileName(TString input, TString output, Float_t cut, Float_t
maxValue, TString extension) {
  TString output = Form("%s",input.Data())  ;
  TString image ="" ;
  if(output.Data() == "pocaPoints3d") {
    image.Append("LambdaCut") ;
    image.Append(Form("%4.2f",cut)) ;
    image.Append("_POCA") ;
  }
  if(output.Data() == "coverage3d")  image.Append("_Coverage") ;
  image.Append(extension) ;
  output.Append(image) ;
```

```
  return output ;
}


TString image2DFileName(TString input, TString reco, TString slicePlane, Float_t
norm, Int_t sliceCut, Int_t number, TString extension) {

  TString sliceAxis ;
  if(slicePlane == "XY") sliceAxis ="Z" ;
  if(slicePlane == "XZ") sliceAxis ="Y" ;
  if(slicePlane == "YZ") sliceAxis ="X" ;

  TString output = Form("%s",input.Data())  ;
  TString slicePlane = Form("%sat%s",slicePlane.Data(),sliceAxis.Data())  ;
  output.Append(reco) ;
  output.Append(slicePlane) ;
  output.Append(Form("%d",number)) ;
  output.Append("_") ;

  TString image ;
  image = Form("%d",sliceCut) ;
  image.Append("mm") ;
  image.ReplaceAll("-","minus") ;
  if(norm !=0) {
    image.Append("_max") ;
    image.Append(Form("%4.0f",norm)) ;
  }
  image.Append(extension) ;

  output.Append(image) ;
  return output ;
}
```

Appendix E: Simulated Scenarios Not in Body of Thesis

The following images are of time exposures of 4 minutes, 10 minutes, and 60 minutes for simulated scenarios mentioned in the body of the thesis. They are presented here in the order in which they are given in the thesis and begin on the following page.

POCA plot for shielded scenario xy, z = -110 mm, with 4 minutes exposure time viewed in the xy plane. The positive z axis is pointing out of the screen.

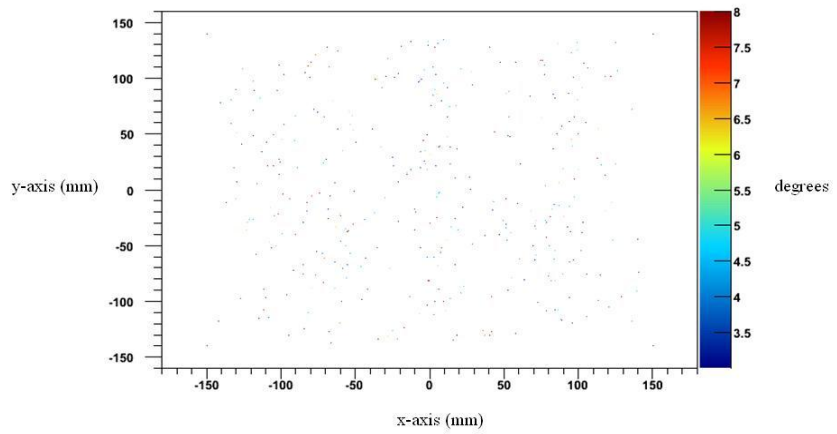

POCA plot for shielded scenario xy, z = -110 mm, with 10 minutes exposure time viewed in the xy plane. The positive z axis is pointing out of the screen.

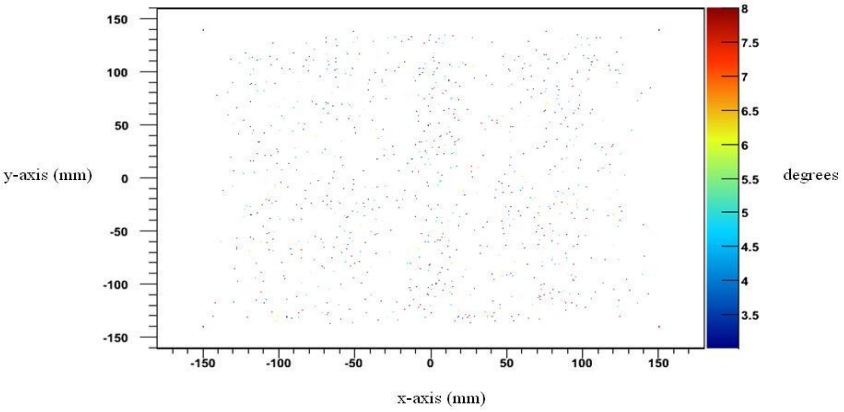

POCA plot for shielded scenario xy, z = -110 mm, with 60 minutes exposure time viewed in the xy plane. The positive z axis is pointing out of the screen.

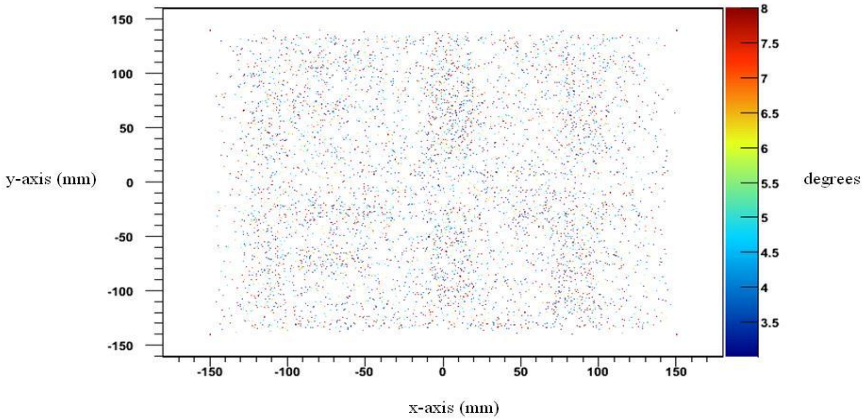

POCA plot for shielded scenario xy, z = 0 mm, with 4 minutes exposure time viewed in the xy plane. The positive z axis is pointing out of the screen.

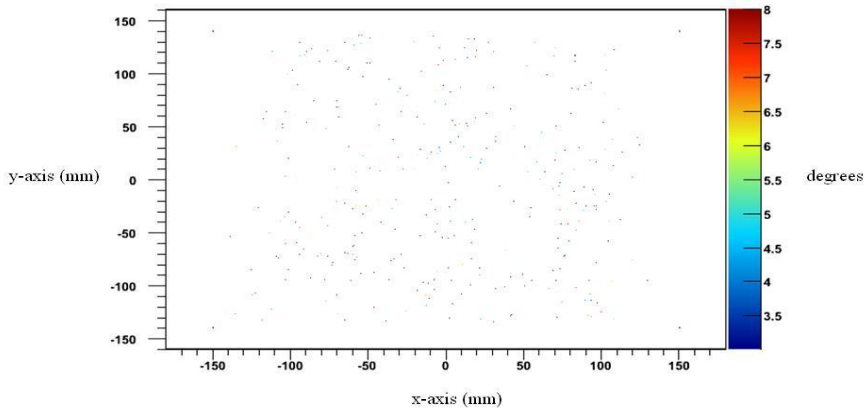

POCA plot for shielded scenario xy, z = 0 mm, with 10 minutes exposure time viewed in the xy plane. The positive z axis is pointing out of the screen.

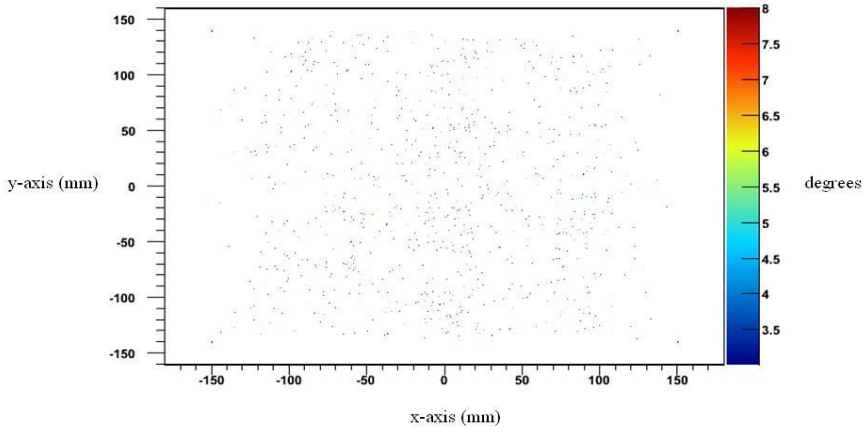

POCA plot for shielded scenario xy, z = 0 mm, with 60 minutes exposure time viewed in the xy plane. The positive z axis is pointing out of the screen.

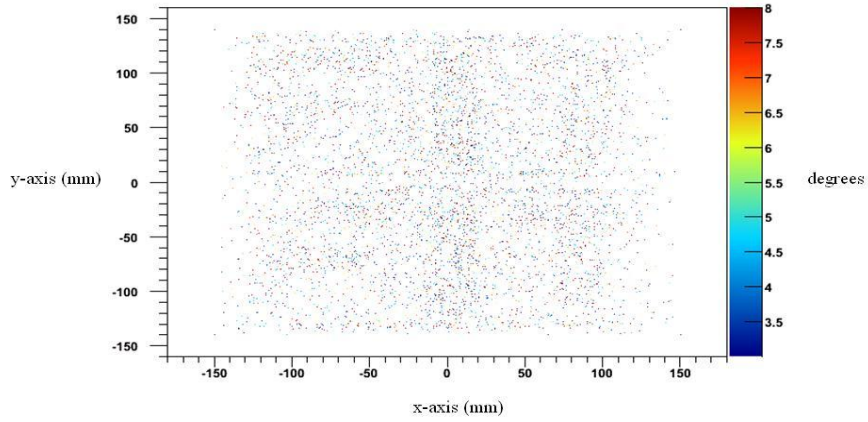

POCA plot for shielded scenario xy, z = 110 mm, with 4 minutes exposure time viewed in the xy plane. The positive z axis is pointing out of the screen.

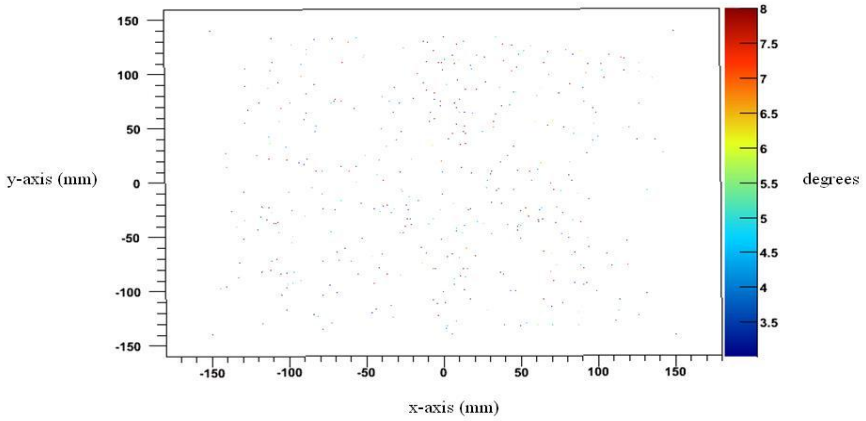

POCA plot for shielded scenario xy, z = 110 mm, with 10 minutes exposure time viewed in the xy plane. The positive z axis is pointing out of the screen.

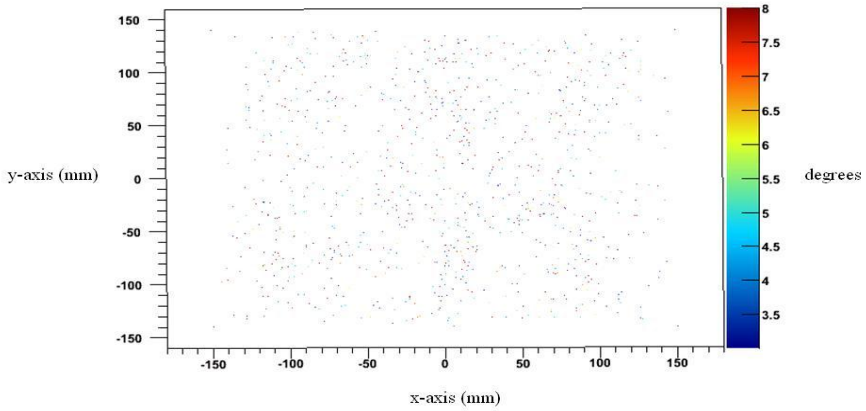

POCA plot for shielded scenario xy, z = 110 mm, with 60 minutes exposure time viewed in the xy plane. The positive z axis is pointing out of the screen.

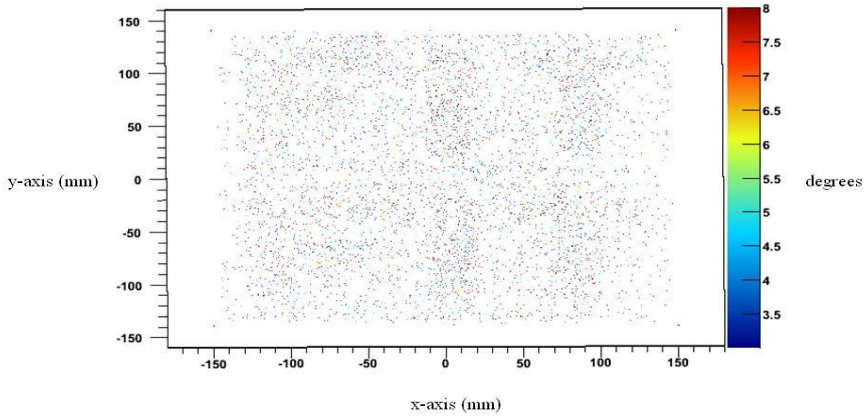

POCA plot for shielded scenario xy, z = -110 mm, with 4 minutes exposure time viewed in the yz plane. The positive x axis is pointing out of the screen.

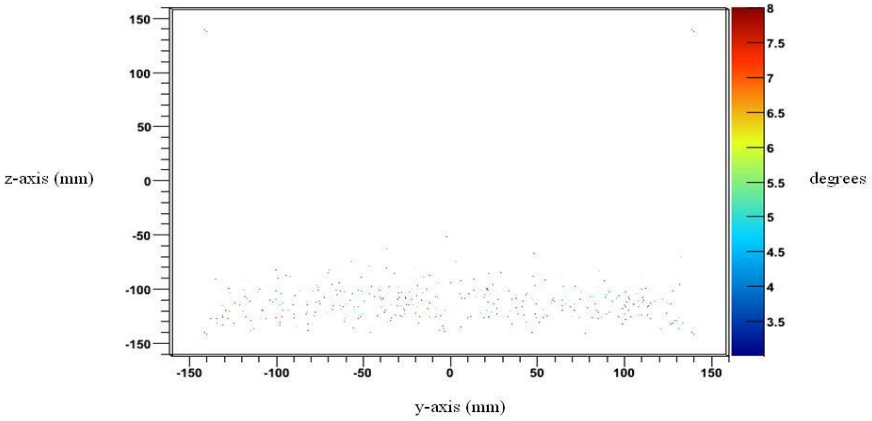

POCA plot for shielded scenario xy, z = -110 mm, with 10 minutes exposure time viewed in the yz plane. The positive x axis is pointing out of the screen.

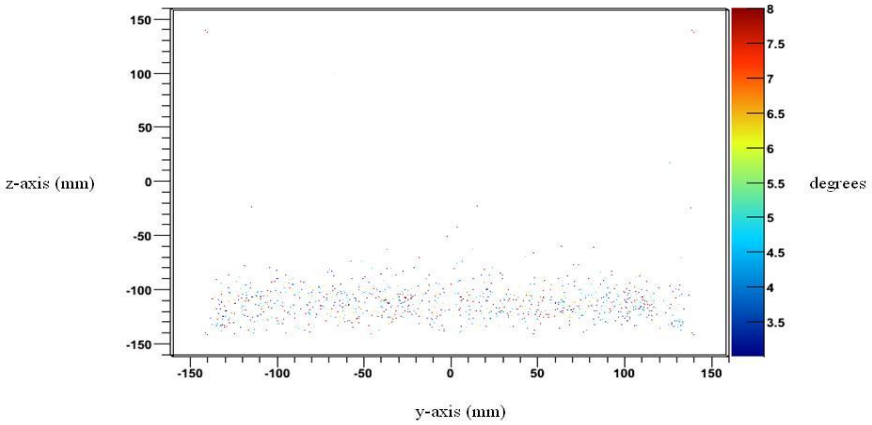

POCA plot for shielded scenario xy, z = -110 mm, with 60 minutes exposure time viewed in the yz plane. The positive x axis is pointing out of the screen.

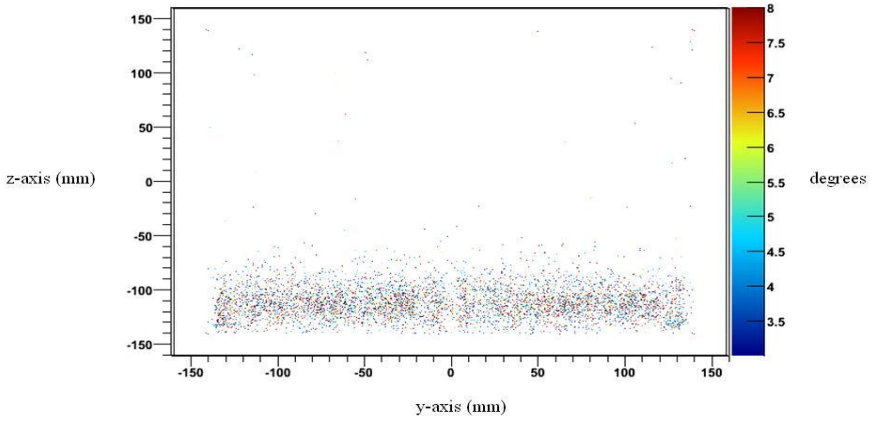

POCA plot for shielded scenario xy, z = 0 mm, with 4 minutes exposure time viewed in the yz plane. The positive x axis is pointing out of the screen.

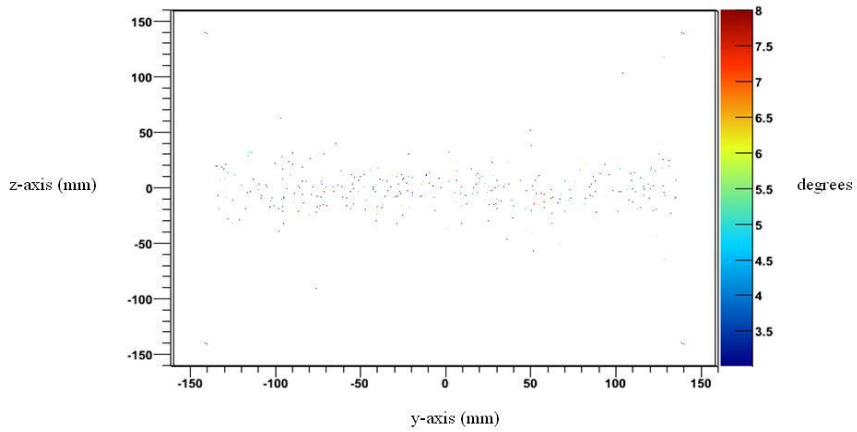

POCA plot for shielded scenario xy, z = 0 mm, with 10 minutes exposure time viewed in the yz plane. The positive x axis is pointing out of the screen.

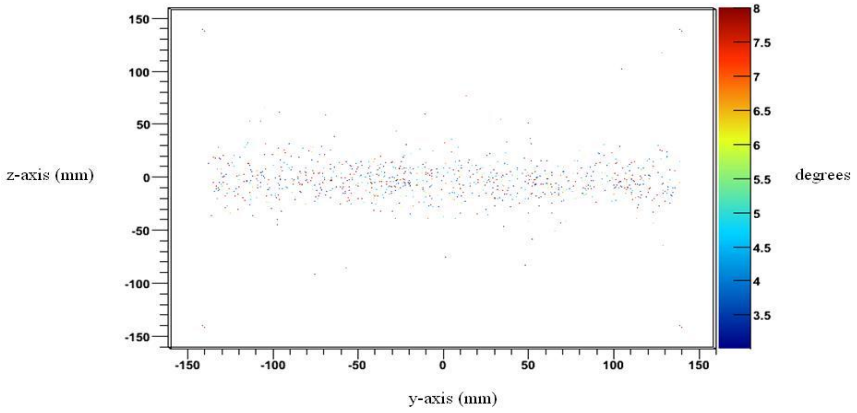

POCA plot for shielded scenario xy, z = 0 mm, with 60 minutes exposure time viewed in the yz plane. The positive x axis is pointing out of the screen.

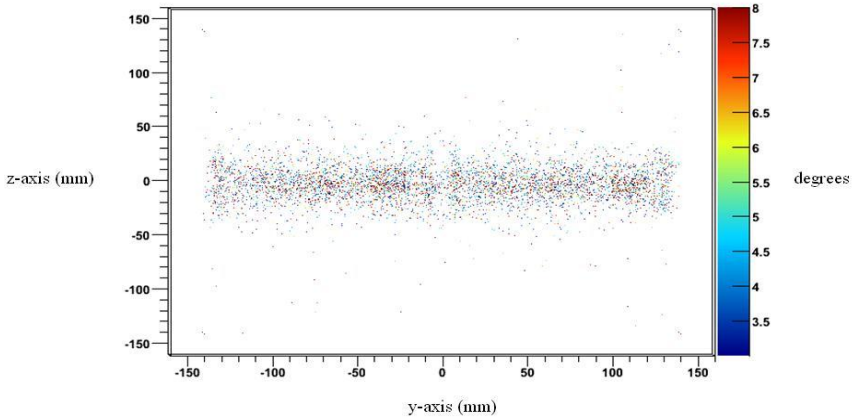

POCA plot for shielded scenario xy, z = 110 mm, with 4 minutes exposure time viewed in the yz plane. The positive x axis is pointing out of the screen.

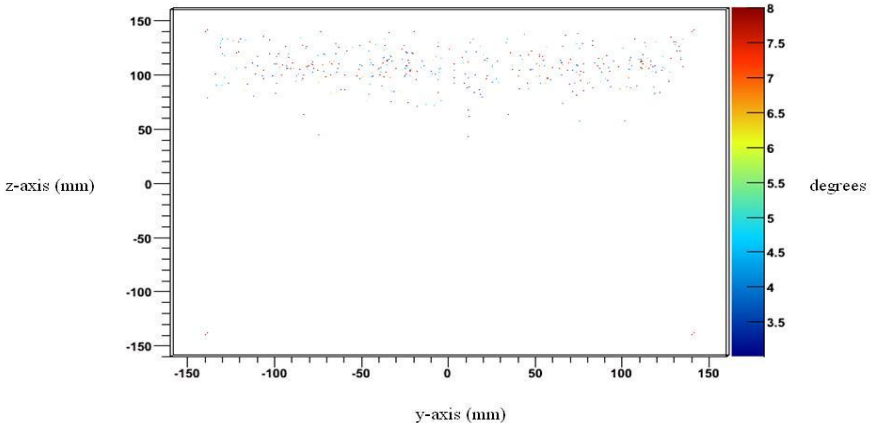

POCA plot for shielded scenario xy, z = 110 mm, with 10 minutes exposure time viewed in the yz plane. The positive x axis is pointing out of the screen.

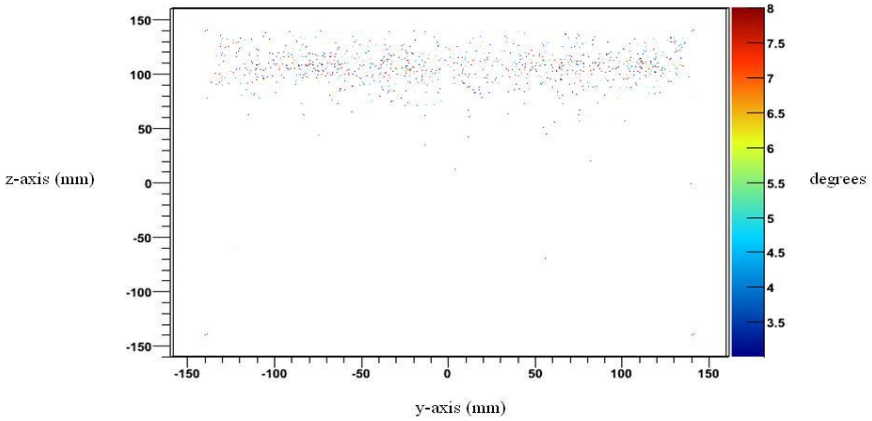

POCA plot for shielded scenario xy, z = 110 mm, with 60 minutes exposure time viewed in the yz plane. The positive x axis is pointing out of the screen.

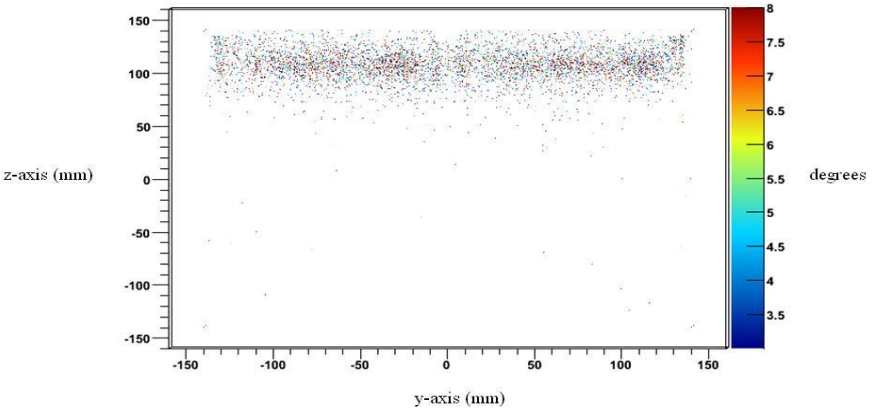

POCA plot for shielded scenario yz, x = -110 mm, with 4 minute exposure time viewed in the yz plane. The positive x axis is pointing out of the screen.

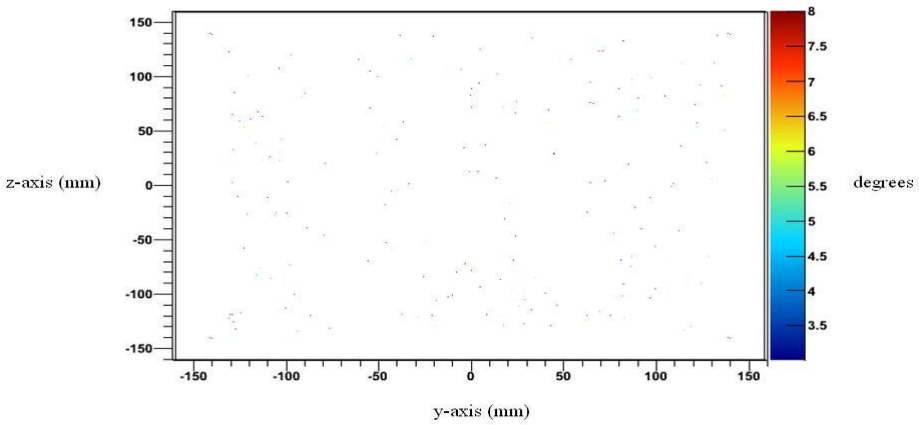

POCA plot for shielded scenario yz, x = -110 mm, with 10 minute exposure time viewed in the yz plane. The positive x axis is pointing out of the screen.

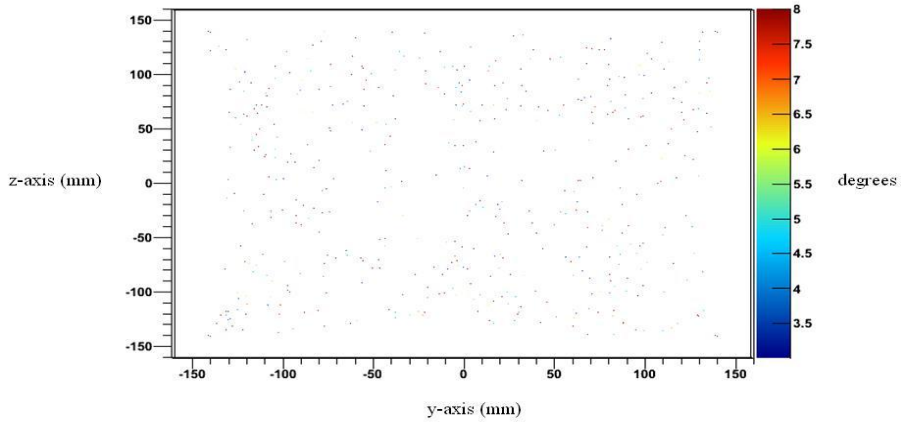

POCA plot for shielded scenario yz, x = -110 mm, with 60 minute exposure time viewed in the yz plane. The positive x axis is pointing out of the screen.

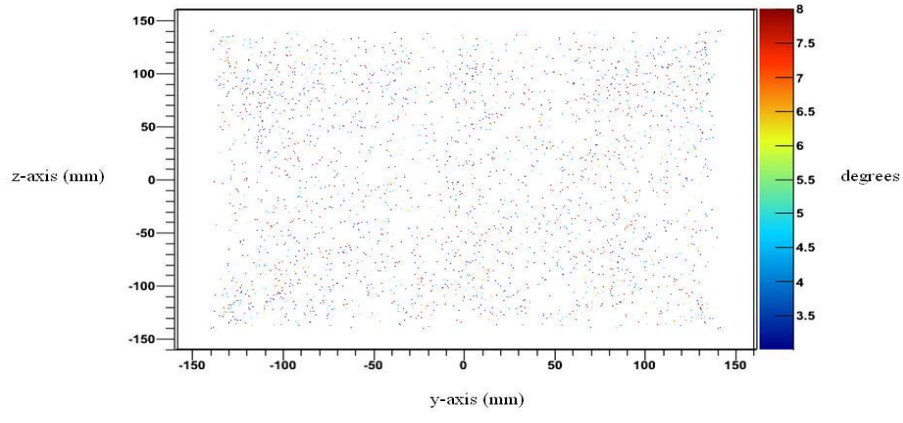

POCA plot for shielded scenario yz, x = 0 mm, with 4 minute exposure time viewed in the yz plane. The positive x axis is pointing out of the screen.

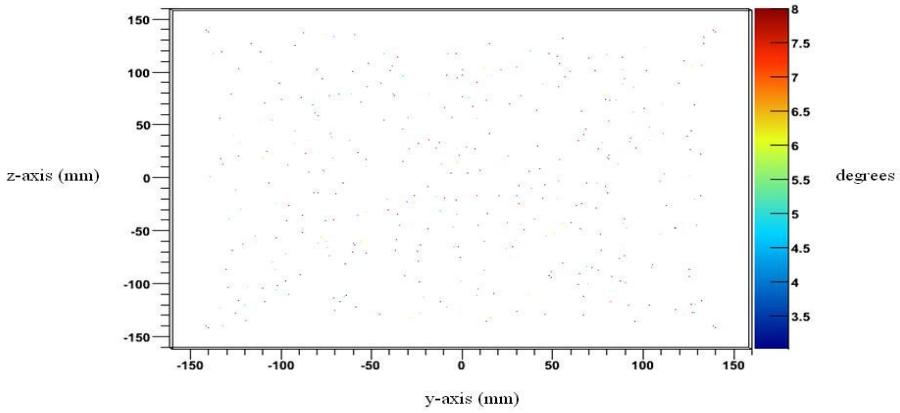

POCA plot for shielded scenario yz, x = 0 mm, with 10 minute exposure time viewed in the yz plane. The positive x axis is pointing out of the screen.

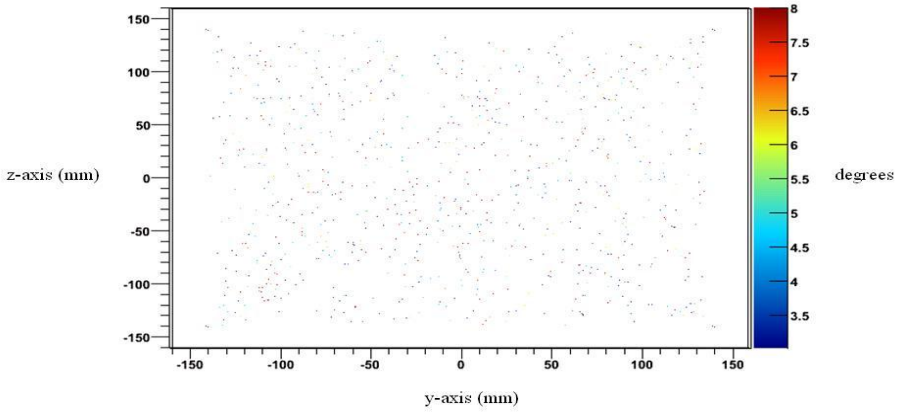

POCA plot for shielded scenario yz, x = 0 mm, with 60 minute exposure time viewed in the yz plane. The positive x axis is pointing out of the screen.

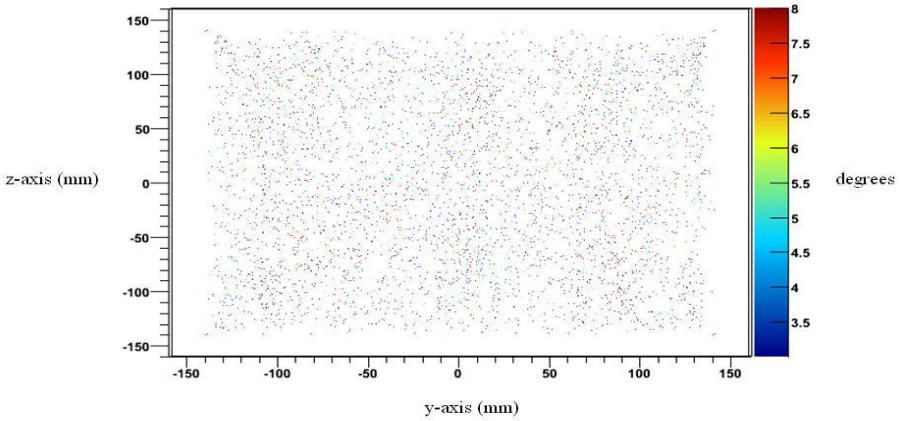

POCA plot for shielded scenario yz, x = 110 mm, with 4 minute exposure time viewed in the yz plane. The positive x axis is pointing out of the screen.

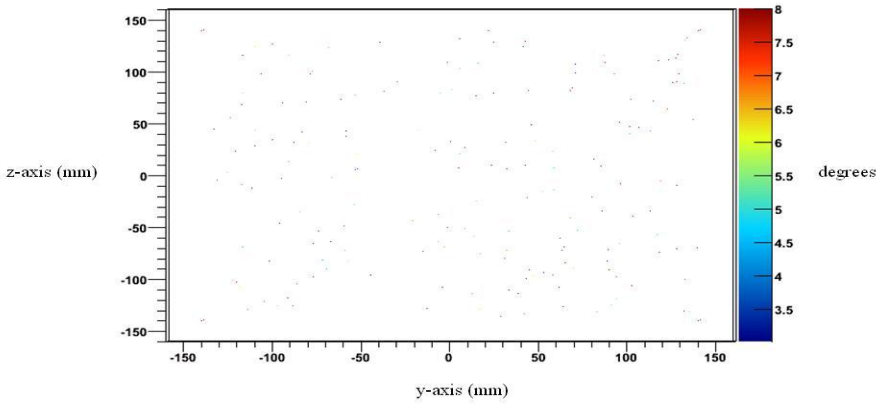

POCA plot for shielded scenario yz, x = 110 mm, with 10 minute exposure time viewed in the yz plane. The positive x axis is pointing out of the screen.

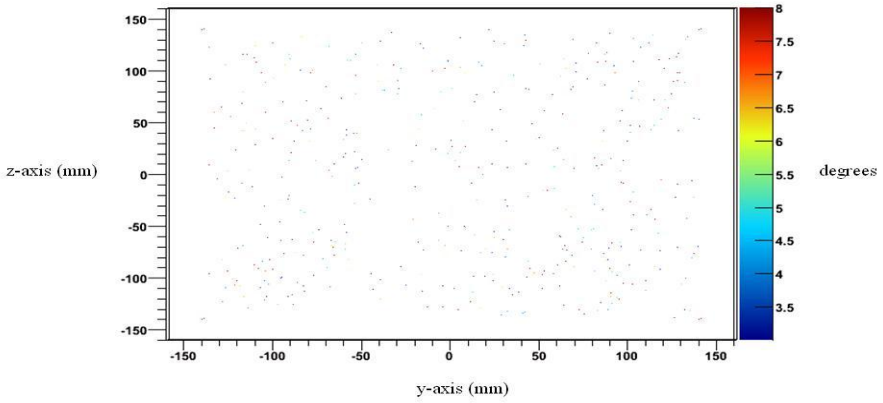

POCA plot for shielded scenario yz, x = 110 mm, with 60 minute exposure time viewed in the yz plane. The positive x axis is pointing out of the screen.

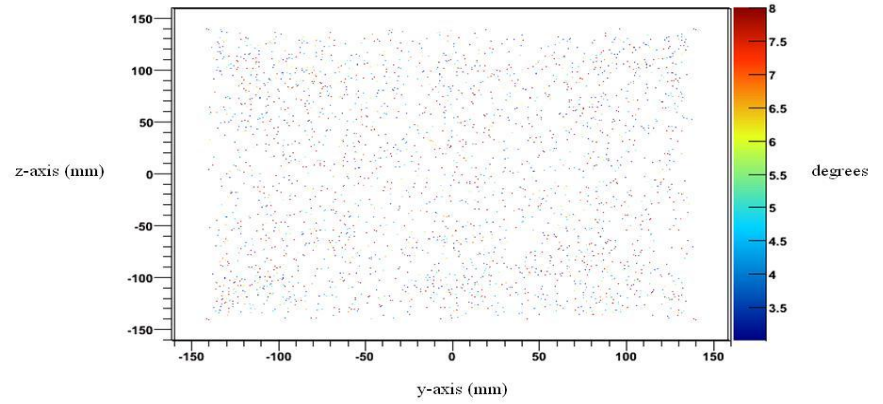

POCA plot for shielded scenario yz, x = -110 mm, with 4 minute exposure time viewed in the xz plane. The negative y axis is pointing out of the screen.

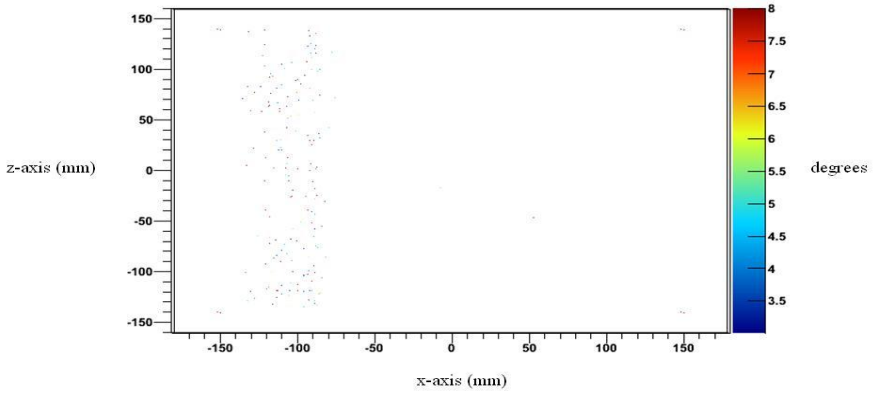

POCA plot for shielded scenario yz, x = -110 mm, with 10 minute exposure time viewed in the xz plane. The negative y axis is pointing out of the screen.

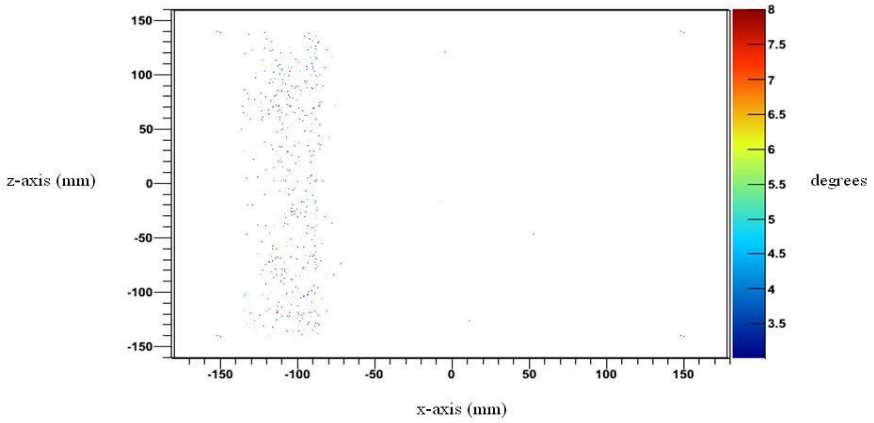

POCA plot for shielded scenario yz, x = -110 mm, with 60 minute exposure time viewed in the xz plane. The negative y axis is pointing out of the screen.

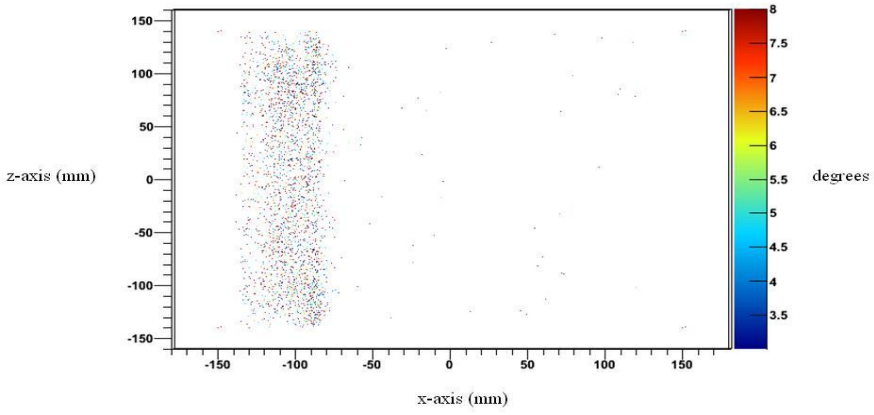

POCA plot for shielded scenario yz, x = 0 mm, with 4 minute exposure time viewed in the xz plane. The negative y axis is pointing out of the screen.

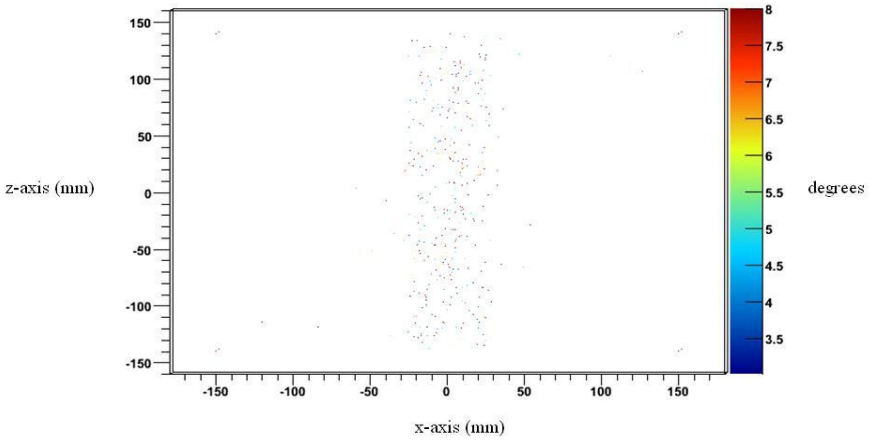

POCA plot for shielded scenario yz, x = 0 mm, with 10 minute exposure time viewed in the xz plane. The negative y axis is pointing out of the screen.

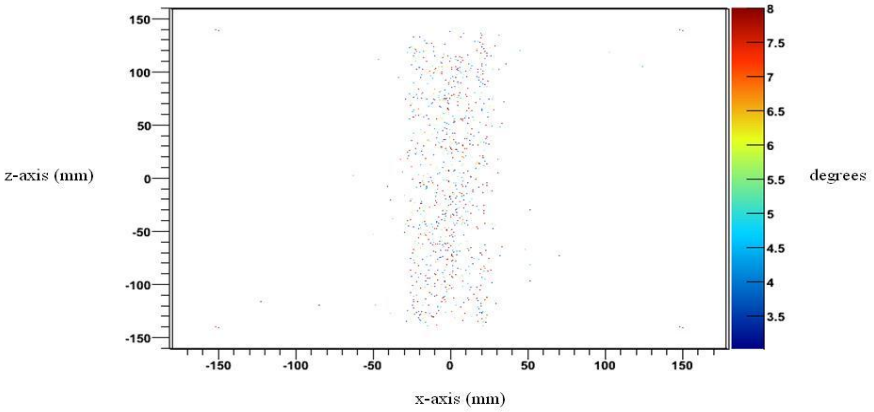

POCA plot for shielded scenario yz, x = 0 mm, with 60 minute exposure time viewed in the xz plane. The negative y axis is pointing out of the screen.

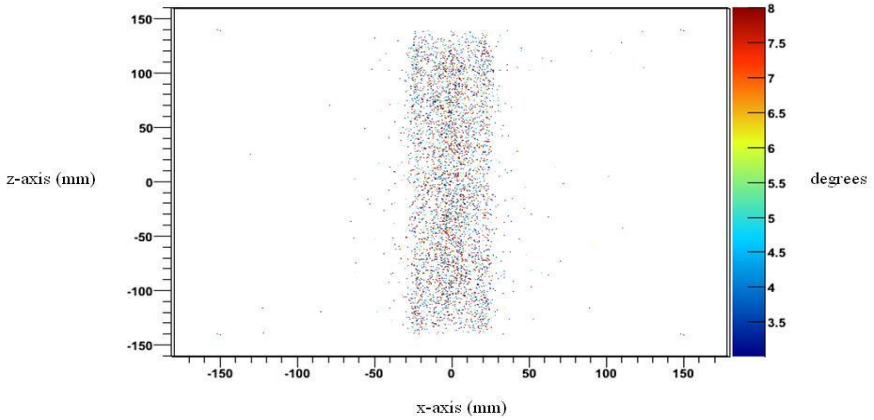

POCA plot for shielded scenario yz, x = 110 mm, with 4 minute exposure time viewed in the xz plane. The negative y axis is pointing out of the screen.

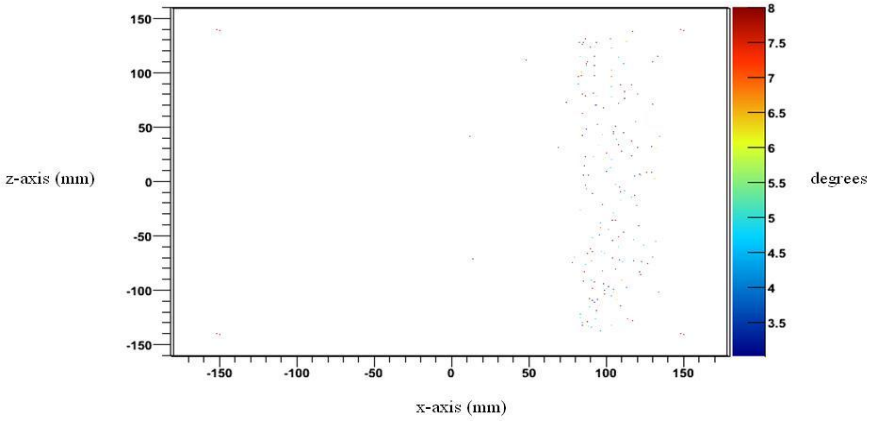

POCA plot for shielded scenario yz, x = 110 mm, with 10 minute exposure time viewed in the xz plane. The negative y axis is pointing out of the screen.

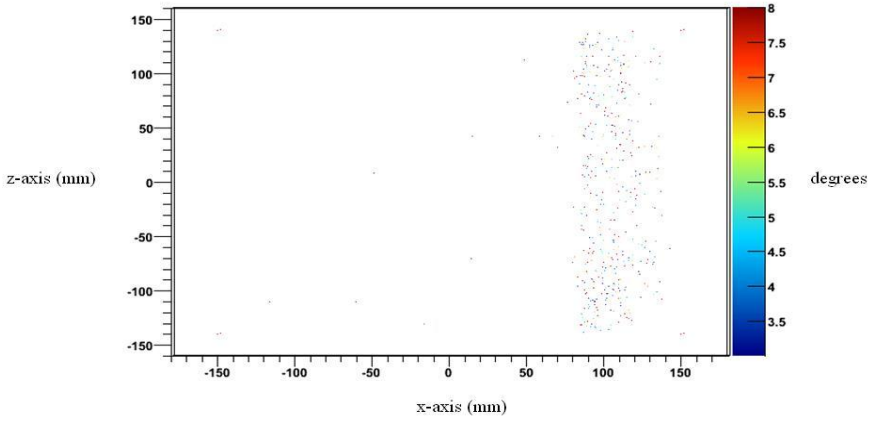

POCA plot for shielded scenario yz, x = 110 mm, with 60 minute exposure time viewed in the xz plane. The negative y axis is pointing out of the screen.

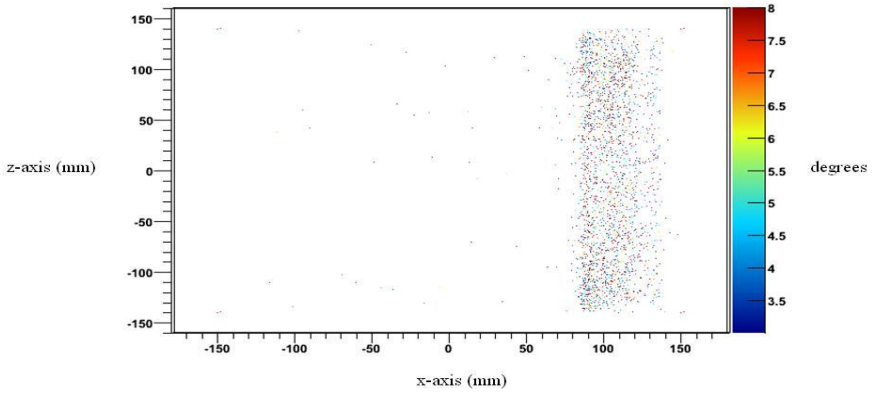

POCA plot for shielded scenario xz, y = -110 mm, with 4 minute exposure time viewed in the xz plane. The negative y axis is pointing out of the screen.

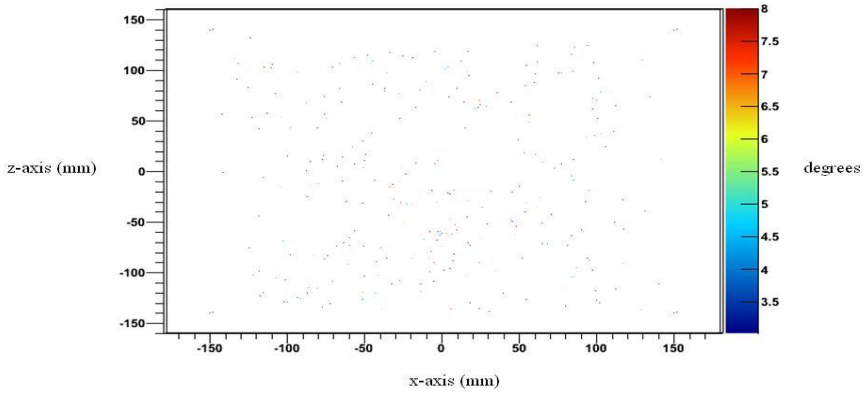

POCA plot for shielded scenario xz, y = -110 mm, with 10 minute exposure time viewed in the xz plane. The negative y axis is pointing out of the screen.

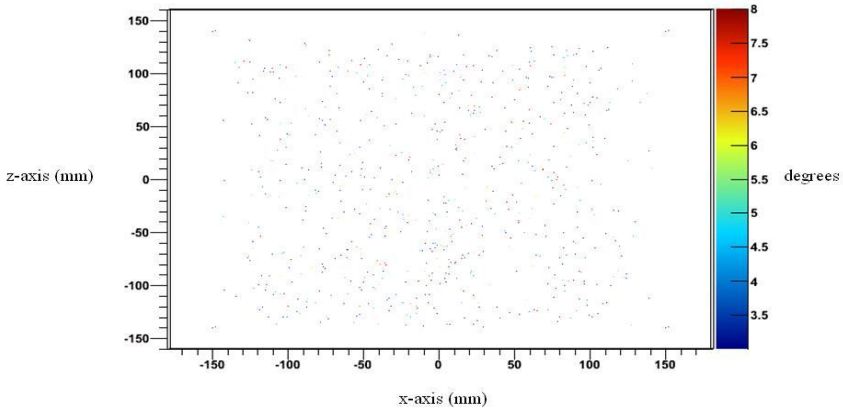

POCA plot for shielded scenario xz, y = -110 mm, with 60 minute exposure time viewed in the xz plane. The negative y axis is pointing out of the screen.

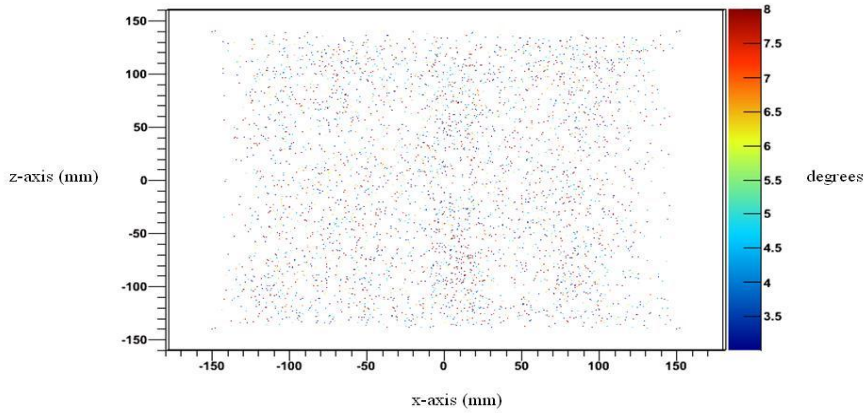

POCA plot for shielded scenario xz, y = 0 mm, with 4 minute exposure time viewed in the xz plane. The negative y axis is pointing out of the screen.

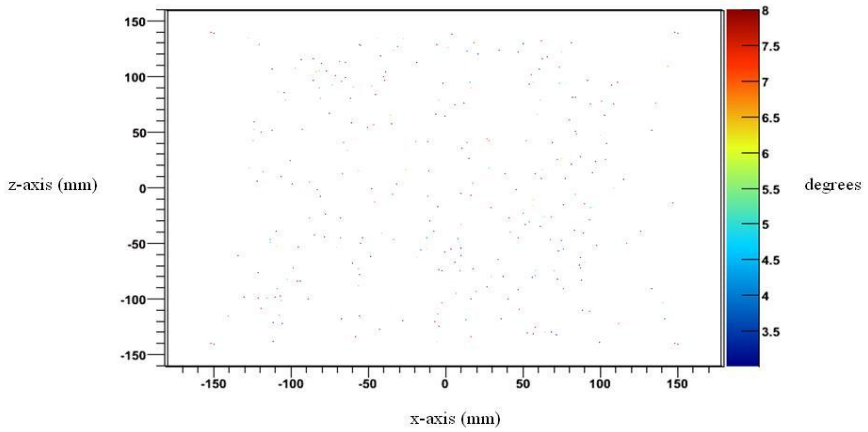

POCA plot for shielded scenario xz, y = 0 mm, with 10 minute exposure time viewed in the xz plane. The negative y axis is pointing out of the screen.

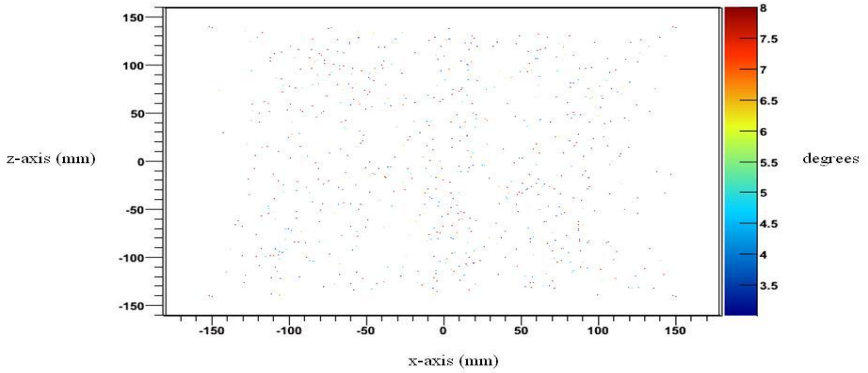

POCA plot for shielded scenario xz, y = 0 mm, with 60 minute exposure time viewed in the xz plane. The negative y axis is pointing out of the screen.

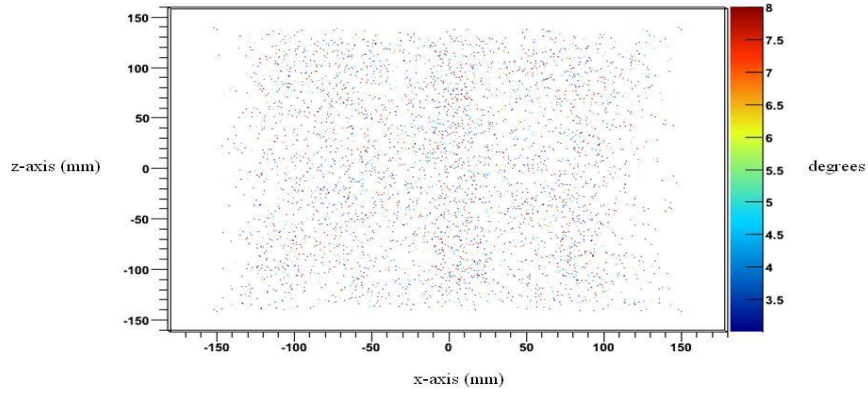

POCA plot for shielded scenario xz, y = 110 mm, with 4 minute exposure time viewed in the xz plane. The negative y axis is pointing out of the screen.

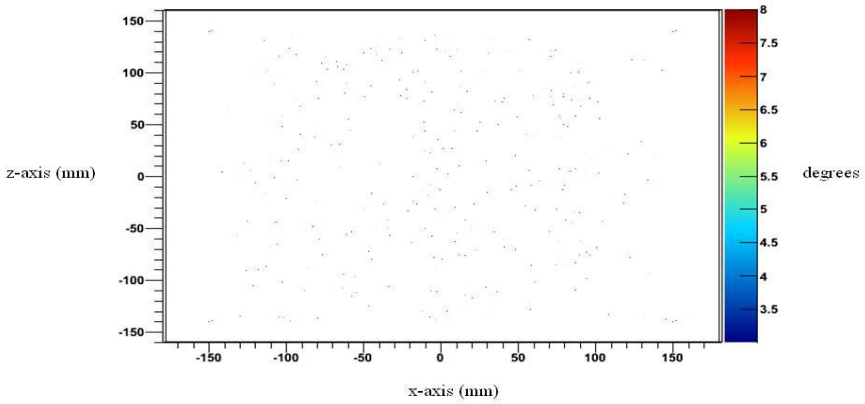

POCA plot for shielded scenario xz, y = 110 mm, with 10 minute exposure time viewed in the xz plane. The negative y axis is pointing out of the screen.

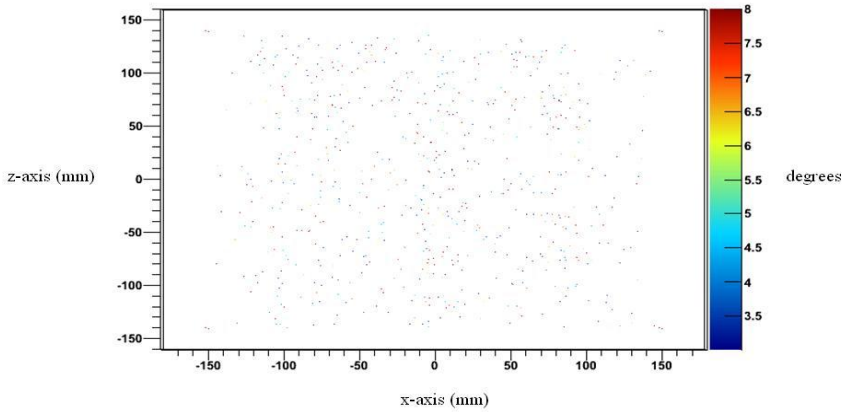

POCA plot for shielded scenario xz, y = 110 mm, with 60 minute exposure time viewed in the xz plane. The negative y axis is pointing out of the screen.

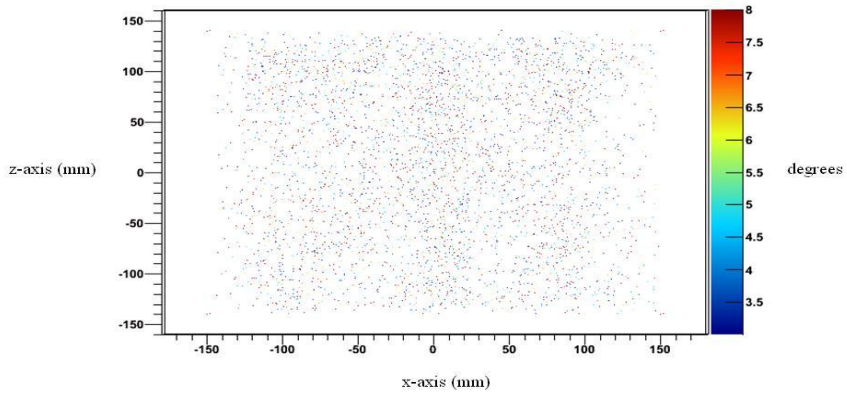

POCA plot for shielded scenario xz, y = -110 mm, with 4 minute exposure time viewed in the yz plane. The positive x axis is pointing out of the screen.

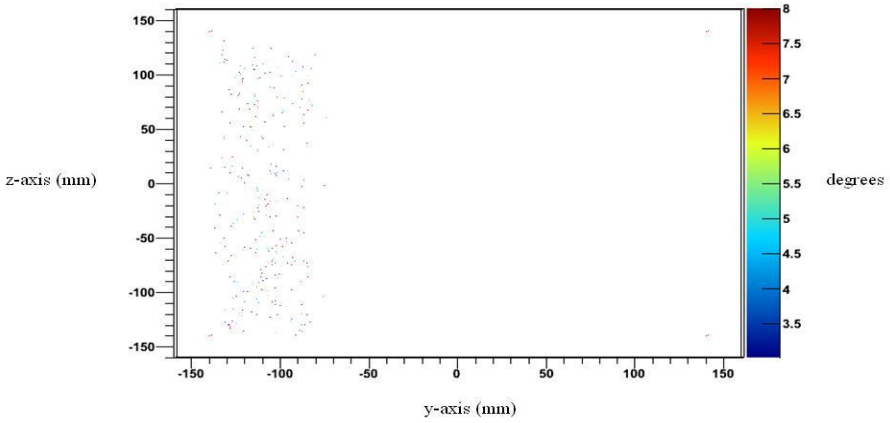

POCA plot for shielded scenario xz, y = -110 mm, with 10 minute exposure time viewed in the yz plane. The positive x axis is pointing out of the screen.

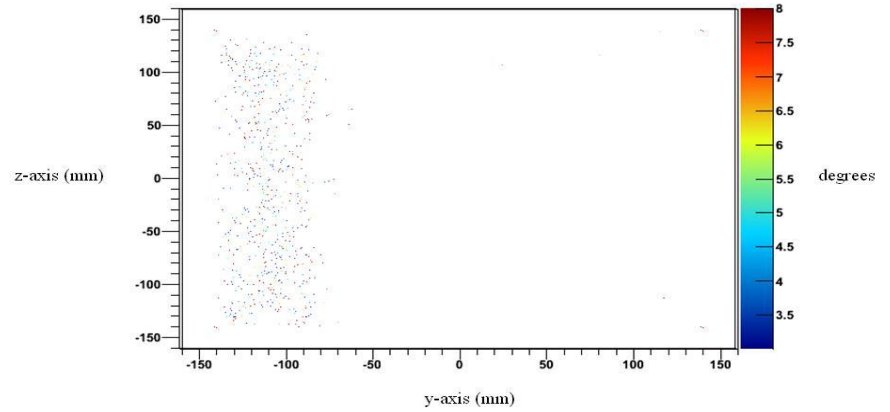

POCA plot for shielded scenario xz, y = -110 mm, with 60 minute exposure time viewed in the yz plane. The positive x axis is pointing out of the screen.

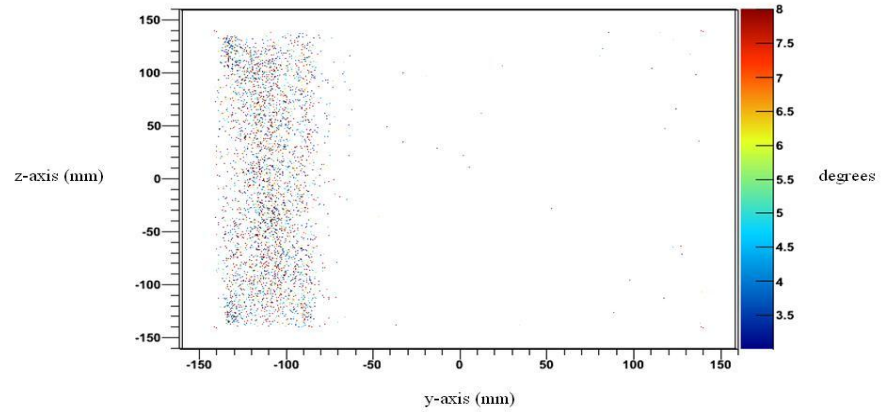

POCA plot for shielded scenario xz, y = 0 mm, with 4 minute exposure time viewed in the yz plane. The positive x axis is pointing out of the screen.

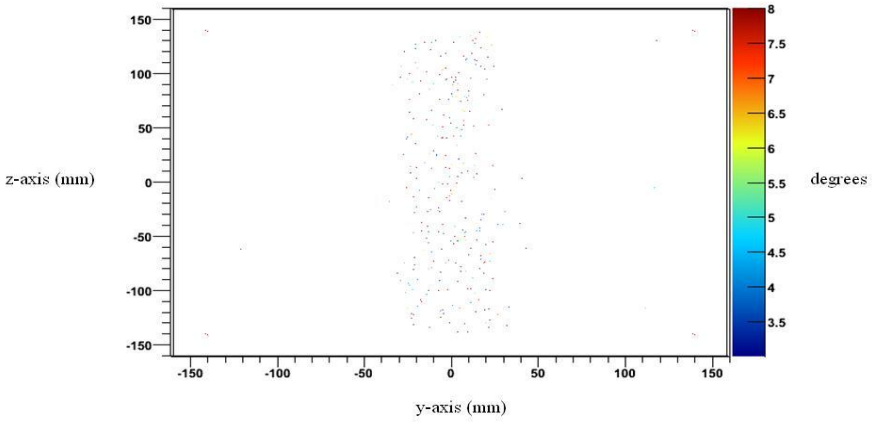

POCA plot for shielded scenario xz, y = 0 mm, with 10 minute exposure time viewed in the yz plane. The positive x axis is pointing out of the screen.

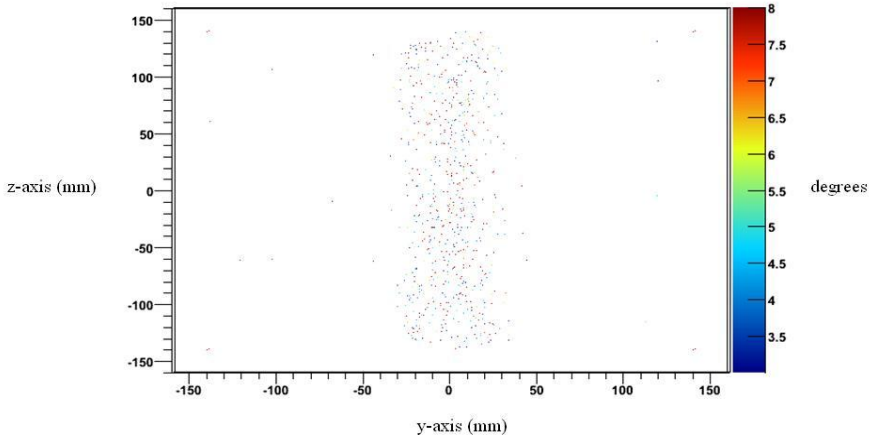

POCA plot for shielded scenario xz, y = 0 mm, with 60 minute exposure time viewed in the yz plane. The positive x axis is pointing out of the screen.

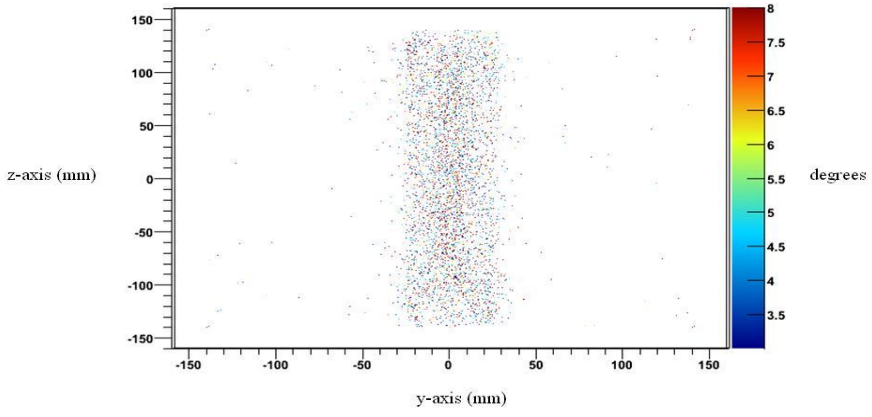

POCA plot for shielded scenario xz, y = 110 mm, with 4 minute exposure time viewed in the yz plane. The positive x axis is pointing out of the screen.

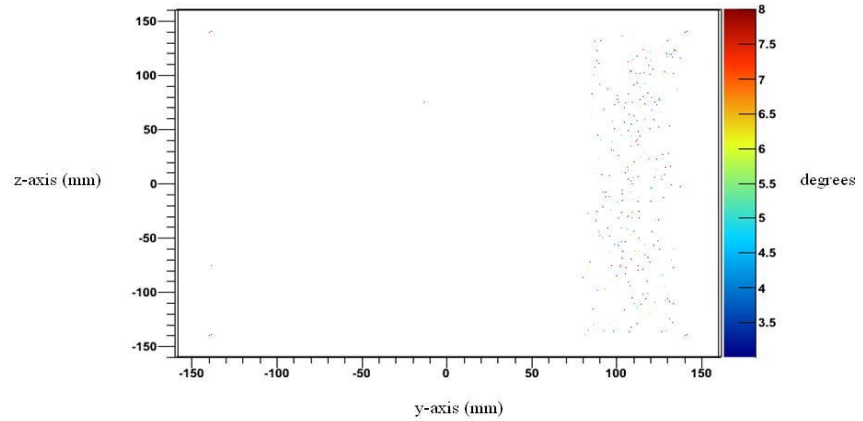

POCA plot for shielded scenario xz, y = 110 mm, with 10 minute exposure time viewed in the yz plane. The positive x axis is pointing out of the screen.

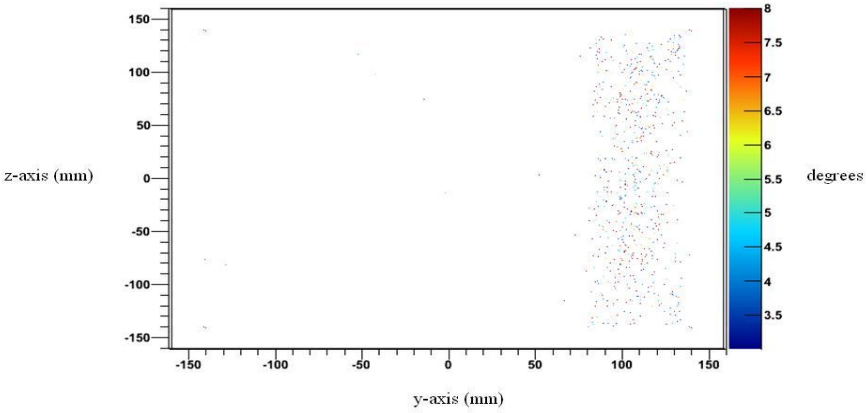

POCA plot for shielded scenario xz, y = 110 mm, with 60 minute exposure time viewed in the yz plane. The positive x axis is pointing out of the screen.

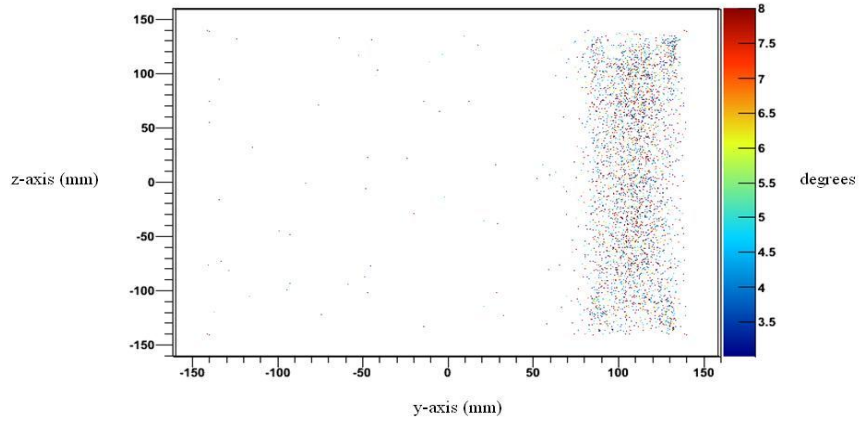

POCA plot of unshielded scenario one, with 4 minutes exposure time. The negative y axis is pointing out of the screen.

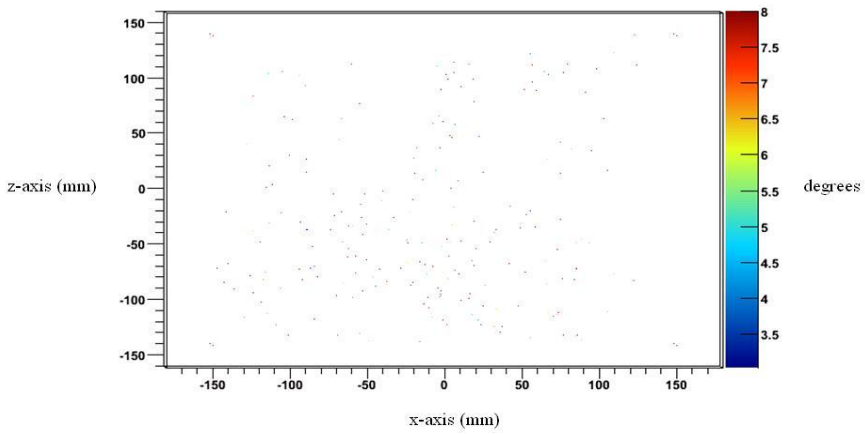

POCA plot of unshielded scenario one, with 10 minutes exposure time. The negative y axis is pointing out of the screen.

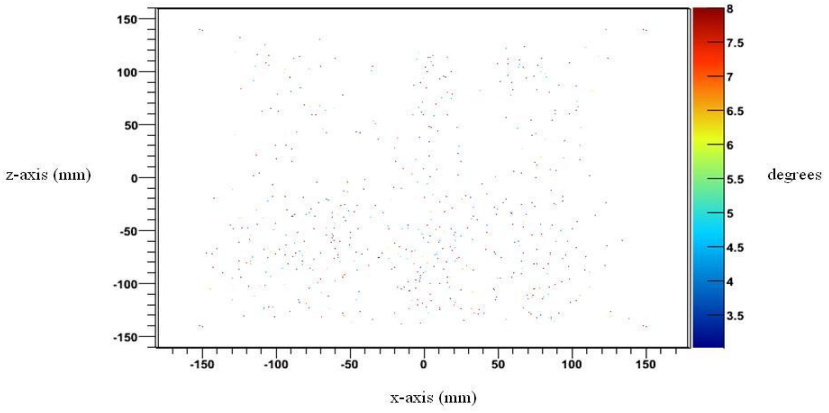

POCA plot of unshielded scenario one, with 60 minutes exposure time. The negative y axis is pointing out of the screen.

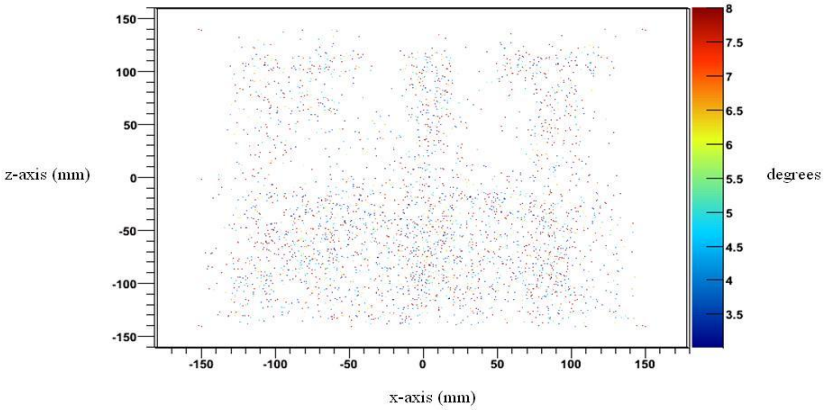

POCA plot of unshielded scenario two, with 4 minute exposure time. The negative y axis is pointing out of the screen.

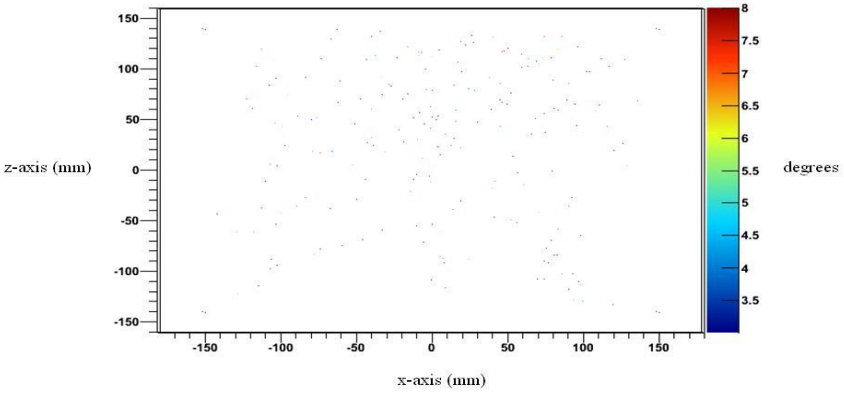

POCA plot of unshielded scenario two, with 10 minute exposure time. The negative y axis is pointing out of the screen.

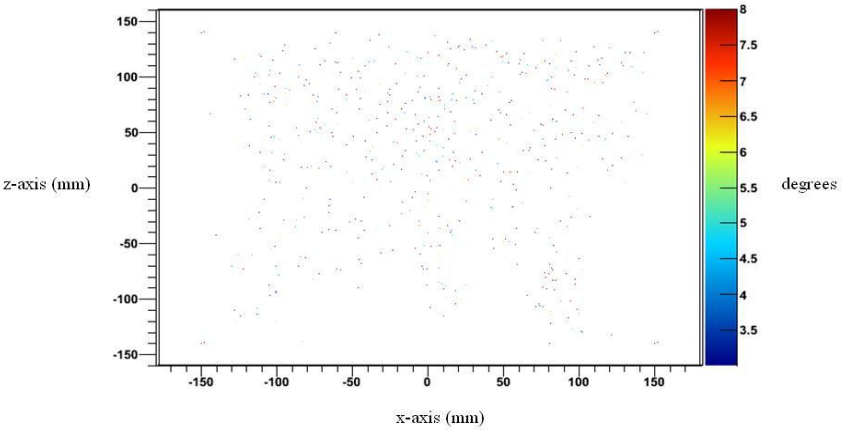

POCA plot of unshielded scenario two, with 60 minutes exposure time. The negative y axis is pointing out of the screen.